



ELSEVIER

Progress in Biophysics & Molecular Biology 86 (2004) 407–485

Progress in  
Biophysics  
& Molecular  
Biology

www.elsevier.com/locate/pbiomolbio

Review

## Ageing and vision: structure, stability and function of lens crystallins

Hans Bloemendal<sup>a</sup>, Wilfried de Jong<sup>a</sup>, Rainer Jaenicke<sup>b,c</sup>, Nicolette H. Lubsen<sup>a</sup>,  
Christine Slingsby<sup>c,\*</sup>, Annette Tardieu<sup>d</sup>

<sup>a</sup> Department of Biochemistry, University of Nijmegen, 6500HB Nijmegen, The Netherlands

<sup>b</sup> Institute of Biophysics and Physical Biochemistry, University of Regensburg, D-93040 Regensburg, Germany

<sup>c</sup> School of Crystallography, Birkbeck College, University of London, Malet Street, London WC1E 7HX, UK

<sup>d</sup> Laboratoire de Minéralogie-Cristallographie, CNRS-Université Paris 6, F-75252 Paris Cedex 05, France

### Abstract

The  $\alpha$ -,  $\beta$ - and  $\gamma$ -crystallins are the major protein components of the vertebrate eye lens,  $\alpha$ -crystallin as a molecular chaperone as well as a structural protein,  $\beta$ - and  $\gamma$ -crystallins as structural proteins. For the lens to be able to retain life-long transparency in the absence of protein turnover, the crystallins must meet not only the requirement of solubility associated with high cellular concentration but that of longevity as well. For proteins, longevity is commonly assumed to be correlated with long-term retention of native structure, which in turn can be due to inherent thermodynamic stability, efficient capture and refolding of non-native protein by chaperones, or a combination of both. Understanding how the specific interactions that confer intrinsic stability of the protein fold are combined with the stabilizing effect of protein assembly, and how the non-specific interactions and associations of the assemblies enable the generation of highly concentrated solutions, is thus of importance to understand the loss of transparency of the lens with age. Post-translational modification can have a major effect on protein stability but an emerging theme of the few

*Abbreviations:*  $\beta$ B2 $\Delta_{\text{NC}}$  and  $\beta$ B2-L $_{\gamma\text{B}}$ ,  $\beta$ B2-crystallin, truncated at N- and C-terminal end and  $\beta$ B2-crystallin with its natural linker replaced by  $\gamma$ B linker;  $\gamma$ B,  $\gamma$ B-N,  $\gamma$ B-C, and  $\gamma$ B-L $_{\beta\text{B2}}$ ,  $\gamma$ B-crystallin, its isolated N- and C-terminal domains, and  $\gamma$ B-crystallin with its natural linker replaced by  $\beta$ B2-linker, respectively;  $\gamma$ S-N,  $\gamma$ S-C, isolated N- and C-terminal domains of  $\gamma$ S-crystallin; CD, circular dichroism; CP, circular permutation or circularly permuted;  $c_{1/2,\text{urea}}$ ,  $c_{1/2,\text{GdmCl}}$ , denaturant concentrations at midpoint of N $\rightarrow$ U transition; 3D, three-dimensional;  $\Delta G$ ,  $\Delta\Delta G$ , and  $\Delta G^\ddagger$ , Gibbs free energy, difference of free energies and free energy of activation, respectively; EM, electronmicroscopy; FRET, fluorescence resonance energy transfer; GdmCl, guanidinium chloride; HMW, high molecular weight; Hsp, sHsp, heat shock protein, small heat shock protein; Ig, immunoglobulin; IR, infrared; MIM, Mendelian inheritance in man; NMR, nuclear magnetic resonance;  $K$ ,  $k$ , equilibrium constant and rate constant, respectively; N, U, I, native, unfolded and intermediate states; Protein S-N or PS-N, Protein S-C or PS-C, N- and C-terminal domains of Protein S from *Myxococcus xanthus*; SAXS, small angle X-ray scattering; SMPI, proteinase inhibitor from *Streptomyces nigrescens*;  $T_m$ ,  $T_c$ , temperatures of thermal denaturation and phase separation, respectively; trh $\beta$ B1, a truncated form of human  $\beta$ B1-crystallin; WmKT, yeast killer toxin from *Williopsis mrakii*

\*Corresponding author. Tel.: 20-7631-6832; fax: 20-7631-6803.

E-mail address: c.slingsby@mail.cryst.bbk.ac.uk (C. Slingsby).

studies of the effect of post-translational modification of the crystallins is one of solubility and assembly. Here we review the structure, assembly, interactions, stability and post-translational modifications of the crystallins, not only in isolation but also as part of a multi-component system. The available data are discussed in the context of the establishment, the maintenance and finally, with age, the loss of transparency of the lens. Understanding the structural basis of protein stability and interactions in the healthy eye lens is the route to solve the enormous medical and economical problem of cataract.

© 2003 Elsevier Ltd. All rights reserved.

*Keywords:* Cataract; Chaperone; Crystallins; Development; Evolution; Eye lens; Protein stability

## Contents

1. Introduction . . . . .	409
1.1. Cataract and lens components . . . . .	410
1.1.1. Cataract as a protein folding disease: the importance of chaperones . . . . .	410
1.1.2. Cataract resulting from altered protein interactions: the importance of solubility . . . . .	411
1.1.3. Lens differentiation: structuring a tissue for transparency . . . . .	412
1.1.4. The crystallins . . . . .	415
1.1.5. Selection of proteins as crystallins: evolution and link to the stress response . . . . .	419
2. Structure of crystallins and their relatives: two families . . . . .	422
2.1. The $\alpha$ -crystallins . . . . .	422
2.2. Structure of the two-domain $\beta$ - and $\gamma$ -crystallins . . . . .	426
2.2.1. The $\beta\gamma$ domain is an independent fold . . . . .	426
2.2.2. Monomeric two-domain $\gamma$ -crystallins . . . . .	428
2.3. $\beta$ -Crystallin oligomers . . . . .	429
2.3.1. Structure of $\beta\text{B}2$ -crystallin . . . . .	429
2.3.2. Structure of human $\beta\text{B}1$ -crystallin . . . . .	429
2.3.3. $\beta$ -crystallin human heterodimers and higher order assembly . . . . .	431
2.4. Microbial relatives and engineered $\beta\gamma$ -crystallins . . . . .	433
2.4.1. Structure of microbial relatives . . . . .	433
2.4.2. Engineered single domain and domain-permuted crystallins . . . . .	434
3. Stability of crystallins . . . . .	435
3.1. Physical basis of protein stability in dilute solution . . . . .	435
3.2. Stability in the cell, macromolecular crowding . . . . .	439
3.3. Stability of $\alpha$ -crystallin . . . . .	440
3.4. Stability of the $\beta$ - and $\gamma$ -crystallins . . . . .	441
3.4.1. $\gamma\text{B}$ -crystallin . . . . .	443
3.4.2. $\gamma\text{S}$ -crystallin . . . . .	445
3.4.3. Stability of $\beta\text{B}2$ -crystallins . . . . .	445
3.5. Stability of microbial $\beta\gamma$ -crystallin proteins . . . . .	448
3.5.1. Spherulin 3a from <i>Physarum polycephalum</i> . . . . .	448
3.5.2. Protein S from <i>Myxococcus xanthus</i> . . . . .	449
4. Multicomponent systems . . . . .	452
4.1. Transparency in multicomponent macromolecular systems . . . . .	452
4.2. Intra- and inter-molecular interactions and associations . . . . .	453
4.3. Interactions at a distance and transparency . . . . .	454
4.4. $\beta$ - and $\gamma$ -crystallin interactions, phase separation . . . . .	456

5. Lens $\alpha$ -crystallins and chaperone function . . . . .	459
5.1. The interaction between $\alpha$ -crystallin and $\beta$ - and $\gamma$ -crystallins . . . . .	460
5.2. Specificity of the $\alpha$ -crystallin chaperone behaviour . . . . .	462
6. Post-translational modification of crystallins . . . . .	463
6.1. Crystallins are extensively modified, outcomes are varied . . . . .	463
6.2. Crystallins are modified at an early age . . . . .	464
6.3. The effect of clipping the arms of the crystallins . . . . .	464
6.4. Deamidation . . . . .	465
6.5. Disulfide bond formation in $\gamma$ S-crystallin . . . . .	466
6.6. Protection by methylation . . . . .	467
7. Conclusions . . . . .	467
Acknowledgement . . . . .	470
References . . . . .	470

## 1. Introduction

The eye and its architecture, at the macroscopic, microscopic and molecular level, is a “joy forever”. Artists, poets and naturalists are equally attracted by its properties (Huxley, 1990; Darwin, 1859). Most impressive is the optical quality of the lens: the cones in the retina are visible through the intact optics of animal and human eyes (Hughes, 1996). The lens is a cellular organ and its transparency is due to its complex architecture and unique protein composition. Unfortunately, the delicate balance required for transparency is easily disturbed with lens opacity, cataract, as the result. Cataract is the most common cause of blindness, and, therefore, of enormous medical (and economical) relevance worldwide. Cataract can have many causes. It can be due to a mutation in one of the lenticular proteins and is then usually already present at birth; it can be one of the symptoms of systemic disease, for example diabetes is a risk factor for cataract; it can also be the result of mere ageing. Lenticular proteins, such as the abundant water-soluble proteins, the crystallins (in mammals:  $\alpha$ A, and  $\alpha$ B;  $\beta$ B1,  $\beta$ B2,  $\beta$ B3,  $\beta$ A3/A1,  $\beta$ A2, and  $\beta$ A4;  $\gamma$ A,  $\gamma$ B,  $\gamma$ C,  $\gamma$ D,  $\gamma$ E,  $\gamma$ F, and  $\gamma$ S), cannot be replaced (see also below) and thus have to last the lifetime of the organism. With time, lens proteins change in conformation and accrue damage due to modifications such as oxidation, deamidation, or cleavage resulting in wrong protein–protein interactions and aggregation. Cataract is then unavoidable. Incidence studies of age-related cataract such as the Beaver Dam Eye Study show that the incidence of three different kinds of cataract increases with age: nuclear cataract, which accounts for about 60% of the age-related cataract, cortical cataract, which accounts for about 30%, while the remaining 10% is a posterior subcapsular cataract (Klein et al., 2002). The total incidence of these three forms of age-related cataract found in the Beaver Dam Eye Study was about 45% for people between the age 55–64 (with 11% having had cataract surgery), of about 75% for people between age 65 and 74 (with 26% cataract surgery) and of about 88% for people older than 75 (with 30% cataract surgery). With increasing age the incidence of lens opacities increases and visual acuity lessens. Ultimately, the only way to restore sight is cataract surgery. Current levels of surgery remain too low to tackle the backlog of cataract blind, estimated to be 16–20 million worldwide, and to stem the rising world incidence due to the ageing population. The social impact and economic cost of cataract

has motivated extensive research on the lens and an enormous amount of knowledge has been accumulated. The premise of this review is that age-related cataract derives from two distinct molecular routes: protein unfolding resulting in protein aggregation and/or altered interaction and association between native crystallins resulting in lesser solubility, and focuses on available experimental data on the structure, folding, stability, solubility and intermolecular interactions of the abundant water-soluble lenticular proteins, the crystallins.

### 1.1. Cataract and lens components

Cataract is a pathological opacity interfering with transparency caused either by disturbances to the regular cytoplasm-membrane lattice repeat of the lens, or by perturbations of the local short-range order of the crystallins in the interior of the fibre cells (Fig. 1). From the physicochemical point of view, the spatial fluctuations of protein density responsible for lens opacification can be attributable at the cellular level to osmotic pressure effects. At the molecular level they can be due to the spontaneous phase separation of the (native) protein solution into coexisting protein-rich and protein-poor phases, or to the intrinsic instability of the cytoplasmic protein solution leading to wrong association i.e. aggregation of partially unfolded protein. Protein–protein interactions leading to the condensation of eye lens proteins into randomly distributed aggregates with average molecular masses beyond 50 MDa, will scatter light (Benedek, 1971, 1997). Mechanistically, condensation of lens protein can be due to unfolding of lens proteins—and cataract could then be considered as a protein folding disease—or due to altered interaction of native proteins—and cataract would then be the consequence of a loss of solubility.

#### 1.1.1. Cataract as a protein folding disease: the importance of chaperones

The present hypothesis for protein folding diseases is that they result from an insufficiency in the protein chaperoning system of the cell. In general, unfolding cytoplasmic protein evokes the



Fig. 1. Slit lamp view of human cataract. A slit lamp image of a slice of a human eye lens along the optical axis using the Scheimpflug principle that allows quantification of the light scatter, kindly provided by Dr. C.K. Patel, Oxford Eye Hospital, UK. This patient has a predominant cortical cataract with the anterior scattering zone indicated by the arrow, which is in a region of the lens where  $\gamma$ S-crystallin is abundant.

heat shock response, while unfolding endoplasmic reticulum protein evokes the unfolded protein response (for review, see Morimoto and Santoro, 1998; van den IJssel et al., 1999; Patil and Walter, 2001; van Montfort et al., 2001; Arrigo and Müller, 2002; Sonna et al., 2002). These two stress induced systems have in common that they inhibit general protein synthesis, and switch the resources of the cell to synthesizing protein chaperones, thus giving cells time and means to deal with the unfolded protein stress. The most prominent cytoplasmic chaperones synthesized as part of the heat shock response are Hsp90, Hsp70 and the small heat shock proteins (sHsps), Hsp27 and  $\alpha$ B-crystallin. Hsp90 and Hsp70 refold proteins in an ATP dependent way, where Hsp90 is dedicated to particular substrates while Hsp70 refolds more general substrates. The sHsps can bind non-native proteins but they cannot refold them. They may help target their substrate for proteolysis or they may store it for later action by a large Hsp. Furthermore, sHsps interact with the cytoskeleton (Nicholl and Quinlan, 1994) and may be instrumental in preserving the integrity of this cellular structure during stress. Protein folding disease would result when the unfolded protein accumulates faster than the chaperoning system can deal with aggregating protein (Dobson, 1999; Csermely, 2001).

Consideration of cataract as a protein folding disease invokes the lack of ability of the mature lens fibre cell to mount a cellular stress response and the use of a prominent lenticular structural protein,  $\alpha$ -crystallin, to function as a chaperone as well. The immature lens fibre cell can still mount the heat shock response and can deal with unfolding protein, although the system may well be overwhelmed if the misfolding protein is a mutant crystallin as the crystallin genes are expressed at very high levels. In this case even the immature lens fibre cell may not be able to escape from the unfolded protein stress, and will cease differentiating, thus disturbing lens morphogenesis (see for example Sandilands et al., 2002). This mechanism explains why the lens phenotype of most misfolded crystallin mutants (such as those involving truncations and frameshifts) is severe and often includes microphthalmia. The mature lens fibre cell lacks protein synthetic capacity and thus cannot increase its protein chaperone content when non-native protein starts aggregating. The mature lens cell does however start with a high concentration of the protein chaperone  $\alpha$ -crystallin, an assembly of the small heat shock proteins  $\alpha$ A- and  $\alpha$ B-crystallin. The prevalent hypothesis for age-related cataract is that, with time, as (other) lenticular proteins unfold and/or become modified and start to unfold, the chaperone capacity of  $\alpha$ -crystallin will be used up and protein aggregates will be formed (Horwitz, 1992; Derham and Harding, 1999; Clark and Muchowski, 2000).

It is noteworthy that the heat shock response attenuates with ageing (Franceschi et al., 2000; Söti and Csermely, 2002). The capacity of ageing cells to deal with unstable proteins thus also decays with age explaining why protein folding disease is more prevalent in the aged. The mature lens fibre cell represents a special case of aged cells: rather than having an attenuated heat shock system, it lacks it completely except for one component,  $\alpha$ -crystallin. Age-related cataract could then well be related mechanistically to other age-related folding diseases (see also Harding, 2002) and serve as a model system for age-related protein folding diseases.

### *1.1.2. Cataract resulting from altered protein interactions: the importance of solubility*

Transparency and high refraction of the lens is due to the short-range order between highly concentrated crystallins. The high level of polydispersity among the crystallin components will not only reduce the risk of protein crystallization, but also contribute to an even and dense packing.

In the lens cytoplasm, the mixture of crystallins displays overall repulsive interactions determined essentially by the dominating effect of  $\alpha$ -crystallin (Vérétout et al., 1989). Changes in solubility or attractive properties can cause cataract without the protein misfolding and before it unfolds. A well-known example is “cold cataract” due to phase separation of the  $\gamma$ -crystallins at low temperature. The importance of solubility is also illustrated by the two human hereditary cataracts shown to be caused by point mutations of surface residues of  $\gamma$ -crystallin. These mutations appear to reduce the protein solubility (Héon et al., 1999; Kmoch et al., 2000) and are unlikely to be rescued by the  $\alpha$ -crystallin chaperone. The post-translational modifications to which crystallins are subject, could cause alterations in protein interaction that are causally involved in ageing cataract.

### 1.1.3. Lens differentiation: structuring a tissue for transparency

The lens is a focusing device that allows images to be formed on the retina. To serve this function, the eye lens has to fulfil two requirements; it has to provide transparency and a high refractive index, i.e. low light scattering and high solubility of its cytoplasmic proteins, the crystallins. From the physical point of view, transparency is limited by absorption and scattering of visible light. In the cataract-free lens, absorption in the visible wavelength range is negligible. The cellular structure of the lens can meet these biophysical requirements because of its unique morphology and composition. In the mature lens, hexagonally packed, long ribbon-like fibre cells, which in man are up to 10 mm long, are arranged in concentric shells, with the oldest cells at the centre and the youngest on the outside (Fig. 2). The shape of the fibre cells is determined and maintained by an extensive cytoskeleton. The critical role played by the exact architecture of the cytoskeleton is indicated by the fact that a lens lacking the lens-specific intermediate filament proteins phakinin (CP49) and filensin is opaque even though the overall fibre cell morphology is normal (Alizadeh et al., 2002). The lens fibre cells have an unusually high protein content: the protein concentration of the round glassy fish lens increases from  $0.13 \text{ g ml}^{-1}$  at the edge to  $1.05 \text{ g ml}^{-1}$  at the centre, while the soft ovoid human lens has a protein concentration around  $0.32 \text{ g ml}^{-1}$ . The abundant water-soluble crystallins account for most of the lens fibre cell protein. Light scattering may originate from the differing refractive indices of the membrane and the

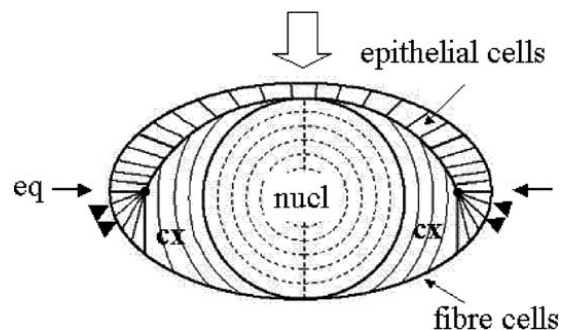


Fig. 2. Schematic drawing of a sagittal section through a vertebrate lens. The monolayer of epithelial cells and the fibre cell mass are indicated. The direction of incident light and the optical axis is represented by the open arrow, the equatorial plane by the two single arrows. The arrowheads show the region where the epithelial cells differentiate to secondary fibre cells. nucl: the nuclear region; cx: the cortical region, eq: the equatorial region.

cytoplasm of the fibre cells, particularly in the cortex (Michael et al., 2003). The experimental evidence for this refractive index difference is clearly seen in the diffraction peaks recorded when laser light is passed through a thin peripheral section of the lens (Benedek et al., 1979). The absence of diffraction when light is directed along the optical axis is presumably a consequence of the continuous gradual change in orientation between layers of cells along this axis. In the centre of the lens, the refractive index of the membranes is the same as that of the cytoplasm and the orientation of the membrane is of lesser importance (Michael et al., 2003).

The lens is determined during early embryonic development (Grainger, 1992) and derives from the ectoderm overlaying the optic cup. The surface ectoderm cells invaginate to form the lens vesicle with cells on the posterior side elongating to primary lens fibre cells filling the vesicle space. Cells on the anterior side remain a monolayer of epithelial cells, with their basal side facing outward and the apical side facing towards the lens fibre cells (Fig. 2). Lens epithelial cells divide in a region just anterior to the equator, the cells at the equatorial zone elongate to form secondary fibre cells which form a continuous layer overlaying the primary fibres (Bron et al., 2000). During differentiation of the fibre cells, the different classes of crystallin genes are expressed in a strict temporal and spatial order (see below). Furthermore, the expression of the crystallin genes is regulated in a developmental manner, with some of the crystallins being expressed primarily in the foetal lens, others only later. Crystallins synthesized during early development will be located in the core of the mature lens; crystallins expressed during later development will abound in the cortex. The design principle of vertebrate lenses is thus one of deposition of complex mixtures of crystallins that vary in their relative proportions along the optical axis and the equatorial plane, put in place by differential gene activity during development (see Section 1.1.4). As the last step in differentiation, fibre cells lose their nuclei, mitochondria and ribosomes in a process resembling the early steps of apoptosis (Bassnett, 2002). This loss of cellular organelles is required for transparency but has as consequence that the terminally differentiated fibre cell can no longer synthesize or degrade proteins. Hence, lens proteins that are located at the centre of the lens, and synthesized during foetal development, cannot be replaced and must last the lifetime of the organism.

Lens growth, development and differentiation is not an autonomous process but is directed by growth factors present in the ocular fluid. In a now classic experiment, Coulombre and Coulombre (1963) showed that inversion of the chicken lens in the optic cup resulted in differentiation of the epithelial cell layer to fibre cells. The quest for the lens differentiation factor in the rat or mouse resulted in the identification of a member of the BMP growth factor family as inducer of the differentiation of the primary lens fibre cells (the cells that derive from the lens vesicle). A member of the FGF family of growth factors is responsible for the induction of differentiation of the secondary fibre cells (McAvoy and Chamberlain, 1989; Faber et al., 2002), although it still is not clear which family member is the *in vivo* inducer of secondary lens fibre cell differentiation (for review, see Chow and Lang, 2001). Lens fibre cells *in vitro* only proceed through the complete programme of differentiation in the presence of continuous growth factor signalling (Peek et al., 1992; Leenders et al., 1997). Growth factor signals also set the level of expression of the various crystallin genes, for example in the presence of insulin or IGF-I relatively less  $\alpha$ -crystallin is made during *in vitro* differentiation of rat lens fibre cells (Civil et al., 2000). Hence, aberrations in ocular growth factor levels at an early age may cause changes in the spectrum of crystallins synthesized and thereby predispose to age-related cataract.

Although all vertebrate lenses are built in the same manner and all contain  $\alpha$ -,  $\beta$ -, and  $\gamma$ -crystallins (see below), there is great variety in certain lens parameters. In most terrestrial animals, the air–cornea interface provides the bulk of refraction with the lens being used for fine focusing over a range of distances. In diurnal animals, this accommodation is commonly achieved by a soft lens moulding into different shapes (Koretz and Handelman, 1988); as an exception, nocturnal animals such as rodents have a very hard lens and cannot accommodate by changing the shape of the lens. In aquatic animals the lens has to provide all the refraction, so fish lenses are spherical and have a very high refractive index at the centre. The fish lens can be readily dissected into two parts, a hard nearly incompressible core region and a soft cortex; in the case of a small fish from Lake Tanganyika, the core radius represents precisely two-thirds of the whole lens radius in all sizes of fish (Fernald and Wright, 1983). The human lens thickness along the optical axis varies with age growing from 3.7 mm at age 20–4.2 mm at age 60, with the equatorial diameter remaining constant at 9 mm after age 30 (Smith et al., 1992). Although the distinction between core and cortex is much less marked in humans compared with fishes, a central core region can be discerned on fine dissection ( $\sim 7$  mm in equatorial diameter), that has a characteristic protein electrophoresis pattern different from the cortex (Garland et al., 1996).

The human and the fish lens represent two extreme kinds of lenses reflecting their different optical specializations. In fish, the lens has a complex continual decrease of refractive indices ( $n$ ) from the centre (1.54) to the surface (1.36) (Kröger et al., 1994). Refractive index gradients have been measured for a wide age range of bovine lenses; it is in place even in the early foetus, spanning from 1.38 at the edge to 1.45 in the centre, and steepening to 1.47 in the centre of the oldest lens (Pierscionek and Augusteyn, 1992). The shape of the very shallow refractive index gradient in the biconvex spheroid human lens is difficult to measure; it is almost constant with  $n \sim 1.40$ .

The above range of refractive index values stem from massive differences in protein concentration. Once proteins have been concentrated to these extremely high values, they are generally not resolvable, and it is not known if they retain the structure of the soluble form. Evidence from Raman spectroscopy indicates that in the core of the rodent lens the bulk of the protein cysteines are oxidized which implies that the proteins are denatured (Yu et al., 1985). However, the “glassy” state is very stable in terms of transparency—the rodent or fish lens can be boiled without losing transparency—whereas the protein solution state of the human lens makes it prone to cataract. These species differences in overall protein levels make it difficult to apply the results of rodent mutation studies to human lens. Presumably, the differences in protein content are correlated with differences in the amount and spectrum of crystallins expressed. However, the complete spectrum of crystallins expressed has been characterized in only a few species. The combination of mass spectroscopy with genomic sequence data will ease the gathering of such data. Determining the crystallin expression pattern is experimentally much more difficult: it requires examination of samples from early embryo through adult, where results are confounded by the fact that later developmental samples also contain the record of the expression pattern at earlier stages. This problem can be circumvented by assaying mRNA rather than protein patterns but this presents an even greater experimental problem. Crystallin expression patterns are only available from chicken, mouse and rat, and man. When the crystallin expression pattern of the rodent lens is compared to that in the human lens (Lampi et al., 1998; Ueda et al., 2002) there is a decrease in expression of the crystallins found in the glassy core of the rodent lens ( $\beta$ B1-,  $\beta$ B3-, and

the  $\gamma$ A-F-crystallins) and an increase of expression of the crystallins found in the softer cortex ( $\beta$ B2- and  $\gamma$ S-crystallin). The differences in these patterns support the notion that these are a determinant of the optical properties of the lens.

#### 1.1.4. The crystallins

The abundant soluble proteins of the vertebrate eye lens are collectively known as the crystallins (Table 1). All vertebrate lenses examined contain three classes of crystallins, the  $\alpha$ -,  $\beta$ - and  $\gamma$ -crystallins, also known as the ubiquitous crystallins, although in widely varying ratios. In addition, some species contain other proteins, they are known as the taxon-specific crystallins. Using a mixture of different sized protein assemblies to fill the lens fibre cells insures polydispersity and prevents crystallization (see also below). In order to fulfil their optical function, crystallins have to be first and foremost soluble. As they have to last the whole life span of the organism they must also be stable.

*1.1.4.1. The  $\alpha$ -crystallins.* There are two  $\alpha$ -crystallin genes,  $\alpha$ A and  $\alpha$ B, encoding proteins that share around 60% sequence identity (Bloemendal and de Jong, 1991). Both  $\alpha$ -crystallins contain the “ $\alpha$ -crystallin domain” characteristic of the sHsps (de Jong et al., 1998). Only  $\alpha$ B-crystallin is still stress inducible. The expression of  $\alpha$ A-crystallin is essentially limited to the lens, only traces are found in some other tissues (Srinivasan et al., 1992), and  $\alpha$ A-crystallin is thus the lens-specific member of the family.  $\alpha$ B-crystallin is more widely expressed, and particularly abundant in brain, heart and muscle (Iwaki et al., 1990). Both  $\alpha$ A- and  $\alpha$ B-crystallin are found in lens epithelial cells but their synthesis is strongly up regulated upon differentiation to the lens fibre cells (McAvoy, 1978; van Leen et al., 1987a).  $\alpha$ A- and  $\alpha$ B-crystallin continue to be synthesized during lens development (Aarts et al., 1989a; Voorter et al., 1990; Lampi et al., 1998; Ueda et al., 2002) and would then be homogeneously distributed throughout the lens. In man, the ratio of  $\alpha$ A- to  $\alpha$ B-crystallin in the foetal lens is about 2:1 and the ratio decreases to about 3:2 in the water-soluble fraction of a lens from a 54/55 year old (Ma et al., 1998). The expression level of  $\alpha$ -crystallin is rather variable between species, just as for the  $\beta\gamma$ -crystallins. It is abundant in man (40% of soluble lens protein), less so in rodents (20%), while from chicken and fish values as low as 10% of the total lens protein have been reported (de Jong, 1981).

The  $\alpha$ -crystallins are presumed to function both as structural proteins and as chaperones in the lens. Possibly the latter function is also required for proper lens development as the lens of the  $\alpha$ A/ $\alpha$ B-crystallin double knock-out mouse is significantly smaller than that of the wild type mouse and fibre cell formation is severely disturbed (Boyle et al., 2003). The  $\alpha$ B-crystallin null mouse has no lens phenotype (Brady et al., 2001), but, because of its shorter lifespan, age-related cataract cannot be studied. The  $\alpha$ A-crystallin null mouse does have cataract, due to inclusion bodies containing  $\alpha$ B-crystallin (Brady et al., 1997) as well as  $\gamma$ -crystallin (Horwitz, 2003), indicating a role for  $\alpha$ A-crystallin in the solubilization of  $\gamma$ -crystallin.

*1.1.4.2. The  $\beta$ - and  $\gamma$ -crystallins.* The oligomeric  $\beta$ - and the monomeric  $\gamma$ -crystallins are both built up out of four Greek key motifs organized into two domains. The main sequence difference is that  $\beta$ -crystallins have N-terminal extensions compared with  $\gamma$ -crystallins, with the basic  $\beta$ -crystallins having in addition C-terminal extensions (Fig. 3). The  $\beta$ -crystallins are a family of basic ( $\beta$ B1,  $\beta$ B2,  $\beta$ B3) and acidic ( $\beta$ A1,  $\beta$ A2,  $\beta$ A3 and  $\beta$ A4) polypeptides (Herbrink et al., 1975; Berbers et al.,

Table 1  
Some crystallin parameters

Crystallin	Residues	Size (kDa)	pI	SwissProt	PDB	MIM
<i>Human lens crystallins</i>						
$\alpha$ A	173	19 909	5.6	P02489	—	123 580
$\alpha$ B	175	20 159	6.8	P02511	—	123 590
$\beta$ B1	251	27 892	8.6	P53674	10ki	600 929
$\beta$ B2	204	23 249	6.5	P43320	—	123 620
$\beta$ B3	211	24 230	5.9	P26998	—	123 630
$\beta$ A1	198	23 191	6.4	P05813	—	123 610
$\beta$ A2	196	21 964	5.9	P53672	—	600 836
$\beta$ A3	215	25 150	5.7	P05813	—	123 610
$\beta$ A4	195	22 243	5.8	P53673	—	123 631
$\gamma$ S	177	20 875	6.4	P22914	1ha4 <sup>a</sup>	123 730
$\gamma$ A	173	20 761	7.8	P11844	—	123 660
$\gamma$ B	174	20 776	7.0	P07316	—	123 670
$\gamma$ C	173	20 747	7.0	P07315	—	123 680
$\gamma$ D	173	20 607	7.2	P07320	1hk0	123 690
<i>Crystallins and homologs with X-ray structures</i>						
Bovine $\gamma$ S	177	20 796		P06504	1a7h <sup>a</sup>	
Bovine $\gamma$ B	174	20 965		P02526	1amm	
Bovine $\gamma$ D	173	20 735		P08209	1elp	
Bovine $\gamma$ E	173	21 008		<sup>b</sup>	1m8u	
Bovine $\gamma$ F	173	20 955		P23005	1a45	
Rat $\gamma$ E	173	21 132		P02528	1a5d	
Rat $\beta$ B2	204	23 250		P26775	1e7n	
Bovine $\beta$ B2	204	23 167		P02522	2bb2	
Met J. 16.5	147	16 452		Q57733	1shs	
Wheat 16.9	151	16 722		S21600 <sup>c</sup>	1gme	
Spherulin 3a	103	11 285		P09353	1ha4	
Protein S	173	18 793		P02966	1nps <sup>d</sup>	
<i>Enzyme-crystallins with X-ray structures</i>						
$\delta$ -crystallin	466 <sup>e</sup>	51 043 <sup>e</sup>		P05083 <sup>e</sup>	1ioa	
$\eta$ -crystallin	501	54 537		Q28399	109j	

<sup>a</sup> Structure of C-terminal domain.

<sup>b</sup> Sequence printed in Norledge et al. (1997a).

<sup>c</sup> The sequence is from GenBank with one sequence change T7S.

<sup>d</sup> Structure of the N-terminal domain.

<sup>e</sup> The sequence is from chicken, the 3D structure is of the turkey protein.

1984; Lampi et al., 1997). The sequences of their corresponding globular domains exhibit between 45 and 60% identity with each other, and about 30% with  $\gamma$ -crystallins (cf. Fig. 3). The  $\beta$ A1- and  $\beta$ A3-crystallins are encoded by the same gene, whereby the synthesis of the  $\beta$ A3-crystallin protein is initiated from a more upstream initiation codon than the  $\beta$ A1-crystallin protein. The only difference between these two proteins is thus the length of the N-terminal arm (Table 1).

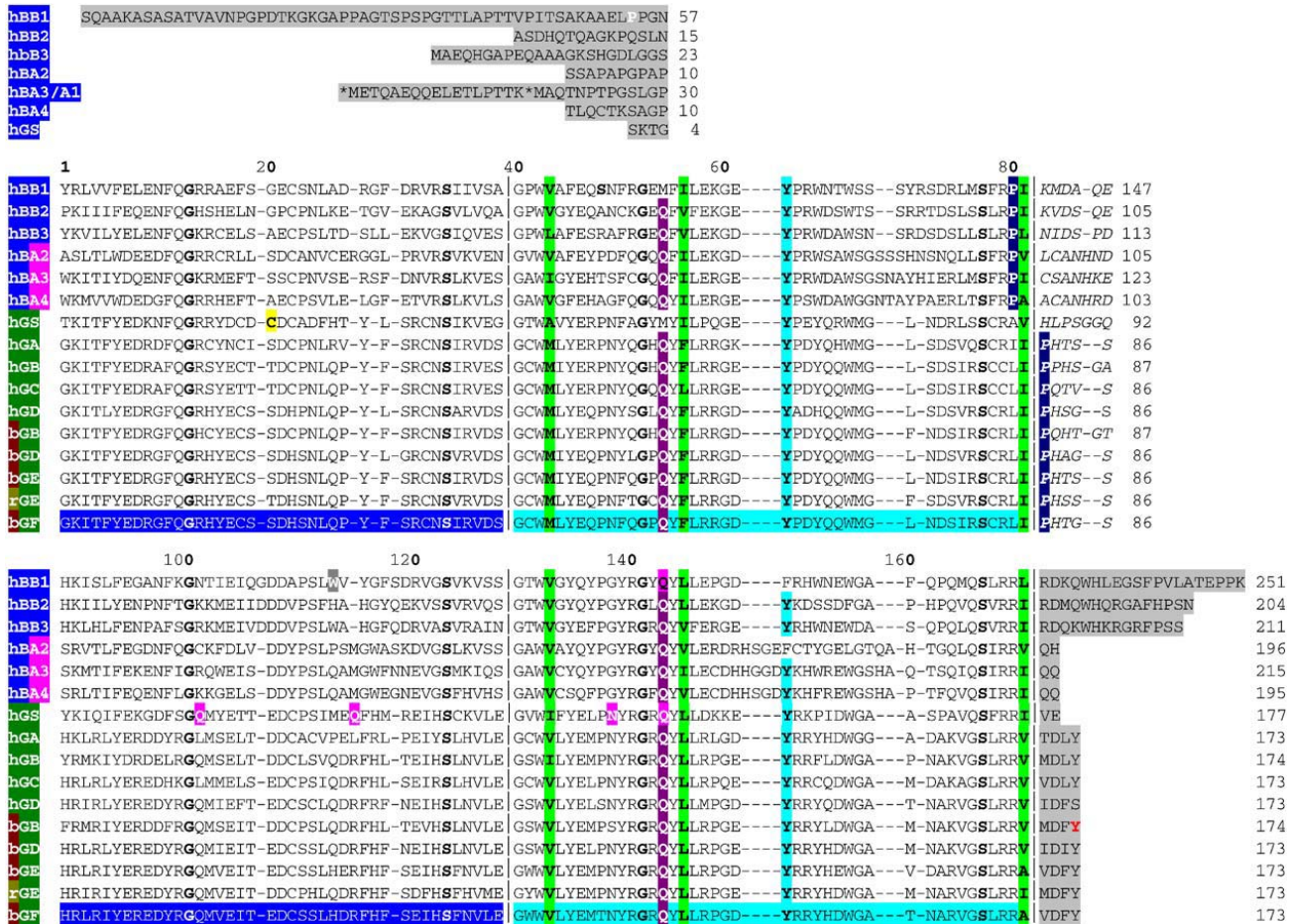


Fig. 3. Sequence alignment of the  $\beta\gamma$ -crystallin family. An alignment of the sequences of the  $\beta\gamma$ -crystallin proteins expressed in the human lens, as well as the bovine and rat  $\gamma$ -crystallins for which X-ray coordinates are available. Details of sequences and PDB's are given in Table 1. The sequences are aligned by domains, Greek key motifs 1 and 3 are in royal blue, and motifs 2 and 4 are in turquoise, to match Fig. 6a. The linkers are in *italics* and the N and C-terminal extensions are highlighted in grey. The motif conserved glycines and serines are in bold. The motif 2 and 4 tyrosine corners are in turquoise. Domain-pairing hydrophobic residues are in green. The conserved interface glutamine is in violet. Prolines in the vicinity of the linkers are in dark blue. Residues mentioned in the text are highlighted. The residue numbers above the alignment are those of bovine  $\gamma$ B-crystallin (indicated by the last digit), while the number to the right of each sequence is that of the corresponding SwissProt entry. \* indicates the two start sites of BA3/A1.

In mammals, the  $\beta$ -crystallin genes are fibre cell specific. Expression of the  $\beta$ -crystallins is under developmental control. The  $\beta$ B1- and  $\beta$ B3-crystallin genes are early genes and their products are found primarily in the lens nucleus, while the  $\beta$ B2-crystallin gene is a late gene, being in rodents only expressed in the post-natal lens (Aarts et al., 1989a; Chambers and Russell, 1991; Ueda et al., 2002). In man, a similar expression pattern is found, but because of the much higher level of  $\beta$ B2-crystallin in the human lens than in the rodent lens (Lampi et al., 1998, 2002b), this protein is prominent at all stages. The acidic  $\beta$ -crystallin genes have a wider expression pattern and their protein products are found both in the centre and the cortex of the lens (Lampi et al., 1998; Ueda

et al., 2002). Curiously, only a trace of the  $\beta$ A2-crystallin protein can be detected in the human lens (Lapko et al., 2003a) although its mRNA is abundant as evidenced from the high frequency of its cDNA in a human lens cDNA library (see <http://neibank.nei.nih.gov>; Wistow et al., 2002), suggesting a block in translation of this mRNA. In contrast, in the mouse or calf lens, this protein is as abundant as  $\beta$ A1-crystallin (Berbers et al., 1984; Ueda et al., 2002). The functional correlate of the species difference in expression pattern of the  $\beta$ -crystallins is not known but likely to be related to the water content of the lens. One of the consequences will be a different spectrum of  $\beta$ -crystallin assemblies across the lens. The  $\beta$ -crystallins assemble into broadly three size categories based on their behaviour during gel permeation chromatography:  $\beta$ H (hexamers/octomers),  $\beta$ L<sub>2</sub> (dimers), and  $\beta$ L<sub>1</sub> being intermediary (Zigler et al., 1980; Bindels et al., 1981; Berbers et al., 1982). As  $\beta$ B1-crystallin correlates with hexamers/octamers, while  $\beta$ B2-crystallin forms a dimer (see below), a shift from higher molecular weight assemblies in time is thus expected and this is indeed found (Ma et al., 1998). In space, this will correlate with a gradient from  $\beta$ H in the nucleus to  $\beta$ L in the cortex (Siezen et al., 1986).

The mammalian genome contains seven  $\gamma$ -crystallin genes. Six of these, the  $\gamma$ A-F-crystallin genes, are closely linked in a tandemly repeated gene cluster and are highly similar in sequence, particularly in their second exon, which encodes the N-terminal domain of the protein. This sequence similarity is, rather unusually, maintained by gene conversion (den Dunnen et al., 1986). The seventh gene, the  $\gamma$ S-crystallin gene, is located on another chromosome and is more divergent in sequence.  $\gamma$ S-crystallin has a short four amino acid<sup>1</sup> residue long N-terminal arm, unlike the  $\gamma$ A-F-crystallins, but lacks the two amino acid residue long C-terminal arm of the  $\gamma$ A-F-crystallins. In addition, the connecting peptide of the  $\gamma$ S-crystallin is one amino acid residue longer than that of the  $\gamma$ B-crystallin and two amino acid residues longer than that of the other  $\gamma$ A-F-crystallins (Table 1; Fig. 3).

The  $\gamma$ -crystallin genes are also fibre cell specific. They are the last crystallins to be made during fibre cell differentiation, being preceded by first the  $\alpha$ -crystallins and then the  $\beta$ -crystallins (McAvoy, 1978; van Leen et al., 1987a; Peek et al., 1992). As a consequence they are not found in the immature fibre cells in the cortical region. Furthermore, the  $\gamma$ A-F-crystallin genes are early genes, that is they are most copiously expressed in early lens development and their products are thus mainly found in the lens core region. The developmental expression pattern of the  $\gamma$ A-F-crystallin genes differs in the time of shut down: some genes, such as the  $\gamma$ E- and  $\gamma$ F-crystallin genes are silenced during (rodent) post-natal development, while  $\gamma$ B-crystallin continues to be synthesized (van Leen et al., 1987b; Ueda et al., 2002). In contrast to the  $\gamma$ A-F-crystallin genes, the  $\gamma$ S-crystallin gene is post-natal in rat. The abundance of its transcript in a cDNA library from two 40-year-old human lenses indicates that it is a late crystallin gene in man as well (Wistow et al., 2002; <http://neibank.nei.nih.gov>). The expression level of the  $\gamma$ A-F-crystallins is quite variable between species and appears to correlate inversely with the water content of the lens nucleus. In the hard rodent lens, the  $\gamma$ A-F-crystallins are all abundant, in the soft human lens, only  $\gamma$ C- and  $\gamma$ D-crystallins are abundant proteins (Siezen et al., 1987; Hanson et al., 1998). The very soft avian lenses contain only  $\gamma$ S-crystallin (van Rens et al., 1991).

*1.1.4.3. The taxon-specific crystallins.* A number of species have highly expressed lens proteins that do not belong to the  $\alpha$ - or  $\beta$  $\gamma$ -crystallin families, the taxon-specific crystallins. Table 2 summarizes a number of examples from different evolutionary lineages. Some of them represent

Table 2  
Enzyme-crystallins in vertebrate and non-vertebrate lenses<sup>a</sup>

Crystallin	Distribution	Identical with (=), or related to (~) <sup>b</sup>
$\delta$	Most birds, reptiles	= Argininosuccinate lyase
$\varepsilon$	Some birds, crocodiles	= Lactate dehydrogenase (LDH-B)
$\zeta$	Guinea pig, camel, llama	= NADPH:quinone oxidoreductase
$\eta$	Elephant shrew	= Aldehyde dehydrogenase I
$\iota$	Gecko ( <i>Lygodactylus picturatus</i> )	= Retinol-binding protein (type 1)
$\lambda$	Rabbit, hare	~ Hydroxyacyl CoA dehydrogenase
$\mu$	Kangaroo, quoll	~ Ornithine cyclodeaminase
$\pi$	Gecko ( <i>Phelsuma serraticauda</i> )	= Glyceraldehyde-3P dehydrogenase
$\rho$	Frogs, gecko ( <i>Lepidodactylus lugubris</i> )	~ NADPH-dependent aldose reductase
$\sigma$	Cephalopods	~ Glutathione S-transferase
$\tau$	Many vertebrates	~ $\alpha$ -enolase
$\upsilon$	Platypus ( <i>Ornithorhynchus anatinus</i> )	= Lactate dehydrogenase A
$\omega/\Omega$	Octopus	~ Alcohol dehydrogenase

Amino acids are abbreviated using the single-letter or three-letter code.

<sup>a</sup> Examples taken from Piatigorsky and Wistow (1989), Wistow (1993, 1995), Jimenez-Asensio et al. (1995), Röhl et al. (1995, 1996), Werten et al. (2000), van Boekel et al. (2001) and van Rheede et al. (2003).

<sup>b</sup> Refers to identical genes, ~ to relationships based on sequence homologies or topological similarities.

central metabolic enzymes occurring in body cells and in the eye lens, and are encoded by the same gene (gene sharing; Piatigorsky and Wistow, 1989, 1991; Wistow, 1993, 1995). During evolution they must have switched directly to their additional role as structural eye-lens proteins by modification of gene expression. In other cases, recruitment followed gene duplication and divergence and hence can be accompanied by loss of catalytic function. This supports the conclusion that taxon-specific enzyme crystallins were not recruited for metabolic or catalytic reasons; instead, their abundance argues that they serve mainly as structural proteins contributing merely to the refractive index and/or to the solubility properties in the complex multicomponent system of the lens. Thermodynamic (and kinetic) stability is another important property of eye-lens proteins. Therefore, it is possible that during evolution proteins were recruited simply because of their high intrinsic stability. Keeping multifunctionality in mind, subsidiary roles such as sequestering NAD(P)H to protect the lens against oxidation or damage from UV radiation, are conceivable (Wistow et al., 1987; Wistow and Piatigorsky, 1987; Piatigorsky and Wistow, 1989, 1991; Jimenez-Asensio et al., 1995; Röhl et al., 1995, 1996; Werten et al., 2000; Berr et al., 2000; van Boekel et al., 2001). A consequence of sharing or recruitment of a gene is that during evolution its different functions may be exposed to widely differing selective constraints so that adaptive changes favourable for one function may be deleterious for another. Conflicts like that may be resolved either by reversing the recruitment or by gene duplication; both strategies have been observed for enzyme-crystallins.

#### 1.1.5. Selection of proteins as crystallins: evolution and link to the stress response

The evolutionary origin of the vertebrate lens remains a matter of debate. The differences in morphology between the vertebrate eye and the various types of invertebrate eyes suggest that

distinct evolutionary pathways are involved (Fernald, 1997). Yet the specification of the vertebrate and the *Drosophila* eye uses homologous regulatory networks in which orthologous proteins participate, showing that the development of these morphologically distinct visual systems has a joint origin (for review, see Chow and Lang, 2001). The  $\alpha\beta\gamma$ -crystallins are specific to the vertebrate lens and must have been recruited as lens proteins in the primitive vertebrate. The evolutionary considerations for recruitment of the  $\alpha\beta\gamma$ -crystallins are the same as those for the taxon-specific genes described above: the ancestral genes must have been genes that were at least potentially transcriptionally active, i.e. either housekeeping genes or stress inducible genes, and recruitment can have been preceded or followed by gene duplication. The origin of the  $\alpha$ -crystallin genes is clear. These proteins belong to the family of the small heat shock proteins (van den Heuvel et al., 1985). A duplication of one of these genes resulted in the  $\alpha A/\alpha B$  crystallin gene pair, where the  $\alpha A$ -crystallin has become lens-specific, while the  $\alpha B$ -crystallin gene has retained a housekeeping function as well (see Section 1.1.4.1) and is still heat shock inducible.

The evolutionary origin of the  $\beta\gamma$ -crystallins is obscure. A vertebrate housekeeping relative directly ancestral to the  $\beta$ - or  $\gamma$ -crystallin genes should be closely related in sequence and share the gene organization. No such genes have been detected in the vertebrate genome. It could be that one of the present-day  $\beta$ - and  $\gamma$ -crystallin genes originally had or even still retains a housekeeping function outside the lens. In case of the  $\gamma$ -crystallins, the most likely candidate is the  $\gamma S$ -crystallin gene as orthologs of this gene are found in all vertebrate lineages examined. In contrast, the other  $\gamma$ -crystallin genes are paralogs and derive from a separate set of gene duplications in for example mammals, amphibians and fish (see also below). Furthermore,  $\gamma S$ -crystallin is expressed outside the lens and its expression pattern suggests a stress-related role (Sinha et al., 1998; Wang et al., 2003). Of the six  $\beta$ -crystallin genes, the  $\beta B2$ -crystallin gene is the one that has the most widespread expression pattern outside the lens, albeit at low level (Dirks et al., 1998; Magabo et al., 2000). A role for this protein in fertility has been suggested (Robinson et al., 2003). The  $\beta B2$ -crystallin gene may thus still retain a housekeeping function.

A stress connection is commonly suggested not only for the  $\alpha$ - but also for the  $\beta\gamma$ -crystallin genes. The promoter regions of the  $\beta\gamma$ -crystallin genes lack heat shock elements and there is no evidence for a role of these proteins in the heat shock response, unlike the  $\alpha$ -crystallins. A shared feature of the promoter regions of the  $\beta\gamma$ -crystallin genes is a Maf Response Element, a target of Maf transcription factors (Ring et al., 2000; Doerwald et al., 2001; Civil et al., 2002). The Maf transcription factors can form heterodimers with AP-1 factors, which are involved in the response to growth factors and to various types of stress (for review, see Motohashi et al., 1997). A Maf transcription factor, MafK, plays a role in the oxidative stress response (Nguyen et al., 2000). If there is a stress connection of the  $\beta\gamma$ -crystallin genes, that connection may well be oxidative stress.

Although the  $\beta$ - and  $\gamma$ -crystallins appear to be close relatives when the protein structure is considered, both being built up out of four homologous Greek key motifs organized into two domains (see also below), genetically they are quite distinct. The  $\beta$ -crystallin genes have six exons with introns separating the motif-encoding regions, while the  $\gamma$ -crystallin genes have only three exons, and lack the intron between the motif-encoding regions, retaining only the intron between the domain-encoding regions (Lubsen et al., 1988). This difference in gene structure suggests divergence between these two gene families at the level of a putative ancestral gene encoding a single motif or single domain and a long separate evolutionary history. It is thus likely that the primordial  $\beta$ - and  $\gamma$ -crystallin genes predated the vertebrates but no clear orthologs in

non-vertebrate species have been detected thus far. A  $\beta\gamma$ -like sequence has been reported from the sponge *Geodia cydonium* (Di Maro et al., 2002). However, this gene does not have introns and the relationship with the mammalian  $\beta\gamma$  genes is difficult to establish. The typical  $\beta\gamma$  double Greek key fold is also found in a number of other proteins such as the human protein AIM1 where the motifs are encoded by separate exons (Ray et al., 1997), EDSP from the amphibian *Cynops pyrrhogaster* (Wistow et al., 1995), while two microbial family members Spherulin 3a from *Physarum polycephalum* and Protein S from *Myxococcus xanthus* are known to have stress-related functions. Putative family members include the yeast-killer toxin WmKT from *Williopsis mrakii* and a proteinase inhibitor SMPI from *Streptomyces nigrescens*.

Genes closely similar to at least some of the six mammalian  $\beta$ -crystallin genes have been detected in amphibians and fish. Since there is no evidence for the existence of a  $\beta$ -crystallin gene family in non-vertebrates, the present scenario is that a series of gene duplications led to a six-membered family during early vertebrate evolution. The various present day  $\beta$ -crystallin genes would then be orthologous in the different vertebrate species, that is they would be direct descendants of the same set of six early vertebrate genes. The evolution of the  $\gamma$ -crystallin genes is more complicated. Of the seven mammalian  $\gamma$ -crystallin genes only the  $\gamma$ S-crystallin gene is common to all vertebrates. It is also the only  $\gamma$ -crystallin gene found thus far in birds. The other six mammalian  $\gamma$ -crystallin genes, the  $\gamma$ A-F-crystallin genes, are unique to mammals.  $\gamma$ -Crystallin genes are present in fish and amphibian genomes as well, but these genes are more closely related to each other than to the mammalian genes, suggesting that these arose from a separate set of gene duplications (Smolich et al., 1993; Pan et al., 1994) and are thus paralogs rather than orthologs of the mammalian  $\gamma$ -crystallin genes. A likely scenario is that the ancestral vertebrate had two  $\gamma$ -crystallin genes. One gene, the  $\gamma$ S-crystallin gene, remained single copy and continued to be expressed in all species after its recruitment for lens expression. Its protein product is most abundant in the water rich region. The product of the other ancestral  $\gamma$ -crystallin gene was apparently particularly suited to a low water environment and its evolution correlates with adaptation to the particular visual requirements imposed by the habitat. Expansion by tandem gene duplications and high-level expression of this gene is found in lineages or species with hard round lenses (for example in fish and rodents), loss of gene copies and down-regulation is seen in lineages or species with soft lenses (for example in birds). In mammals this adaptation is illustrated by man: although the human genome contains the usual six mammalian  $\gamma$ A-F-crystallin genes, only two, the  $\gamma$ C and  $\gamma$ D genes are highly active. A low level of expression of the  $\gamma$ A and  $\gamma$ B genes is found, while the  $\gamma$ E and  $\gamma$ F genes have become pseudogenes (Brakenhoff et al., 1990).

The frequent recruitment of genes to serve as crystallin genes might suggest that many proteins could be a “crystallin”. Indeed, the refractive-index increment of proteins does not vary much. Yet in spite of the plasticity of the lens in accepting other proteins as crystallins, the  $\alpha$ -,  $\beta$ - and  $\gamma$ -crystallins are highly conserved proteins, with little variation in protein sequence. For example, the rate of change in the  $\beta$ A3/1-crystallin is less than that of the  $\text{Na}^+ \text{K}^+$  ATPase  $\beta$ -subunit (Aarts et al., 1989b) and even the peculiar dual translation initiation site of the  $\beta$ A1/3-crystallin gene has been retained in time (Werten et al., 1996). The fact that these proteins are under severe constraint imposed by the selection pressure of visual acuity is also illustrated by the  $\alpha$ -crystallin genes of the blind mole rat. In this rodent the lens has degenerated and selection pressure due to the need for vision is no longer applied. Consequently, the  $\alpha$ A-crystallin gene has accumulated mutations at an

accelerated rate, while the  $\alpha$ B-crystallin gene, which also has a non-lens function, has evolved at the same rate as in other rodents (Hendriks et al., 1987).

These evolutionary considerations suggest that the  $\alpha$ -,  $\beta$ - and  $\gamma$ -crystallins are essential to the function of the lens although the expression level is adapted to the optical properties of the lens. Indeed, as described above, loss of the  $\alpha$ -crystallins leads to aberrant fibre cell differentiation. No hereditary cataracts due to a lack of a  $\beta$ - or  $\gamma$ -crystallin are known, all the hereditary cataract mutations linked to these genes cause protein misfolding and aggregation or contain point mutations which result in properly folded proteins with lower solubility. Yet, except for the single instance of the lower fertility of the Philly mouse (Robinson et al., 2003), with a  $\beta$ B2-crystallin mutation, no phenotype other than cataract has been reported for these mutations. The available evidence thus suggests that the evolutionary conservation of the crystallin genes in sequence and their divergence in expression patterns is due to the selective advantage of visual acuity and further suggests that building a transparent lens requires a finely tuned mixture of specialized proteins.

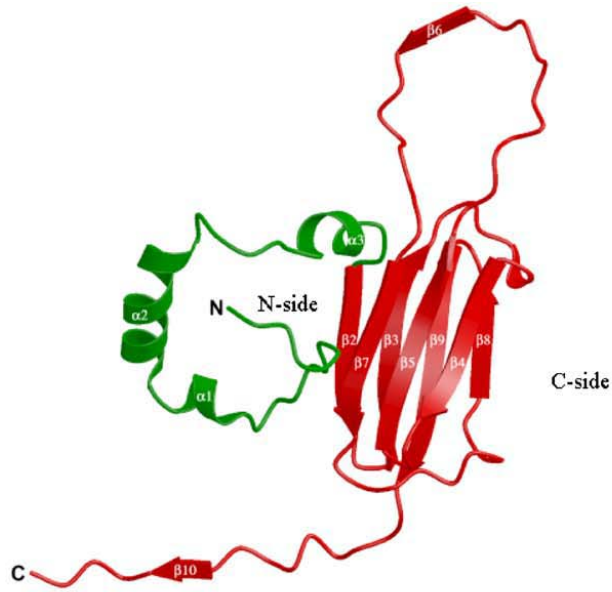
## 2. Structure of crystallins and their relatives: two families

### 2.1. The $\alpha$ -crystallins

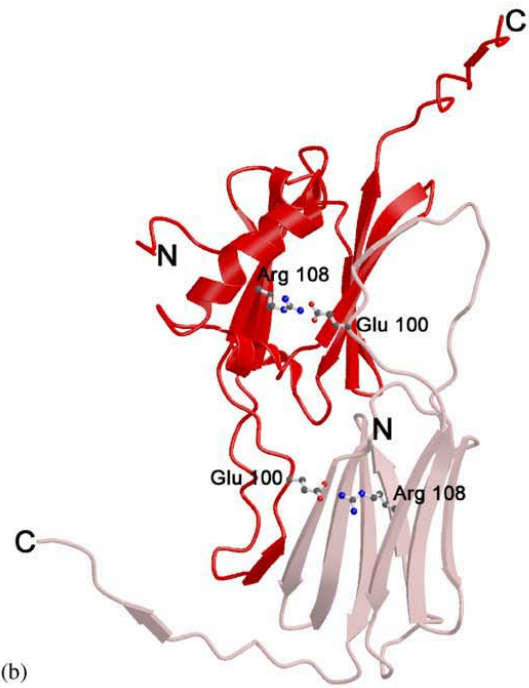
Vertebrate  $\alpha$ -crystallins, like many sHsps, form polydisperse multimers (MacRae, 2000).  $\alpha$ -Crystallins have molecular masses between 300 and 1200 kDa, depending on the solvent conditions and other variables. CD- and IR-based secondary structure predictions for the  $\alpha$ -crystallin subunit suggested predominantly  $\beta$ -sheet and less than 20% helix content. Due to the polydisperse size distribution of both the natural and recombinant protein, crystallization of vertebrate  $\alpha$ -crystallin has been unsuccessful so far. Thus, presently neither the detailed 3D structure of the subunit nor the topology of the subunit assembly is known. Classification of

---

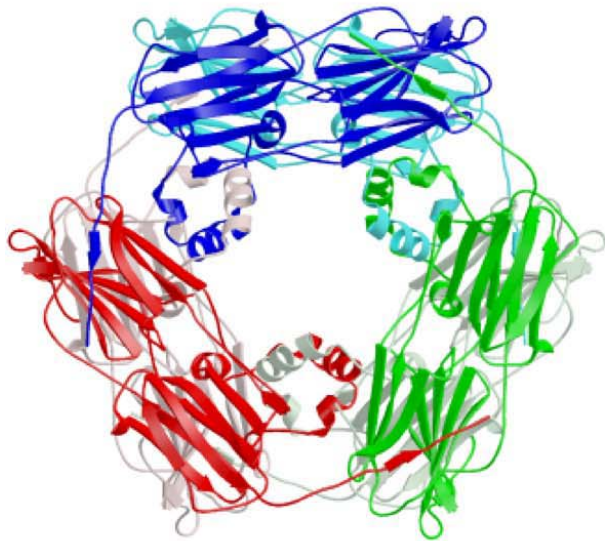
Fig. 4. Structure of a plant small heat shock protein assembly (based on Figs. 2 and 4c from van Montfort et al., 2001, reproduced with permission from <http://www.nature.com/nsb/>). (a) Ribbon diagram of the monomer with the N-terminal arm shown in green, the  $\alpha$ -crystallin domain and C-terminal extension in red with the N- and C-termini, and secondary structure elements labelled. (b) The dimer showing the monomer with the ordered N-terminal arm in red and the monomer with the disordered N-terminal arm in pink, as viewed down the approximate 2-fold axis. Note how a  $\beta$ -strand from a long loop in one monomer extends a  $\beta$ -sheet in the partner monomer. The dimer interface is stabilized by an ion pair between Arg 108 and Glu 100. Arg 108 is structurally conserved throughout the sHsp family and when mutated in  $\alpha$ A- or  $\alpha$ B-crystallin causes cataract and muscle myopathy, respectively. (c) *Top*: The overall structure shows that the dodecamer is arranged as two disks, each comprising six monomers, with overall 32 symmetry. The top view is looking down the crystallographic 3-fold axis which is perpendicular to the 3 crystallographic 2-fold axes. The dimers in the top disk are displayed in red, green and blue, the dimers in the bottom disk are shown in pink, sage and turquoise. The ordered N-terminal arm from each of 3 dimers in one disk makes a 2-fold interaction with an N-terminal arm from the other disk, resulting in three helical domains in the centre of the double disk. *Bottom*: A side view (showing eight dimers for clarity) showing the loosely knotted paired helices of the red and sage green dimers. (d) A close up view of the intramolecular interactions between the N-terminal arm (green) and the surface hydrophobic patch on the  $\alpha$ -crystallin domain (red). The conserved residues in a conserved sequence motif in the N-terminal arm and the interacting hydrophobic residues in the  $\alpha$ -crystallin domain are indicated.



(a)

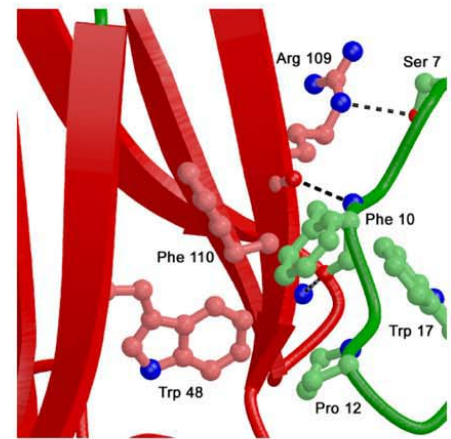


(b)



(c)

7 10  
**S-X-X-F-D**  
 48 108 109 110  
**(W) R (R) (F)**



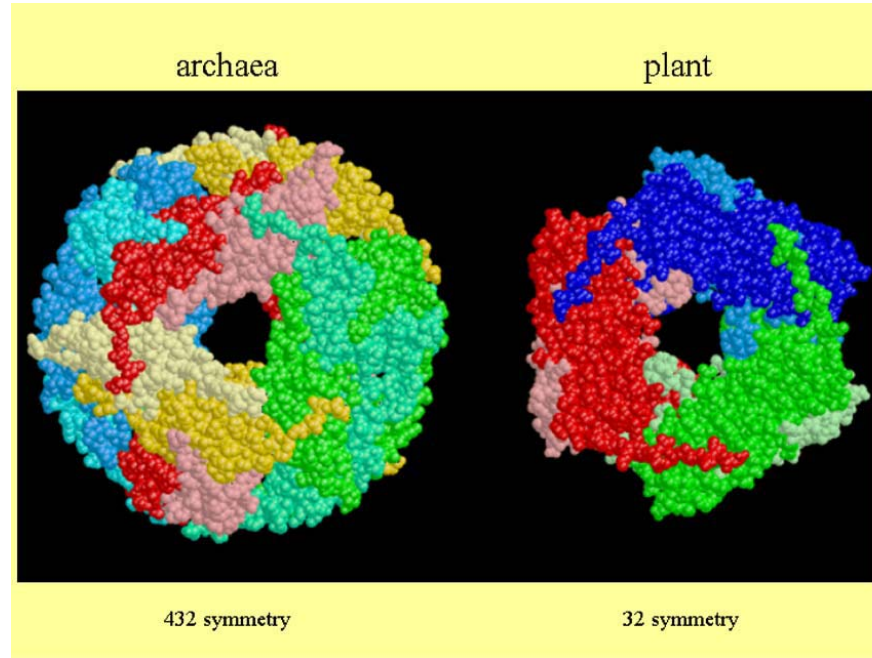
(d)

cryo-electron micrographs and 3D image reconstruction of the recombinant homotypic human  $\alpha$ B-crystallin showed that the assembly consists mainly of protein shells of  $\sim 19$  nm diameter with a central cavity  $\sim 8$  nm in diameter (Haley et al., 1998).

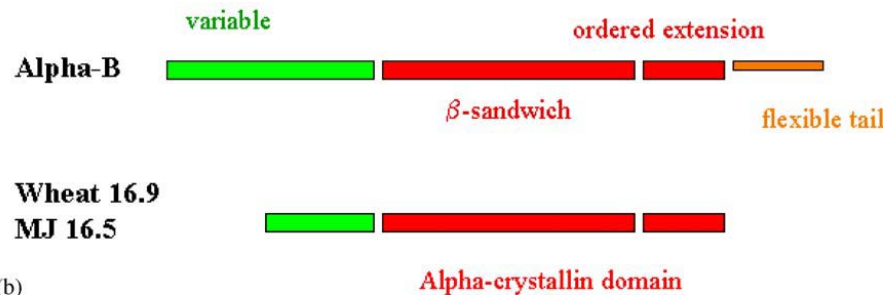
sHsp sequences are characterized by a C-terminal “ $\alpha$ -crystallin domain” linked to a variable N-terminal region (de Jong et al., 1998). It was proposed that the “ $\alpha$ -crystallin domain” might resemble an Ig fold (Mornon et al., 1998). This hypothesis was confirmed when the first X-ray structure of an “ $\alpha$ -crystallin domain” was solved from an archaeal hyperthermophile (Kim et al., 1998), followed by the 2.7 Å X-ray structure of the first sHsp assembly from a higher organism, wheat (van Montfort et al., 2001). Looking in detail at one monomer of the plant sHsp (Fig. 4a), the domain fold is seen to be composed of a two sheet  $\beta$ -sandwich structure surrounded by “loose ends”, in contrast with the neat arrangement of strands in the  $\beta\gamma$ -crystallin domain (see next section). This is considered to represent an “unfinished domain”, as the edges of both sheets on the two sides of the sandwich (labelled the N- and C-sides) need partners for stabilization of the fold. The first step in assembly is the formation of a dimer by reciprocal strand-exchange, in which the  $\beta_6$ -strand from one monomer becomes an edge strand of one  $\beta$ -sheet on the N-side of the subunit partner in the dimer (Fig. 4b). Then six dimers assemble to form the dodecamer (Fig. 4c). This stage of the assembly requires the N-terminal region from six monomers to assemble into 3 sets of paired helices inside a ring of paired “ $\alpha$ -crystallin domains”. A side view shows the discs of the  $\beta$ -sandwiches packed face-to-face with the paired N-terminal helices in the middle (Fig. 4c). The 12 ordered C-terminal extensions are also helping to bind the assembly together. The side view shows for example that for the red dimer of “ $\alpha$ -crystallin domains”, the two ordered C-terminal extensions are clearly in different orientations which allow the binding of domains within a ring and between rings. The binding of the ordered C-terminal extension derives from a hydrophobic I-X-I motif in the final strand that covers a hydrophobic crevice and seals both  $\beta$ -sheets edges on the C-side of the sandwich. Whereas all 12 C-terminal extensions are ordered in this assembly structure, only six of the N-terminal regions are visible as loosely knotted paired helices. The other six N-terminal regions are not visible and presumed to be disordered.

Comparison of the two sHsp X-ray structures allowed definition of common features across two kingdoms and showed that the drive for assembly likely stemmed from the search of the “unfinished  $\alpha$ -crystallin domain” for partners. The  $\beta$ -sandwich domain fold has the same topology as the monomeric human co-chaperone p23 (Weaver et al., 2000), but in this case the fold is patched intramolecularly (van Montfort et al., 2001). For the oligomers, higher assembly completes the fold by patching the edges of the  $\beta$ -sheets on both sides of the sandwich. Both the prokaryote and the eukaryote proteins patch the N-side edge of the  $\beta$ -sheet by forming similar dimers by strand exchange from a long loop (Fig. 4b) and thus the basic structural unit of both assemblies is a dimer. The edges of both sheets are patched on the C-side of the  $\beta$ -sandwich by the conserved hydrophobic I-X-I sequence motif in the C-terminal extension, but here it is from another dimer. The prokaryote uses these contacts to assemble as a spherical 24-mer with 432 symmetry (Fig. 5a). The plant sHsp assembles with 32 symmetry (Fig. 4c) by using an additional edge patch on the N-side provided by a conserved sequence motif in the N-terminal region (Fig. 4d) to contribute towards the fold of the loosely knotted dodecameric assembly (Fig. 4c).

The final assembly of the plant sHsp thus differs from the shell-like archaeal 24-mer and the proposed cryoEM structure for human  $\alpha$ B-crystallin. Analysis of sHsp sequences indicated that whereas patching the C-side of the  $\beta$ -sandwich with a C-terminal extension may be a conserved



(a)



(b)

Fig. 5. Comparison of archaeal and plant sHsp assemblies. (a) Comparison of the quaternary structures of the dodecameric wheat Hsp16.9 double disk with 32 symmetry on the right and the spherical *Methanococcus jannaschii* Hsp16.5 24-mer with 432 symmetry on the left. Dimers are shown in uniform colours (based on Fig. 3a from van Montfort et al., 2001, reproduced with permission from <http://www.nature.com/nsb/>). (b) The conserved  $\alpha$ -crystallin domain as recognized by sequence profile searches is shown in red. It comprises two structural modules, the  $\beta$ -sandwich and the ordered extension. The hinge connecting these two modules is flexible allowing different assemblies. The flexible tail is shown in orange and corresponds with the regions classed as mobile when the assembly is investigated by NMR spectroscopy. The N-terminal regions (green) are variable in length and sequence.

feature throughout the family, metazoans differ in the region of the dimerization loop (van Montfort et al., 2002). Systematic site-directed spin labelling of  $\alpha$ -crystallin is consistent with this fold topology for the monomer, but indicates a different dimerization motif (Koteiche and Mchaourab, 1999) as does low angle X-ray scattering (Feil et al., 2001). Recent nanoelectrospray mass spectrometry results suggest that a monomer, rather than a dimer, is the assembly unit (Aquilina et al., 2003). However, the conserved sequence motif used for the N-side patch is found in a subclass of the human sHsps that includes lens  $\alpha$ -crystallins and Hsp 27 (Fig. 4d). The

topological equivalents of the arginine mutation in  $\alpha$ A-crystallin that causes congenital blindness and the corresponding mutation in  $\alpha$ B-crystallin that causes a desmin-related myopathy are found to be associated with this edge  $\beta$ -strand protection, albeit in different ways, in the two resolved structures (Fig. 4b).

In summary, the “ $\alpha$ -crystallin domain” in the  $\alpha$ -crystallins is likely to have the  $\beta$ -sandwich fold in which the C-side protection is provided by the conserved I-X-I motif from the ordered extension of a partner subunit. However, to predict how the fold is completed on both edges of the N-side of the sandwich is much more difficult as metazoan sequences differ significantly from the sequences of observed structures in the regions that perform the patching function. The  $\alpha$ -crystallins also have an additional C-terminal tail for which there is evidence of conformational flexibility (Fig. 5b).

In connection with the functionally relevant quaternary structure of  $\alpha$ -crystallin, a number of models have been proposed, based on hydrodynamic data and subunit-exchange, as well as light scattering, X-ray small-angle scattering, cryo-electron microscopy, image-reconstruction and homology-modelling (Tardieu et al., 1986; Groenen et al., 1994b; Haley et al., 1998; Horwitz et al., 1998a; Abgar et al., 2000). There seems to be general agreement that under physiological conditions the quaternary assembly is characterized by a relatively fast subunit-exchange, indicating a certain degree of conformational flexibility of the  $\alpha$ -crystallin protomers (Bova et al., 1997; Ehrnsperger et al., 1999; Abgar et al., 2000; Datta and Rao, 2000; Haley et al., 2000; Reddy et al., 2000; Vanhoudt et al., 2000; Putilina et al., 2003).

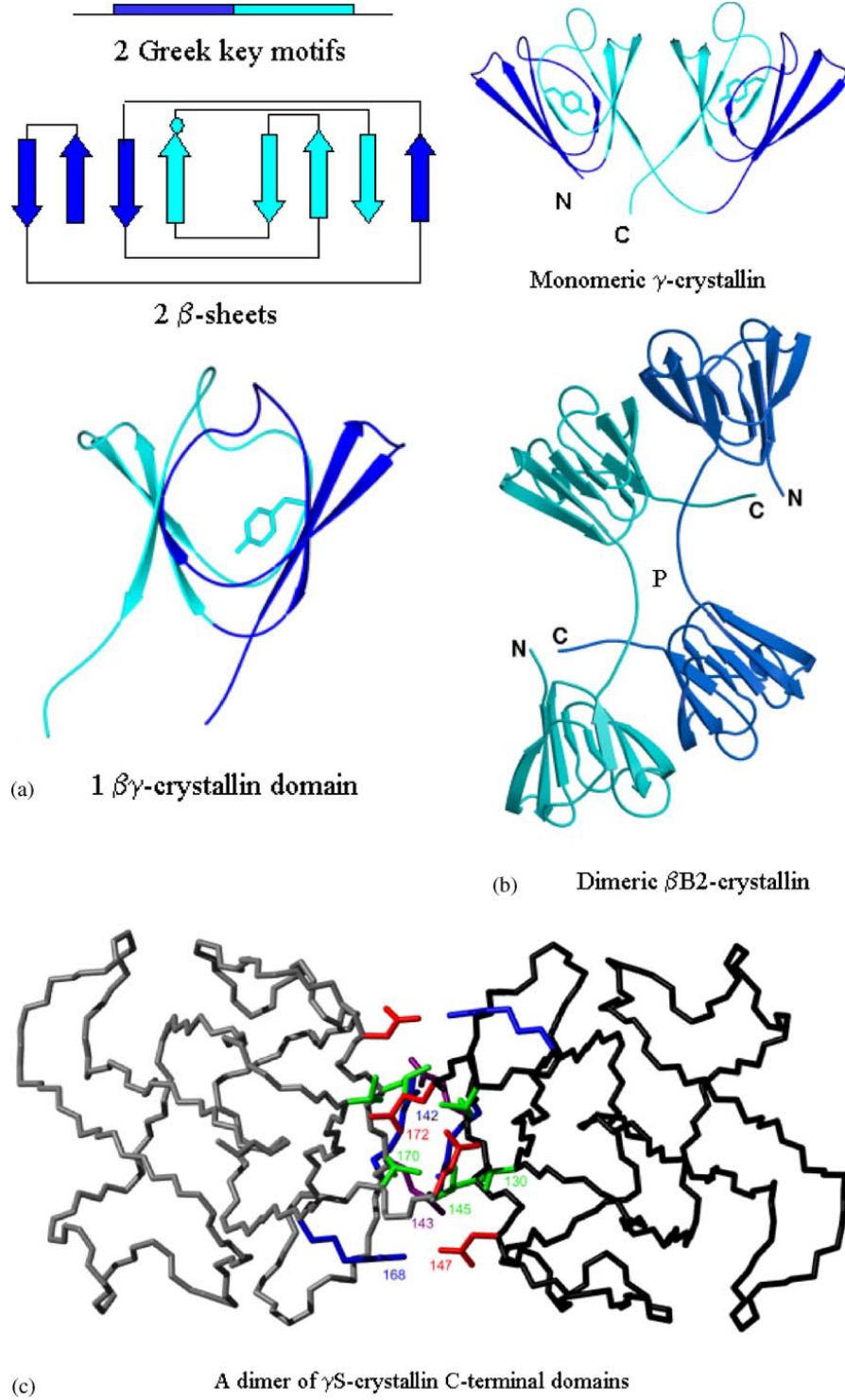
## 2.2. Structure of the two-domain $\beta$ - and $\gamma$ -crystallins

### 2.2.1. The $\beta\gamma$ domain is an independent fold

In protein structure there is a common secondary structural motif called a Greek key, well known from Attic vases (Fig. 6a). This motif of four  $\beta$ -strands is unable to fold on its own (Kretschmar, 1999) and thus requires support, but only rarely is this provided by a direct structural repeat as a result of an ancient gene duplication. A double Greek key represents the common feature in  $\beta\gamma$ -crystallins from eye lens as well as ancient relatives found in microbial organisms. The two consecutive Greek key motifs comprising eight  $\beta$ -strands intercalate to form

---

Fig. 6. The modular structure of the  $\beta\gamma$ -crystallins. (a) Each  $\beta\gamma$ -crystallin domain is made from two linear sequence-related Greek key motifs that intercalate on folding to form two  $\beta$ -sheets. The second motif (shown in turquoise) is more sequence conserved among family members and contains a tyrosine corner positioned between the 3rd and 4th  $\beta$ -strands (indicated by the turquoise filled circle). The two sheets form a compact and pseudo-symmetric  $\beta\gamma$ -crystallin domain. (b) All lens  $\beta\gamma$ -crystallins comprise two domains. In the monomeric  $\gamma$ -crystallins the N- and C-terminal domains pair in a symmetrical manner about an approximate dyad using mainly residues from motifs 2 and 4. In the dimeric  $\beta$ B2-crystallin, the N-terminal domain pairs with the C-terminal domain of the partner subunit, in a process known as domain swapping. (c) The detail of this N and C domain pairing interface is taken from the artificial domain pairing found in the crystal structure of human  $\gamma$ S-C-terminal domain. The heart of the interface is formed mainly by hydrophobic residues from motifs 2 and 4, indicated in green in the alignment in Fig. 3, and some of these are shown here in green. Surrounding this core are polar and charged residues including a conserved glutamine (violet Fig. 3) whose side chain contacts the main chain of the partner domain (based on Fig. 2 from Purkiss et al. (2002) reproduced with permission from Journal of Biological Chemistry).



two  $\beta$ -sheets that pack together to form a  $\beta$ -sandwich domain. Although  $\beta$ -sandwich domains are common in proteins, in  $\beta\gamma$ -crystallins they are characterized by their high internal conformational symmetry and by a conserved folded hairpin structure for each motif. Sequence–structure alignment of all the Greek key motifs shows that two quite distal residues, a glycine and a serine (Fig. 3), are the most conserved and are involved in stabilizing the supersecondary fold by packing this  $\beta$ -hairpin over the  $\beta$ -sheet (Blundell et al., 1981). The double Greek key domain has a complex topology in that each linear 4-stranded motif exchanges its third  $\beta$ -strand to a  $\beta$ -sheet belonging to its partner motif, an essentially cooperative act (Fig. 6a). This theme of mutual exchange is seen at higher levels of the complex hierarchy of  $\beta\gamma$ -crystallins (Fig. 6b; Bax et al., 1990). When the structure is viewed in terms of the two  $\beta$ -sheets forming a  $\beta$ -sandwich or a  $\beta$ -barrel, there are many connections (arches) that cross from one sheet to another and, unlike the jelly roll motif, cannot be conceptualized as folding from a single long  $\beta$ -hairpin (Branden and Tooze, 1998). There is an obvious asymmetry in that only one tyrosine corner is present (Figs. 3 and 6a) (Hemmingsen et al., 1994; Clout et al., 2001).

### 2.2.2. Monomeric two-domain $\gamma$ -crystallins

Rounds of gene duplication of the Greek key motif sequences have resulted in genes encoding two-domain polypeptides which in the case of  $\gamma$ -crystallins form monomers. The X-ray structures of several  $\gamma$ A-F-crystallin family members have been solved now in a variety of crystal lattices, and the N and C domains are always paired in a specific symmetrical manner about a hydrophobic interface (Figs. 3 and 6b). What is clear from the spatial structures is that the pairing appears to mimic an ancestral single domain form that dimerized (Blundell et al., 1981). Protein engineering experiments (detailed later) have since attempted to quantify the contribution of this interface to the energetics of binding and its dependence on the linker. So far only the C-terminal domain of bovine and human  $\gamma$ S-crystallin has been solved by X-ray crystallography (Basak et al., 1998; Purkiss et al., 2002), and therefore only the “artificial” interfaces formed from self-association of the  $\gamma$ S C-terminal domains have been determined (Fig. 6c). However, it can be inferred from modelling studies that  $\gamma$ S-crystallin, apart from a 4-residue N-terminal extension, differs from  $\gamma$ A-F-crystallin mainly in the interface region between the domains. The linker region is one residue longer in  $\gamma$ S-crystallin than in  $\gamma$ B-crystallin, while in the remaining  $\gamma$ -crystallins it is one residue shorter (Fig. 3). The charged residues are paired in a different way from the  $\gamma$ B-crystallin structure, which may be correlated with their specific differences in solvation, phase separation and stability (Cooper et al., 1994b; Zarina et al., 1994; Liu et al., 1996).

It is of interest to compare the sequences and structures of  $\gamma$ -crystallins with low and high phase separation temperatures ( $T_c$ ). However, it has sometimes been difficult to assign the correct sequences to proteins purified from lenses. The best estimate of the current situation is that bovine  $\gamma$ E-, rat  $\gamma$ E-, and bovine  $\gamma$ F-crystallin are high  $T_c$  proteins while bovine  $\gamma$ B-, human  $\gamma$ D-, and bovine  $\gamma$ D-crystallin are low  $T_c$  proteins. When these sequences are aligned (Fig. 3), they do not partition at any single charged position. The 3D structures for these sequences are available (Table 1). As would be expected, they have all crystallized in different lattices and therefore exhibit diverse intermolecular contacts. Although it is clear that in all cases the charged side chains engage in close intramolecular and intermolecular ion pairs, the detail is both sequence- and lattice-dependent.

### 2.3. $\beta$ -Crystallin oligomers

#### 2.3.1. Structure of $\beta$ B2-crystallin

The main sequence difference between monomeric  $\gamma$ -crystallins and oligomeric  $\beta$ -crystallins is the presence of sequence extensions in the oligomers (Fig. 3). The crystal structure of bovine  $\beta$ B2-crystallin focused attention on the linker peptide between the N- and C-terminal domains, and away from the extensions. These were not visualized in the electron density (Bax et al., 1990), were observed to be flexible by 2D NMR (Carver et al., 1993b; Cooper et al., 1993, 1994a) and consequently were judged not to be involved in stabilizing the dimer interface. As depicted in Fig. 6b, there is a close spatial relationship between  $\gamma$ B- and  $\beta$ B2-crystallin. The N- and C-terminal domains are clearly very similar, and in both cases, the domain pairing exhibits pseudo 2-fold symmetry. The distinction between the proteins derives mainly from the linker conformation: in the 21 kDa  $\gamma$ B-crystallin monomer, the V-shaped connecting peptide allows intramolecular domain interactions, whereas in  $\beta$ B2-crystallin the linker is straight, thus favouring quaternary interactions between the dumb-bell shaped 23 kDa subunits (Fig. 6b). As a consequence of the topological similarity of the  $\beta$ - and  $\gamma$ -crystallin domains, their interactions are analogous, except for their *intermolecular* and *intramolecular* character.

At first sight it seemed that the sequence of the linker might be responsible for directing  $\beta$ -crystallin polypeptides into oligomers by domain swapping. For  $\gamma$ B-crystallin, it was proposed that Gly 86 in the interdomain region was critical to allow a V-shaped conformation essential for the monomeric domain paired state. In addition the  $\beta$ - and  $\gamma$ -crystallins had prolines in characteristic sequence positions close to the linker region (Fig. 3). However, exchanging the linker peptides by engineering the  $\beta$ B2- and  $\gamma$ B-crystallin linkers ( $L_{\beta B2}$  and  $L_{\gamma B}$ ) between the  $\gamma$ B- and  $\beta$ B2-crystallin domains challenged the swapping hypothesis as both linker mutants are *monomeric* (Table 3).

The transition of a tertiary interaction in  $\gamma$ -crystallins to a quaternary interaction in a  $\beta$ -crystallin gives an idea how oligomers may have evolved from precursor monomers by using a domain interface either within one and the same polypeptide chain or between two of them (Bax et al., 1990). 3D domain swapping has been proposed as the first stage of a general mechanism for forming oligomeric proteins from their monomeric forms (Bennett et al., 1994, 1995; Schlunegger et al., 1997), with additional stability being gained in a second step through the evolution of a new interface. 3D domain swapping in the  $\beta$ -crystallin example appears to be at the first stage, as the swapped domains are kept at “arms length” by their extended linkers (Fig. 6b). The story of  $\beta$ -crystallin assembly is, however, more complicated and involves a higher order interface observed in the  $\beta$ B2-crystallin crystal lattice structure (Fig. 7). In the  $\beta$ B2-crystallin crystal structure, the pair of subunits, related by a crystallographic dyad (P), is considered to be the solution dimer. In the crystal lattice two such dimers are packed together about 2 further dyads (Q and R). The interface that holds the solution dimer together is defined as the PQ interface (and is centred around equivalent hydrophobic interactions to the two-domain pairing in  $\gamma$ -crystallins; Fig. 3), and the dimer–dimer interface is defined as QR.

#### 2.3.2. Structure of human $\beta$ B1-crystallin

Extensive crystallization trials failed to crystallize full length human  $\beta$ B1-crystallin and therefore the first glimpse came with the 1.4 Å crystal structure of a truncated human

Table 3  
Molecular characteristics of rat  $\beta$ B2-crystallin and  $\beta$ B2-mutants<sup>a</sup>

$\beta$ B2-variant	Residues	$M_{\text{calc}}$ (kDa)	$M_{\text{obs}}$ (kDa)	$s_{20,w}$ (S)	State of association	$c_{1/2,\text{urea}}$ (M)
$\beta$ B2	205 (–16 to 185)	23.38	$42.6 \pm 1.9$	4.23	Dimer	2.6 <sup>b</sup>
$\beta$ B2-N	107 (–16 to 88)	12.03	$19.8 \pm 3.1$	1.85	Dimer <sup>c</sup>	1.2
$\beta$ B2-C	99 (88–185)	11.64	$10.6 \pm 1.0$	1.21	Monomer	2.9
$\beta$ B2 $\Delta_{\text{NC}}$	178 (–1 to 173)	20.50	$38.5 \pm 2.5$	3.42	Dimer	1.7
$\beta$ B2 $\Delta_{\text{NC}}$	178 (–1 to 173)	20.50	$72.2 \pm 2.8$	5.34	Tetramer	1.8
CP- $\beta$ B2	176	20.13	$39.5 \pm 1.8$	3.34	Dimer	2.2
$\beta$ B2-L $_{\gamma\text{B}}$	(cf. Fig. 2)	23.33	$22.0 \pm 1.8$	2.53	Monomer	2.2
$\gamma\text{B-L}_{\beta\text{B2}}$		20.96	$22.5 \pm 2.0$	2.50	Monomer	2.1/5.1 <sup>d</sup>

<sup>a</sup>  $M_{\text{calc}}$  and  $M_{\text{obs}}$ : molecular masses, calculated and taken from ultracentrifugal analysis;  $s_{20,w}$ : sedimentation coefficient; state of association taken from ultracentrifugal analysis and gel permeation chromatography;  $c_{1/2,\text{urea}}$ : transition midpoints of urea denaturation. Data from Trinkl et al. (1994), Mayr et al. (1994, 1997), Norledge et al. (1996, 1997b), Jaenicke (1999), Wieligmann et al. (1998, 1999) and Wieligmann (2000).

<sup>b</sup> Measurements in 0.1 M sodium phosphate pH 7.0 plus 0.3 M ammonium sulfate, 5 mM DTT and 2 mM EDTA. At  $\sim 5 \mu\text{g/ml}$ ,  $\beta$ B2 exhibits concentration-dependent dissociation to partially unfolded monomers; at 200  $\mu\text{g/ml}$ , the dimer–monomer transition shows enhanced cooperativity with  $c_{1/2,\text{urea}} = 2.9 \pm 0.1$ .

<sup>c</sup> At  $< 50 \mu\text{g/ml}$ , dissociation to unfolded monomers according to  $M_2 \rightleftharpoons 2I \rightleftharpoons 2U$ .

<sup>d</sup> Transition midpoints for the C-/N-terminal domains of  $\gamma\text{B}$ .

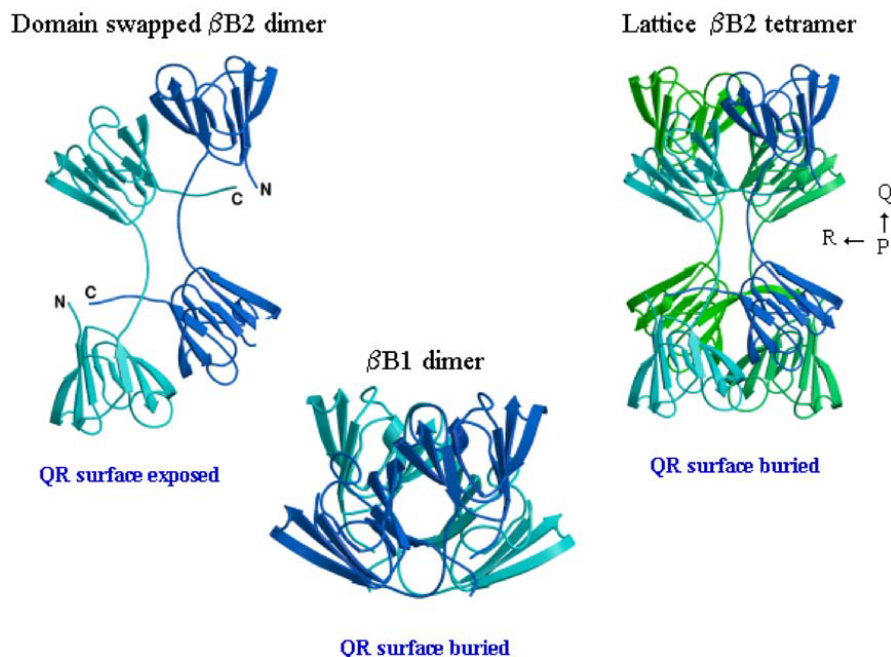


Fig. 7.  $\beta$ B2- and  $\beta$ B1-crystallin assemblies. The domain swapped  $\beta$ B2-crystallin dimer represents the solution dimer. In the crystal lattice there is a strong dimer–dimer interface (defined as the QR interface). The crystal structure of dimeric truncated  $\beta$ B1-crystallin showed that the subunits are engaged in intramolecular domain pairing, as in  $\gamma$ -crystallins, but that the monomer–monomer interface resembled one-half of the QR interface of the  $\beta$ B2-crystallin tetramer.

$\beta$ B1-crystallin (trh $\beta$ B1) which lacks more than the first 41 N-terminal residues (Bateman et al., 2001; van Montfort et al., 2003). The trh $\beta$ B1 monomer, comprising residues 54–236 (corresponding to –4–174 of the topological numbering based on the  $\gamma$ B-crystallin sequence), is composed of the two characteristic  $\beta\gamma$ -crystallin domains, which are connected by a linker that is the same length as in  $\beta$ B2- and  $\gamma$ B-crystallin (Fig. 3). Surprisingly, the N- and C-terminal domains of trh $\beta$ B1 pair in the same intramolecular fashion as in  $\gamma$ -crystallin and the respective linkers have a similar conformation (Fig. 7). The two monomers form a dimer related by an approximate 2-fold axis which is similar to the QR interface of the  $\beta$ B2-crystallin lattice tetramer. The domain arrangement is also similar to that of the engineered circularly permuted rat  $\beta$ B2-crystallin (cp $\beta$ B2) dimer (Wright et al., 1998). The solution dimer of trh $\beta$ B1 is thus similar to the top half of the  $\beta$ B2 lattice tetramer (Fig. 7) and the topology is unlikely to depend on linker sequences or the adjacent conserved prolines (Fig. 3).

### 2.3.3. $\beta$ -crystallin human heterodimers and higher order assembly

Now that expression clones and purification protocols for human  $\beta$ -crystallins are available, the next step in analyzing the complex formation of  $\beta$ -crystallins, namely determining the quaternary level of structure, can be taken. The full-length human  $\beta$ B1-crystallin behaves as a dimer (Lampi et al., 2001), but undergoes further self-association at high protein concentrations (Bateman et al., 2001), unlike  $\beta$ B2-crystallin. The size of the refolded human  $\beta$ A4-crystallin (Bateman et al., 2003) has not been determined but the bovine homolog behaves as a dimer (Slingsby and Bateman, 1990).  $\beta$ A3-crystallin when freshly prepared is a dimer by dynamic light scattering. However, on gel permeation chromatography,  $\beta$ A3-crystallin at pH 5.8 was prone to higher order aggregation even in the presence of a reducing agent. Although similar aggregation behaviour occurs with a calf-rat  $\beta$ A3-crystallin chimera, in the human  $\beta$ A3-crystallin it is more marked. These solution conditions, one pH unit away from physiological, have allowed the trapping of a potential intermediary state involving aggregation before insolubilization. Definition of experimentally accessible soluble non-native states will aid in understanding the conformational changes that crystallins undergo during their long life in the lens.

Selected pairs of homodimers have been shown to subunit-exchange to form hetero-oligomers. Human  $\beta$ A4-crystallin readily oligomerizes with human  $\beta$ B1-crystallin, a hetero-oligomer that can be purified because its pI differs markedly from that of the constituent subunits (Bateman et al., 2003). A truncated version of human  $\beta$ B1-crystallin, which lacks the first six amino acids of the N-terminal arm, formed assemblies with either  $\beta$ A4-crystallin or  $\beta$ A3-crystallin that were larger than heterodimers. The size of this  $\beta$ A3/ $\beta$ B1 $\Delta$ N6-crystallin hetero-oligomer is indicative of a tetramer, but the equilibrium shifts to lower size at lower protein concentration indicative of a tetramer–dimer equilibrium. These results show that the basic  $\beta$ -crystallin can subunit-exchange to form higher order hetero-oligomers with  $\beta$ A3-crystallin, and that the hetero-oligomer is more stable, in terms of resistance to time-dependent aggregation, than the  $\beta$ A3-crystallin homodimer.

Two homodimer models are available for basic  $\beta$ -crystallins, the  $\beta$ B1-crystallin dimer or the  $\beta$ B2-crystallin dimer. It is unknown which arrangement the acidic  $\beta$ -crystallin homodimers take. It is also unknown what sort of heterodimer forms following subunit-exchange of  $\beta$ B2-crystallin homodimer and truncated  $\beta$ B1-crystallin homodimer, in other words which shape is dominant. The  $\beta$ B2-crystallin lattice tetramer serves as a potential model for heterotetramers of domain swapped dimers. The  $\beta\gamma$ -crystallin domain system is thus certainly versatile in terms of domain

assembly and may well have evolved to generate conformational and combinatorial diversity in the oligomeric  $\beta$ -crystallins. Not only might this be a device for inhibiting crystallization at the high protein concentration of the lens, but it could also contribute to forming a range of oligomeric sizes that in turn contributes to providing an even protein distribution and refractive index (Fig. 8).

Although higher assemblies of  $\beta$ -crystallins can be made in vitro, the size reached is not yet as large as the in vivo assemblies. These findings provide an experimental basis to address the role of the N-terminal extension of  $\beta$ B1-crystallin in higher assemblies. Clipping of this extension is associated with disassembly and insolubilization in the human lens. Light scattering indicated dimers at low protein concentration that self-associate as a function of protein concentration. Major truncations from the N-terminal extension lead to anomalous behaviour on gel permeation chromatography and altered solubility indicative of altered interactions (Bateman et al., 2001, 2003; Lampi et al., 2001).

The crystal packing of trh $\beta$ B1 shows that even a truncated form of human  $\beta$ B1-crystallin can contribute to assembly (van Montfort et al., 2003). The trh $\beta$ B1 structure shows Pro 54 stacking against the side chain of Trp 174 (Fig. 3) from a crystallographically related dimer consistent with the region of the N-terminal sequence extension that is adjacent to the domain having a role in higher assembly. Intriguingly, both circular dichroism and fluorescence spectroscopy show that homodimer surface tryptophans become buried in  $\beta$ A3/ $\beta$ A1- $\beta$ B1-crystallin heteromers (Bateman et al., 2003). Therefore dimer–dimer interactions of the N-terminal sequence extension in the trh $\beta$ B1 crystal structure may be typical of more complex higher order molecular weight interactions between basic and acidic  $\beta$ -crystallins in the lens.

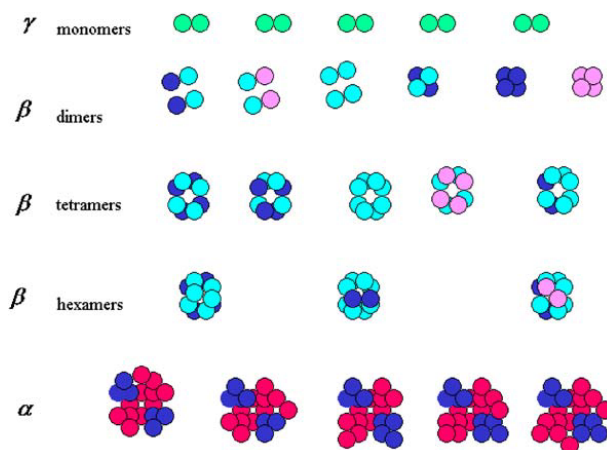


Fig. 8. Structural polydispersity in the lens crystallins. The lens  $\alpha\beta\gamma$ -crystallins constitute an array of differently sized proteins. Although the  $\gamma$ -crystallin family members are individually monodisperse, the oligomeric crystallins have the potential of greater polydispersity. In the case of dimeric  $\beta$ -crystallins, not only is there the potential combinatorial diversity due to the identity of monomer components, but also there is the possibility of conformational diversity generated through use of interface selection in subunit pairing. This diversity can then only be increased in the higher-order  $\beta$ -crystallin assemblies, although little precise information is available about them. In the case of  $\alpha$ -crystallin, not only is there the potential for diversity in the location of the  $\alpha$ A- and  $\alpha$ B-crystallin subunits in the assembly, there is also evidence for variation in the number of assembly subunits. The  $\alpha$ -crystallin cartoon is based on the model of heteromeric lens  $\alpha$ -crystallin by Tardieu and colleagues (Tardieu et al., 1986).

#### 2.4. Microbial relatives and engineered $\beta\gamma$ -crystallins

There are no monomeric single-domain eye lens crystallins in nature. However, there are extremely stable microbial proteins with a double Greek key topology such as SMPI from *Streptomyces* (Ohno et al., 1998) and WmKT from yeast (Antuch et al., 1996), which may be examples of convergent evolution (Clout et al., 1997). There are also ancient family members in the microbial world such as the single domain Spherulin 3a (Wistow, 1990) from *Physarum*, and the two-domain spore coat component known as Protein S (Wistow et al., 1985) from *Myxococcus* which play a role in the organisms' stress response. During stress, such as starvation, the *Physarum* plasmodium divides into dehydrated spherules containing several nuclei that over-express specific proteins, the most abundant being Spherulin 3a (Bernier et al., 1986, 1987). Upon starvation, *Myxococcus* cells differentiate into durable myxospores protected by a multi-layered spore coat containing Protein S (Kaiser et al., 1979; Inouye et al., 1980). These microbial relatives and recombinant single domains of  $\beta\gamma$ -crystallins have been used to address issues concerning evolutionary relationships, oligomeric stability (see later) and solubility (Rudolph et al., 1990; Mayr et al., 1994; Jaenicke, 1999; Wenk et al., 1999, 2000). The microbial relatives are amenable to rigorous thermodynamic characterization (see later) and hence provide a benchmark for the less ideal multi-state behaviour of lens crystallins.

##### 2.4.1. Structure of microbial relatives

NMR and X-ray studies have shown that Protein S comprises two similar domains connected by a short linker with each domain comprised of two similar Greek key motifs, a short  $\alpha$ -helix, and a pair of calcium binding sites (Bagby et al., 1994a–c; Wenk et al., 1999). Each domain has a single tyrosine corner (Fig. 9), and although compared with the lens  $\beta\gamma$ -crystallins the motifs are permuted, the resultant core packing is similar to lens crystallins (Clout et al., 1997). This structural similarity increases the likelihood that they are ancestrally related to the lens

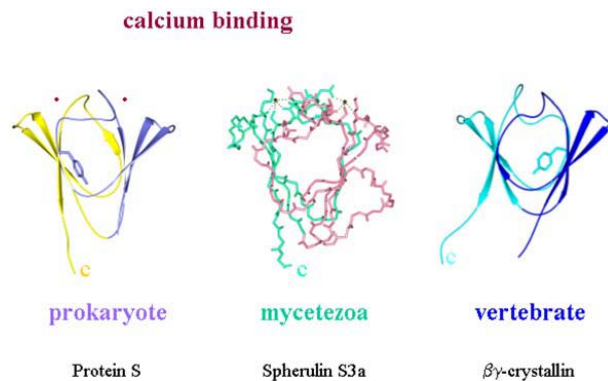


Fig. 9. Comparison of Protein S and Spherulin 3a with the  $\beta\gamma$ -crystallin fold and showing the calcium binding sites. The double Greek key fold in two microbial proteins is very similar to the vertebrate  $\beta\gamma$ -crystallin domain fold. The prokaryote Protein S fold is more similar to that of the vertebrate  $\beta\gamma$ -crystallin domain fold as it includes a tyrosine corner, although the motifs are permuted with respect to each other. The mycetezoa Spherulin 3a fold is more distant from the other two and includes an N-terminal arm that extends one of the  $\beta$ -sheets. However, both microbial proteins have very similar pairs of calcium binding sites that are used to stabilize the fold. Although the Spherulin 3a fold is expressed as a monomer, none of the domains exist in isolation in solution, they domain pair in different ways.

$\beta\gamma$ -crystallins (Clout et al., 2001). The single domain Spherulin 3a protein (Fig. 9) is more distantly related to lens  $\beta\gamma$ -crystallins, it does not have a tyrosine corner but does have an N-terminal arm that extends a  $\beta$ -sheet that is unique to Spherulin 3a (Rosinke et al., 1997). However, the domain comprised a pair of 2-fold symmetric calcium-binding sites (Fig. 9) that were very similar to those found in the N-terminal domain of Protein S (Wenk et al., 1999; Clout et al., 2001). This structural similarity to Protein S supports membership of Spherulin 3a to the  $\beta\gamma$ -crystallin fold family. However, sequence/structure comparisons showed that these calcium-binding sites are not conserved in lens crystallins (Clout et al., 2001), although recent experimental studies have attributed equivalent binding sites to lens  $\beta\gamma$ -crystallins (Rajini et al., 2001).

Higher domain assembly in the microbial proteins is quite different from the lens crystallins. The X-ray crystal structure of Spherulin 3a shows a 2-fold symmetric dimer held together by an extensive interface but different from domain pairing in lens  $\beta\gamma$ -crystallins (Fig. 6b and c) (Clout et al., 2001). No concentration-dependent dissociation of the dimer was observed by ultracentrifugal analysis, indicating that the monomer fold may be dependent on dimerization (Kretschmar et al., 1999a, b). Attempts to construct subdomains from a Spherulin 3a single motif were unsuccessful due to aggregation and/or misfolding and subsequent degradation of the truncated protein (Kretschmar, 1999). In the absence of reducing agents intermolecular cystine bridges lead to the formation of higher oligomers. The X-ray structure shows that they are suitably placed for forming a symmetric tetramer. The two domains in Protein S form an intramolecular interface, but it is non-symmetric and hence quite different from both the  $\beta\gamma$ -crystallin and the Spherulin 3a domain-pairing interfaces.

#### 2.4.2. Engineered single domain and domain-permuted crystallins

The idea that symmetrical domain pairing in  $\beta\gamma$ -crystallins evolved from an ancestral single domain homodimer (Blundell et al., 1981) was supported by the observation that the N-terminal domain of rat  $\beta$ B2-crystallin forms a homodimer in solution (Wieligmann et al., 1999) that resembled the prototype interface (Clout et al., 2000). However, isolated domains of  $\gamma$ B-crystallin (or  $\gamma$ S-crystallin) form neither homodimers nor heterodimers in solution (Mayr et al., 1997); obviously, the domain interactions in the intact two-domain protein require the high local concentrations defined by the short linker peptide. Several of these C-terminal domains can form homodimers in their crystal lattices, thus demonstrating that the interface region of the C-terminal domain is complementary to itself. However, crystallographic studies showed that the complete C-terminal domain of bovine  $\gamma$ B-crystallin (with its four-residue C-terminal extension) forms heterologous interactions with other domains leading to the solvent exposure of the natural interface. On the other hand, this same C-terminal domain, truncated by just the C-terminal tyrosine residue, does form a symmetrical homodimer of domains in the crystal lattice. The correct dimerization is inhibited by the C-terminal tyrosine alone (Norledge et al., 1996). The consequence is that single domains unable to domain pair can decrease in protein solubility from ca. 500 to <10 mg/ml indicating how, at the limit of solubility, misassembly due to wrong domain interactions leads to aggregation, precipitation and sometimes crystallization (Norledge et al., 1996; Mayr et al., 1997).

In following up the hypothesis that the linker between the domains and the extensions at the terminal ends determine the state of association of  $\beta\gamma$ -crystallins, another series of experiments made use of circular permutants of the domains. In these constructs the N- and C-terminal

domains are linked inversely, and the original polypeptide chain clipped at the linker region allowing a stable structure to be formed. In numerous cases, circularly permuted proteins (CP-Ps) have been shown to possess native structure and function (cf. Jaenicke, 1999), proving that vectorial folding from the N- to the C-terminus is not a necessary requirement for correct folding. In designing a circularly permuted  $\beta$ B2-crystallin construct (CP- $\beta$ B2), an attempt was made to mimic  $\gamma$ -crystallin by clipping the linker of  $\beta$ B2 $_{\Delta$ NC, and joining residues 175 and –1. The protein formed a dimer in solution (cf. Table 3). At first sight, this suggested that the intended  $\gamma$ -crystallin like topology was not realized. However, the crystal structure revealed that the native domain-swapped  $\beta$ B2 subunit had converted to intramolecular domain pairing on permutation (Wright et al., 1998) like the crystal structure of truncated human  $\beta$ B1-crystallin (van Montfort et al., 2003). The two  $\gamma$ -crystallin like monomers associate to form a dimer that resembles one half of the native lattice tetramer, and also like the human  $\beta$ B1-crystallin (van Montfort et al., 2003). Urea- and temperature-induced denaturation transitions gave evidence for a slight increase in stability, in keeping with the additional buried domain interfaces. However, ( $c_{1/2,urea}$ ) and  $T_m$  were in no way comparable with the extreme stability limits of bovine  $\gamma$ B-crystallin, thus indicating that the stability in this case does not follow the topology and domain organization, but resides in the individual domains (Wieligmann et al., 1998, 1999).

### 3. Stability of crystallins

Age-related cataract resulting from wrong protein–protein assemblies or associations can be caused by protein unfolding. Understanding crystallin stability, and the effect of post-translational modifications thereon, is a prerequisite for trying to decrease the rate of protein unfolding and thus delay age-related cataract.

#### 3.1. Physical basis of protein stability in dilute solution

The stability of proteins refers to either covalent or conformational changes. Non-covalent denaturation is not necessarily reversible, especially in the case of modular or oligomeric proteins, which are prone to aggregation and coagulation due to wrong interdomain or intersubunit interactions as side-reactions on the folding/association pathway (Jaenicke and Seckler, 1997). To quantify the thermodynamic stability of a given protein, the transition from the native (N) to the denatured (U) state needs to be complete and fully reversible (Pfeil, 1998). If both requirements are fulfilled, the “two-state equilibrium”



allows the free energy of stabilization ( $\Delta G_{stab}$ ) to be calculated according to

$$\Delta G_{stab} = -RT \ln K \quad (2)$$

(with  $R$  is the gas constant,  $T$  the absolute temperature and  $K$  the equilibrium constant). For small, monomeric, single-domain proteins, which usually obey the two-state approximation, the analysis is straightforward. However, for more complex (multi-domain or oligomeric) proteins,

often this is not the case, either because intermediates (*I*) give rise to more than one transition,



or because side reactions, such as misfolding and/or aggregation interfere with the two-state equilibrium



In such cases, *relative* stabilities have often been used to obtain at least qualitative data, e.g. for homologs from different species, or for wild-type and mutant proteins. To give the rank order of stability, here commonly the onset of thermal unfolding or deactivation ( $T_m$ ), or the denaturant concentration at the  $N \rightarrow U$  transition midpoint ( $c_{1/2, \text{urea}}$ ,  $c_{1/2, \text{GdmCl}}$  for urea and guanidinium chloride as chaotropic additives) are used, ignoring reversibility. As shown in Table 4, the denaturation of small standard globular proteins is characterized by a Gibbs free-energy change of the order 40 kJ/mol ( $\sim 10$  kcal/mol); small proteins exhibit even smaller  $\Delta G_{\text{stab}}$  values (cf. data for mesophilic, thermophilic and hyperthermophilic cold-shock protein). Thus, in spite of the large number of non-covalent contacts maintaining the native structure, the free energy of stabilization is minute compared to the total molecular energy (Baldwin and Eisenberg, 1987). It represents a small difference between large numbers, originating from the contributions of attractive and repulsive forces that are responsible for the close packing and the minimization of hydrophobic surface area characteristic for the native state of globular proteins in aqueous solution. In terms of the relevant weak interactions, it is the equivalent of a few hydrogen bonds or hydrophobic interactions, or just one or two ion pairs; with this subtle compensation, it allows the functionally important compromise between rigidity (stability), on the one hand, and flexibility (folding/function/degradation), on the other (for details, see Dill (1990) and Jaenicke (1991a, b, 1999)). Obvious differences in  $\Delta G_{\text{stab}}$  are attributable to different purposes of proteins; for example, structural proteins and proteins from thermophiles need to be more stable than protein hormones or normal mesophilic enzymes involved in metabolic regulation. Evidently, crystallins with their anomalous long-term stability belong to the first category, but still, their free energy of stabilization does not exceed the above range significantly. At this point, examples such as RNase A, lysozyme, Spherulin 3a, and myoglobin illustrate that changes in net charge, or ligand binding may strongly effect the free energy of stabilization (Privalov, 1979, 1982, 1992; Pfeil, 1998; Kretschmar and Jaenicke, 1999; Wenk et al., 2000).

The fact that proteins exist close to the borderline of denaturation does not allow general strategies of protein stabilization to be formulated (Böhm and Jaenicke, 1994; Jaenicke and Böhm, 1998). As a state function,  $\Delta G_{\text{stab}}$  is additive. According to the Gibbs–Helmholtz equation

$$\Delta G_{\text{stab}} = \Delta H_{\text{stab}} - T\Delta S_{\text{stab}}, \quad (5)$$

it is composed of enthalpic and entropic contributions attributable to weak interactions, on the one hand, and water release (from ionized and non-polar residues) or changes in the rotational

Table 4  
Stability parameters of selected globular proteins in aqueous solution<sup>a</sup>

Protein <sup>b</sup>	Number of residues	<i>N</i>	Molecular mass (kDa)	pH	<i>T</i> <sub>m</sub> (°C)	Δ <i>G</i> <sub>stab</sub> (kJ/mol)	Denaturation approach
<i>Monomers</i>							
CSP ( <i>B. subtilis</i> )	67	1		7.0	50	11.1±0.5	G, heat, kinetics
Cytochrome <i>c</i> (B) (chicken)	104	1	12.4	6.5		35.1 32.1	G G
Barnase	110	1	12.4	6.3		36.9±1.7	U
Staphylococcal nuclease	149	1	16.7	7.0		23.4±0.2	G (20°C)
<i>Oligomers</i>							
MDH (mitochondrial)		2	70	7.5		15.1/19.2	(2 transitions, G)
GroEL ( <i>E. coli</i> )		14		7.8		13.3±1.3/ 54.6±6.4	U
<i>Effect of net charge</i>							
Ribonuclease A	124	1	13.7	3.0 3.5 6.0 7.0 8.5		18.7±0.9 24.2±1.6 36.9±2.2 38.7±1.3 38.9±2.8	G G G G G
Lysozyme (hen egg white)		1	14.4	0.64 2.03 6.0-7.0		11.4±0.5 17.1±0.8 36.0±3.0	G G G
α-Chymotrypsin		1	21.6	4.0-7.0		50.0±1.5	G
<i>Effect of ligands</i>							
Myoglobin (horse) (Apo-Mb)	153	1	16.9	7.0		44.8±3.8 ~10	G, U, acid G, U, acid
Spherulin 3a (C4S) (+ 3 mM Ca <sup>2+</sup> )	103	2	22.4	7.0	53 69	81 137	G, U, acid
<i>Effect of fragmentation</i>							
Thermolysin	316	1	34.2	7.0	87	55	G, heat
(121–316 fragment)		1	20.9	7.0	74	47	G, heat
(225–316 fragment)		1	9.56	7.0	65	26	
γS-Crystallin (H)	177	1	21.5	7.0	75 <sup>c</sup>	84±10 <sup>c</sup>	G, heat, DSC
(N-terminal domain)	90	1	10.5	7.0		42±5 <sup>c</sup>	G, heat, DSC
(C-terminal domain)	87	1	10.4	7.0		48±5 <sup>c</sup>	G, heat, DSC
<i>Proteins from mesophiles and thermophiles</i>							
CSP							
( <i>B. subtilis</i> )	67	1	7.0	50		11.1±0.5	G, heat
( <i>B. caldolyticus</i> )	66	1	7.0	72		20.4±0.9	G, heat
( <i>T. maritima</i> )	66	1	7.0	85		26.9±1.2	G, heat

Table 4 (continued)

Protein <sup>b</sup>	Number of residues	<i>N</i>	Molecular mass (kDa)	pH	<i>T<sub>m</sub></i> (°C)	$\Delta G_{\text{stab}}$ (kJ/mol)	Denaturation approach
<b>DHFR</b>							
( <i>E. coli</i> )		1	17.6	7.8		27 ± 3	U
( <i>T. maritima</i> )	169	2	38.4	7.8		142 ± 10	G, U (15°C)
<b>PGK</b>							
( <i>S. cerevisiae</i> )	415	1	43.2	7.0		20.6 ± 2.0	G
(Horse)				7.4		25.0 ± 2.0	G
( <i>Thermus therm.</i> )				7.5		49.7 ± 0.9	G
( <i>T. maritima</i> )				7.0	100	106 ± 10	G, heat
<b>Crystallins</b>							
$\alpha$ -Crystallin				7.4		25 ± 5	DSC
$\gamma$ B-Crystallin (B)	174	1	21.0	2.0	55/48 <sup>d</sup>		DSC
$\gamma$ S-Crystallin (H)	177	1	21.5	7.0	75	84	G, heat, DCS

<sup>a</sup> Number of residues refers to the length of the polypeptide chain, *n* to the state of association in the native state, *T<sub>m</sub>* to the midpoint of thermal transition, and  $\Delta G_{\text{stab}}$  to the Gibbs free energy of stabilization. If not stated otherwise, data refer to 25°C. Denaturation approaches: Unfolding accomplished by guanidinium chloride (G), urea (U), thermal denaturation (heat), or by differential scanning calorimetry (DSC).

Thermodynamic data taken from Vita et al. (1989), Perl et al. (1998), Pfeil (1998), Dams and Jaenicke (1999), Kretschmar (1999), Kretschmar and Jaenicke (1999), Kretschmar et al. (1999a, b) and Wenk et al. (2000).

<sup>b</sup> Proteins: CSP, cold-shock protein from *Bac. subtilis*, *Bac. caldolyticus*, and *Thermotoga maritima*;  $\gamma$ B and  $\gamma$ S-crystallin from bovine (B) and human (H) eye lens; DHFR, dihydrofolate reductase from *E. coli* and *Thermotoga maritima* (mesophilic monomer vs hyperthermophilic dimer); lysozyme from hen egg-white (EW); MDH, malate dehydrogenase from pig; Mb, myoglobin from horse, with and without (apo-Mb) its heme group; PGK, phosphoglycerate kinase from yeast, horse, *Thermus aquaticus*, and *Thermotoga maritima*; protein S (Protein S) from *Myxococcus xanthus*; Spherulin 3a (cys→ser mutant) from *Physarum polycephalum*; thermolysin from *Bac. thermoproteolyticus* (complete molecule and two C-terminal fragments, illustrating the incremental nature of  $\Delta G_{\text{stab}}$ , cf. Vita et al., 1989).

<sup>c</sup> Zero net charge at pH 7 allows cooperative N ↔ U transition of both domains to be monitored. Correcting  $\Delta G_{\text{stab}}$  for the molecular masses of  $\gamma$ S,  $\gamma$ S-N and  $\gamma$ S-C yields  $\Delta G^* = 4.2 \pm 0.3$  J/g.

<sup>d</sup> Bimodal transition of N- and C-terminal domain in intact  $\gamma$ B-crystallin (cf. Rudolph et al., 1990).

and translational degrees of freedom (proline/glycine substitutions, deletion of loops, altered states of oligomerization), on the other. Details regarding the increments have been worked out for ultrastable proteins from hyperthermophiles (Jaenicke and Böhm, 2001; Petsko, 2001; Jaenicke and Sterner, 2002).

Apart from the free energy differences between N and U, a high free energy of activation ( $\Delta G_{\text{N} \rightarrow \text{U}}^\ddagger$ ) along the N → U unfolding pathway may govern protein stability as a consequence of a decreased unfolding rate (“kinetic stabilization”). If the reaction mechanism does not show full reversibility (Eqs. (3) and (4)), the overall kinetics may be modelled by



with I as a partially unfolded intermediate, and  $k_{N \rightarrow I}$ ,  $k_{I \rightarrow N}$  and  $k_{I \rightarrow U}$  as rate constants for the respective reversible and irreversible transitions. Now, the observed rate of the overall process  $k_{\text{obs}} = (k_{N \rightarrow I} \cdot k_{I \rightarrow U}) / (k_{I \rightarrow N} + k_{I \rightarrow U})$  is determined by the rate of partial unfolding ( $k_{N \rightarrow I}$ ), since only I undergoes irreversible denaturation to U. Obviously, for the long-term stability of eye lens crystallins, i.e. for lens transparency, the kinetic stability of N may be highly significant, because low unfolding rates under physiological conditions keep the level of unfolded protein low, this way minimizing irreversible processes such as chemical modification and subsequent aggregation. Kinetic barriers to unfolding have indeed been suggested for bovine  $\gamma$ F-crystallin and human  $\gamma$ D-crystallin (Das and Liang, 1998; Kosinski-Collins and King, 2003). In the case of Spherulin 3a, reversible unfolding experiments have shown that in the presence of  $\text{Ca}^{2+}$  unfolding is slowed down by an order of magnitude; the free energy of stabilization of unliganded and liganded Spherulin 3a was found to be 80 and 140 kJ/mol, respectively (Kretschmar et al., 1999b).

In concentrated protein solutions, there are two further kinetic effects in connection with protein stability. Firstly, there is the kinetic competition between folding and assembly of either subunits or domains according to Eq. (4), and secondly, effects of viscosity and crowding (cf. Section 3.2). The formation of the native quaternary structure as well as proper docking of domains requires complementary interfaces formed in precursor reactions preceding association. Collisions of intermediates with internal residues on their periphery are expected to cause misassembly, i.e. aggregation, precipitation into inclusion bodies, amyloid formation, etc. (Jaenicke and Seckler, 1997). It is within this context, whereby  $\beta\gamma$ -crystallins are formed from multi-domain monomers and oligomers, and  $\alpha$ -crystallin is constructed from a domain whose fold and stability is dependent on higher assembly, that “kinetic partitioning” causes many of the crystallins to aggregate irreversibly on unfolding. Although these characteristics hinder their measurement of free energy of stabilization and make them challenging molecules for understanding the molecular origins of their stability, they are likely responsible for crystallin aggregation with time in the lens. Insights into this aggregation process may lead to its inhibition in the lens.

### 3.2. Stability in the cell, macromolecular crowding

Protein folding/unfolding has been reported to be viscosity dependent (Bieri and Kiefhaber, 2000). In the corresponding in vitro studies, it is difficult to separate effects of friction from the stabilization caused by viscogenic additives (e.g. sucrose or other polyols). However, performing experiments at constant protein stability showed clearly that both the rates of unfolding and folding are viscosity dependent (Jacob, 2000). Considering the viscosity of highly concentrated cytosol in the eye-lens fibre cells, one would predict that the native state of crystallins in situ may also be favoured by *friction-induced kinetic stabilization*. Further stabilization may come from *macromolecular crowding*, as a consequence of excluded-volume effects at high protein concentration. A general view of *excluded-volume effects* on reactions that lead either to protein assembly or aggregation has recently been given by Minton (2000a). At the given high protein level, in which the different macromolecular species occupy a large fraction of the total volume of the solution, crowding may affect a wide variety of reactions: (i) Folding and association of proteins (Jaenicke, 1996, 1998), (ii) binding of folding/unfolding intermediates to molecular chaperones, e.g.  $\alpha$ -crystallin (Horwitz, 1992; Carver et al., 1994a; Ehrnsperger et al.,

1998; van den Berg et al., 1999, 2000; Berr et al., 2000), (iii) reversible binding of folding intermediates to (non-chaperone) proteins, (iv) as a consequence of (iii), self-assembly of homo- or hetero-oligomers and multimers (Lindner and Ralston, 1995, 1997; Liu et al., 1996; Rivas et al., 1999), (v) irreversible aggregation of misfolded proteins to form large particles (Wilf et al., 1985; Jaenicke and Seckler, 1997; Lansbury, 1999; Dobson, 1999), and finally, (vi) assembly of proteins to membranes, e.g. of fibre cells. In the various processes, interactions may be individually weak, however, the cumulative effect may be significant in a crowded environment, for the simple reason that steric repulsion by excluded volume effects reduces the configurational entropy. This, in turn, increases the Gibbs free energy of the solution and, hence, stabilizes the native structure of globular proteins relative to less compact non-native structures (Tellam et al., 1983; Minton, 2000a, b). At the upper limit of solubility, where phase separation may take place, “overcrowding” may enhance aggregation reactions of non-native proteins, leading to increased light scattering. Apart from thermodynamic stabilization, volume exclusion in crowded solutions may also reduce the rates of diffusion-controlled reactions as a consequence of decreased diffusional mobility of the reactants. On the other hand, high protein levels have been shown to enhance both the tendency and the rate of protein aggregation (Jaenicke, 1987; Jaenicke and Seckler, 1997; Minton, 2000a, b; Jaenicke and Slingsby, 2001).

Protein components taken out of the cell and purified to homogeneity, often exhibit drastic destabilization compared to their *in vivo* characteristics. Apart from the above friction-dependent and macromolecular crowding effects on stabilization, *extrinsic factors* such as ions, cofactors or substrates as well as *compatible solutes* need to be considered as well. Typical compatible solvent components are proline, glycerol or other polyhydric compounds. Their stabilizing effects are linked to the preferential hydration of proteins, due to non-specific interactions related to the perturbation of the solvent structure in contact with the protein surface. The predominant mechanism is an increase in the surface tension of water by the osmolyte; the system reacts by maintaining a minimal total protein–solvent interface, corresponding to maximal hydration and a deficiency of cosolvent in the protein surface (Carpenter et al., 1993; Timasheff and Arakawa, 1997; Knapp et al., 1999).

### 3.3. Stability of $\alpha$ -crystallin

Native (bovine)  $\alpha$ -crystallin when isolated from the lens is a polydisperse hetero-assembly containing about 40 subunits of  $\alpha$ A- and  $\alpha$ B-crystallin in a ratio of 3 to 1 (for review, see Horwitz, 2003). Homotypic  $\alpha$ A- or  $\alpha$ B-crystallin, prepared from recombinant proteins or following reassembly of one type of subunit after purification from disaggregated lens  $\alpha$ -crystallin, assemble into smaller homo-oligomers of about 30–35 subunits with, for  $\alpha$ B-crystallin, a dominant species of 28 subunits (Aquilina et al., 2003).  $\alpha$ -Crystallin can be readily denatured by heat, urea or GdmCl, following pathways that include both changes in the secondary structure and the state of assembly but, not surprising given the complexity of the  $\alpha$ -crystallin assembly, both assembly size and chaperone properties of renatured  $\alpha$ -crystallin differ from native  $\alpha$ -crystallin (Doss-Pepe et al., 1998; Putilina et al., 2003). Upon heating, both infrared and circular dichroism spectroscopy showed that  $\alpha$ -crystallin undergoes a thermal transition around 61°C (Surewicz and Olesen, 1995; Das et al., 1997; Raman and Rao, 1997). It was shown later on that in addition to the local changes,  $\alpha$ -crystallin doubles in size and number of subunits around 60°C but does not aggregate

further (Burgio et al., 2000; Putilina et al., 2003). When separate subunits are used,  $\alpha$ A-crystallin also remains soluble up to 100°C but  $\alpha$ B-crystallin starts to precipitate around 65°C (Sun et al., 1998; van Boekel et al., 1999; Liang et al., 2000). The observation that some  $\alpha$ -crystallins do not precipitate under severe stress conditions is consistent with the notion that the  $\alpha$ A subunit in particular can bind and hence chaperone itself (see Section 7).

As followed by fluorescence emission, bovine  $\alpha$ -crystallin is 50% unfolded at approximately 1 M GdmCl (Santini et al., 1992; Das and Liang, 1997; Table 5). However, as  $\alpha$ A-crystallin contains only a single Trp (at position 9) and  $\alpha$ B-crystallin contains only two (at positions 9 and 60), fluorescence emission would only report on the unfolding of the N-terminal region. It is thus not surprising that difference absorbance at 287 nm or far-UV CD measurements indicate that  $\alpha$ -crystallin only unfolds at a higher GdmCl concentration, with 50% loss of structure at about 1.5 M GdmCl (Das and Liang, 1997) or 2.6 M GdmCl (Santini et al., 1992). Urea denaturation showed less difference between the physical techniques used to follow unfolding: fluorescence spectroscopy showed  $\alpha$ -crystallin to be 50% unfolded at about 2.9 M urea (van den Oetelaar and Hoenders, 1989a; Santini et al., 1992), while difference absorbance at 287 nm gave a value of about 3.2 M urea (Santini et al., 1992). In these experiments only a single transition was seen, yet the stabilities of  $\alpha$ A- and  $\alpha$ B-crystallin have been reported to be quite different. In urea, bovine  $\alpha$ B-crystallin was 50% unfolded at about 1 M while for bovine  $\alpha$ A-crystallin about 3 M was required (as indicated by Trp fluorescence, van den Oetelaar and Hoenders, 1989a). Using GdmCl as denaturing agent, the  $\Delta G$  for human  $\alpha$ A-crystallin was reported to be around 27 kJ/mol and that for  $\alpha$ B-crystallin 21 kJ/mol (Sun et al., 1999). Carver et al. (1993a) have probed the stability of the (bovine)  $\alpha$ A- and  $\alpha$ B-crystallin using NMR. The C-terminal domain of  $\alpha$ B-crystallin started unfolding at 2.5 M urea, the N-terminal domain only at 4.0 M urea. For unfolding of the C-terminal domain of  $\alpha$ A-crystallin 4 M urea (at pH 3.9) is required. Hence, most data indicate that  $\alpha$ B-crystallin is less stable than  $\alpha$ A-crystallin and that this protein is stabilized in the  $\alpha$ -crystallin assembly by its interaction with  $\alpha$ A-crystallin (Sun and Liang, 1998).

Studies on the stability and/or chaperone properties of  $\alpha$ -crystallin have used either bovine lens  $\alpha$ -crystallin or human recombinant  $\alpha$ A- or  $\alpha$ B-crystallin. At present there is no evidence that human  $\alpha$ -crystallin behaves significantly different from its bovine ortholog or from the individual subunit assemblies. Nevertheless, caution should be taken in extrapolating data obtained with bovine  $\alpha$ -crystallin to human  $\alpha$ -crystallin. Human  $\alpha$ A-crystallin differs at eight positions from bovine  $\alpha$ A-crystallin (A4T, E91D, S142C, P147Q, S148T, G153T, S155A, S168T; notation is for bovine  $\rightarrow$  human); human  $\alpha$ B-crystallin at four (A40T, I61F, A132T, A152V). It is clear that in other crystallins, for example  $\gamma$ S- or  $\beta$ B2-crystallin, seemingly innocuous changes in amino acid sequence can result in marked differences in stability: human  $\gamma$ S-crystallin is more stable than bovine  $\gamma$ S-crystallin; human  $\beta$ B2-crystallin aggregates upon thermal denaturation, bovine  $\beta$ B2-crystallin does not (see below). Caution should be taken as well in extrapolating data obtained with homotypic oligomers of  $\alpha$ A- or  $\alpha$ B-crystallin to the heteromeric native lens  $\alpha$ -crystallin.

### 3.4. Stability of the $\beta$ - and $\gamma$ -crystallins

The unfolding of the  $\beta$ - and  $\gamma$ -crystallins is most easily monitored by fluorescence. The  $\gamma$ -crystallins have a total of four buried Trp residues, two in motif 2 and two at equivalent

Table 5  
Stability of crystallins<sup>a</sup>

Protein	$C_{1/2,urea}$ (M)	$C_{1/2,GdmCl}$ (M)	$\Delta G$ (kJ/mol)	$T_m$ (°C)	
$\alpha$ (bovine)	3.2	1.5–2.6		61	Not reversible
$\alpha A$ (human)			27		Reversibility not demonstrated
$\alpha B$ (human)			21		Reversibility not demonstrated
$\beta A1$ (human)	3.8				
$\beta A3$ (human)	3.4				
$\beta A1$ (calf/rat)	3.4				
$\beta A3$ (calf/rat)	3.4				
$\beta A4$ (human)	4.7				Renatured protein
$\beta B1$ (human)	5.9			67	
$\beta B1$ (human) N-terminal domain	4.9		51		Measured in the full length protein using a spin label
$\beta B2$ (human)		1; 2.2	49		Bimodal transition, Reversibility not demonstrated
$\beta B2$ (rat)	2.6	0.8 (at pH 6.0)			Folding not reversible
$\gamma B$ (bovine)	2.1/5.1 (at pH 2.0)	2.6 (at pH 6.0)		55/48 (at pH 2.0)	Bimodal transition N- and C-terminal domains
$\gamma C$ (human)		2.3	36		Reversibility not demonstrated
$\gamma D$ (human)		3.7		43 (at pH 2.0)	Folding not reversible at 25°C
$\gamma F$ (bovine)	3.7 (in 1.5 M GdmCl)	3	35		Reversibility not demonstrated
$\gamma S$ (human)	8.0	2.6	84	75	
$\gamma S$ (human) N-terminal domain			42		
$\gamma S$ (human) C-terminal domain			48		
$\gamma S$ (bovine)	7.0	2.1			

<sup>a</sup>The transition midpoints for urea, GdmCl or thermal denaturation are indicated as well as the Gibbs free energy ( $\Delta G$ ) where known. For references, see legends to Tables 3 and 6 and van den Oetelaar and Hoenders (1989a), Santini et al. (1992), Mayr et al. (1994), Trinkl et al. (1994), Werten et al. (1996), Das and Liang (1997, 1998), Sun and Liang (1998), Wieligmann et al. (1998, 1999), Pande et al. (2000), Wieligmann (2000), Fu and Liang (2002), Kim et al. (2002), Bateman et al. (2003) and Kosinski-Collins and King (2003).

positions in motif 4 (Fig. 3). The  $\beta$ -crystallins also contain Trp residues at the same motif 2 and 4 positions (except for  $\beta B2$ -crystallin where the second Trp in motif 4 has been replaced by a Phe) but they also have Trp residues at more exposed positions in the motif fold and even in the C-terminal extension. In those cases where protein unfolding has also been followed by the change in CD spectrum, a good agreement with stability measurements obtained by following changes in Trp fluorescence was found (Das and Liang, 1998; Wenk et al., 2000; Fu and Liang, 2002; Kim et al., 2002).

A survey of data concerning stability of the  $\beta$ - and  $\gamma$ -crystallins (and, for comparison,  $\alpha$ -crystallins) culled from the literature is presented in Table 5. These data should be interpreted with caution as stability measures are dependent upon the experimental conditions (pH, ionic

strength, temperature and protein concentration) which may differ between laboratories. For instance, the literature data suggest that human  $\beta$ B2-crystallin is more stable than the rat  $\beta$ B2-crystallin, yet a direct comparison of the urea denaturation of these two proteins showed identical behaviour (unpubl. results). Furthermore, as argued above, for thermodynamic calculations reversible denaturation needs to be shown; this was found to be a problem in the case of dimeric rat  $\beta$ B2-crystallin (Jaenicke, 1999), bovine  $\gamma$ B-crystallin (Rudolph et al., 1990) and human  $\gamma$ D-crystallin (Kosinski-Collins and King, 2003). The latter protein did fold reversibly in above 1 M GdmCl, neutral pH and 37°C, with aggregation into fibrils competing with refolding at lower chaotrope concentration (Kosinski-Collins and King, 2003). In general, these data show that the  $\gamma$ -crystallins are more stable than the  $\alpha$ - and  $\beta$ -crystallins, with  $\gamma$ S-crystallin probably less stable than the other branch of  $\gamma$ -crystallins given the conditions required for denaturation of the  $\gamma$ A-F-crystallins.

With respect to the stability of the  $\beta$ -crystallins it must be remembered that, except for  $\beta$ B2-crystallin which is found in the lens as a homodimer, these proteins are taken out of context, as they naturally occur as heteromers. The stabilization of  $\beta$ -crystallins by heterodimerization is evident from the fact that both  $\beta$ B1- and  $\beta$ A3-crystallin tend to aggregate while the  $\beta$ A3/ $\beta$ B1-crystallin hetero-oligomer is stable (Bateman et al., 2001, 2003). The effect of  $\beta$ -crystallin hetero-oligomer formation on thermodynamic stability has not yet been systematically explored. One of the experimental problems encountered is the difference in fluorescence yield from the different  $\beta$ -crystallins upon denaturing, which for example makes it impossible to detect the signal from  $\beta$ A4-crystallin in the context of the  $\beta$ A4/ $\beta$ B1-crystallin hetero-oligomer. In the case of the  $\beta$ A1/ $\beta$ B1-hetero-oligomer, clear stabilization of the  $\beta$ A1-crystallin was seen. CD spectra of this hetero-oligomer suggested that hetero-oligomer formation was accompanied by a change in secondary structure (Bateman et al., 2003). For three crystallins, bovine  $\gamma$ B-crystallin, human and bovine  $\gamma$ S-crystallin and rat  $\beta$ B2-crystallin extensive experiments have been undertaken to determine the contribution of domain stability and domain interaction to the stabilities of these proteins. These results will be discussed in more detail below.

#### 3.4.1. $\gamma$ B-crystallin

Intact bovine  $\gamma$ B-crystallin requires complete protonation and high concentrations of chaotropic agents to accomplish denaturation.  $\gamma$ B-Crystallin preserves its native structure at pH 1–10; in 0.1 M phosphate, at pH 7, it is stable up to 75°C and, even at pH 2, to reach the unfolded state requires exceedingly high urea concentrations (Fig. 10a, upper frame). Thermal denaturation beyond the given temperature limit is only partially reversible so that calorimetry does not allow thermodynamic data to be determined (Rudolph et al., 1990). At pH 2 a three-state  $N \rightleftharpoons I \rightleftharpoons U$  unfolding mechanism is found, in which in the intermediate the C-terminal domain is unfolded while the N-terminal domain remains in its native state (Rudolph et al., 1990). At pH 2 the free energies of the N- and C-terminal domains are found to be 5 and 16 kJ/mol, respectively (Mayr et al., 1997). This difference is explained by the difference in net-charges: both have an equal number of acidic and basic residues, however, in the C-terminal domain the total number is higher. The resulting charge difference of +3 is responsible for the difference in stability. At pH 4–7, the charge difference, and thus the population of the intermediate, becomes negligible (Fig. 10a, lower frame).

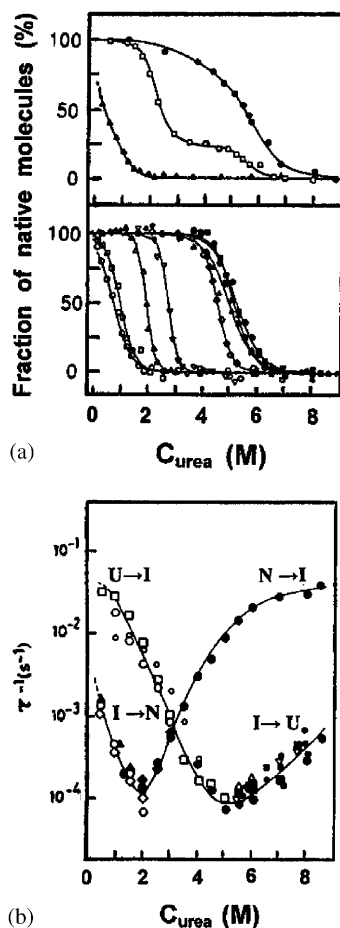


Fig. 10. Urea-dependent equilibrium unfolding of bovine  $\gamma$ B-crystallin and its isolated domains  $\gamma$ B-N and  $\gamma$ B-C (with permission, Rudolph et al., 1990; Mayr et al., 1997). (a) Comparison of intact  $\gamma$ B and its isolated N-terminal (closed symbols) and C-terminal domains (open symbols). *Upper frame*:  $\gamma$ B ( $\square$ ),  $\gamma$ B-N ( $\bullet$ ) and  $\gamma$ B-C ( $\blacktriangle$ ) in 0.1 M NaCl/HCl pH 2.0, 20°C, monitored by fluorescence emission. *Lower frame*:  $\gamma$ B-N at pH 2.0 ( $\blacktriangle$ ), pH 3.0 ( $\blacksquare$ ), pH 4.0 ( $\bullet$ );  $\gamma$ B-C at pH 2.0 ( $\circ$ ), pH 2.5 ( $\square$ ), pH 3.0 ( $\triangle$ ), pH 3.5 ( $\nabla$ ), pH 4.0 ( $\diamond$ ) at 1  $\mu$ M protein concentration in 100 mM NaCl/HCl, Gly/HCl and 60 mM formate buffer, 20°C. (b) Rates of unfolding/refolding at 0.2 mg/ml, in 0.1 M NaCl/HCl pH 2.0, 20°C, monitored by fluorescence emission of native  $\gamma$ B at 360 nm (unfolding  $\bullet$ , folding  $\circ$ ), 320 nm (unfolding  $\blacksquare$ , folding  $\square$ ), GPC/FPLC (unfolding  $\blacklozenge$ , folding  $\diamond$ ); fluorescence emission of intermediate (I) at 360 nm (unfolding  $\blacktriangle$ , folding  $\triangle$ ) and 320 nm (unfolding  $\nabla$ ). Fluorescence emission of  $\gamma$ B-N at 360 nm (unfolding  $\bullet$ , folding  $\circ$ ) and 320 nm (unfolding  $\blacksquare$ ); 1  $\mu$ M protein concentration, 20°C. For intact  $\gamma$ B-crystallin at pH 2, both the bimodal unfolding equilibrium transition (in the upper frame of a), and the crossing point in the chevron plots of the corresponding kinetics (in b) confirm the three-state unfolding/folding mechanism  $N \rightleftharpoons I \rightleftharpoons U$  (Eq. (3)).

Unfolding experiments showed that for the isolated domains less stringent pH conditions are required for denaturation, confirming the correlation between the local charge distribution and domain stability, on the one hand, and the contribution of domain pairing to the intrinsic stability of the intact two-domain protein, on the other (Fig. 10a). The interaction and mutual stabilization of domains depend on their close proximity, illustrating the significance of the *local concentration* of the interacting modules (Jencks, 1969; Kirby, 1980). The importance of the spatial and

chemical complementarity of the interacting surfaces may be illustrated by point mutations in the domain interface in intact  $\gamma$ B-crystallin, in which hydrophobic residues make van der Waals contacts with each other (Palme et al., 1997, 1998a, b). A demonstration of the linker length on stabilization was provided by a circular permutation experiment in which the choice of the clipping sites allows the local concentration and the correct interaction of the domains to be optimized. In the case of  $\gamma$ B-crystallin, circular permutation was accomplished by deleting Gly 86 in the original linker, and by changing Thr 87 and Thr 85 into the new N- and C-termini; triglycine and pentaglycine were inserted as connectors (Table 6, upper part). Both constructs, CP- $\gamma$ B(G<sub>3</sub>) and CP- $\gamma$ B(G<sub>5</sub>), were found to be monomeric, showing identical equilibrium unfolding transitions, with no effects of the local domain concentration and no indication for hydrophobic docking of the domains. Instead, the transitions resembled the superimposed transitions of the separate N- and C-terminal domains of the parent molecule.

#### 3.4.2. $\gamma$ S-crystallin

In human  $\gamma$ S-crystallin the charge difference between the two domains at low pH is negligible. As a consequence, chaotropic agents induce reversible two-state N  $\leftrightarrow$  U equilibrium transitions without detectable amounts of the “tailed one-domain intermediate”. This holds over a wide temperature and pH range, allowing a detailed thermodynamic analysis (Wenk et al., 2000). Interestingly, bovine and human  $\gamma$ S-crystallin and their isolated domains, in spite of their high structural homology, differ in their free energies of stabilization and their tendency to form *nicked*  $\gamma$ S, i.e. heterodimers of the isolated domains (Table 6, lower part). Since the 3D structure of the complete protein is still unknown, no rationale for the differences can be given. In summarizing presently available data,  $\gamma$ S- and  $\gamma$ B-crystallin differ in their structurally and thermodynamically relevant characteristics at three levels: (i) the length of the connecting peptides, four in  $\gamma$ B-crystallin, five in  $\gamma$ S-crystallin, (ii) the distribution of ion pairs on the surface of the two molecules, and (iii) the interactions at the interfaces between the domains. In the case of  $\gamma$ B-crystallin, the latter prevent a sound thermodynamic analysis; for  $\gamma$ S-crystallin and its isolated domains this was accessible. The results show that, in spite of the fact that we are dealing with “ultrastable proteins”, the free energy of stabilization is marginal:  $\Delta G_{\text{stab}}$  for intact  $\gamma$ S-crystallin and its N- and C-terminal domains amounts to 84, 42 and 48 kJ/mol, respectively. Correcting for the molecular mass, all three values coincide ( $\Delta G_{\text{stab}}^* = 4.0 \pm 0.5$  kJ/g); this shows clearly that in  $\gamma$ S-crystallin, domain interactions do not contribute significantly to the overall stability, in contrast to  $\gamma$ B-crystallin (Mayr et al., 1994, 1997; Palme et al., 1997, 1998a, b; Wenk et al., 2000).

#### 3.4.3. Stability of $\beta$ B2-crystallins

The dimeric  $\beta$ B2-crystallin shows a two-step unfolding reaction with a concentration-dependent first step (Wieligmann et al., 1999). The intermediate in the unfolding reaction is a partially unfolded monomer, with an unfolded N-terminal domain and a folded C-terminal domain. Dissociation of the dimer and unfolding of the N-terminal domain are thus simultaneous. Reversibility of the unfolding/dissociation reaction can be accomplished; however, the concentration-dependent association step does not allow the two-state approximation to be applied for a quantitative thermodynamic evaluation. Using a three state model, Fu and Liang (2002) calculated a  $\Delta G$  of 36.6 kJ/mol for the first transition (N  $\leftrightarrow$  U) and a  $\Delta G$  of 12.7 kJ/mol for the second transition (U  $\leftrightarrow$  N) for human  $\beta$ B2-crystallin (at 0.1 mg/ml). These numbers must be

Table 6  
Molecular characteristics of  $\gamma$ B- and  $\gamma$ S-crystallin variants<sup>a</sup>

Variant	Residues	$M_{\text{calc}}$ (Da)	$M_{\text{obs}}$ (Da)	pH	$z$	$T_m$ (°C)	$\Delta G$ (kJ/mol)	$\Delta G^*$ (kJ/g)	$c_{1/2,\text{urea}}$ (M)
<i>Bovine <math>\gamma</math>B-crystallin and <math>\gamma</math>B-mutants</i>									
B $\gamma$ B	(1–174)	20 965	20 700	2.0	29	48/55			2.1/5.1 <sup>b</sup>
(F56W)		21 005	21 500	2.0	29				1.5/4.0 <sup>b,c</sup>
(F56A)		20 890	20 200	2.0	29				1.0/4.0 <sup>b,c</sup>
(F56D)		20 934	21 000	2.0	~29				0.8/4.0 <sup>b,c</sup>
B $\gamma$ B-N	(1–87)	10 403	11 000	2.0	13				5.0
B $\gamma$ B-C	(87–174)	10 692	10 750	2.0	16		4.7 ± 0.2		0.7
B $\gamma$ B-C	(87–174)			2.5	15		7.3 ± 0.5		0.95
B $\gamma$ B-C	(87–174)			3.0	14		25.5 ± 1.6		1.95
B $\gamma$ B-C	(87–174)			3.5	12		34.8 ± 2.6		2.75
B $\gamma$ B-C	(87–174)			4.0	9		36.0 ± 1.9		4.50
B $\gamma$ B[N + C] <sup>d</sup>		21 095	12 000	2.0	29				0.7/5.1 <sup>b</sup>
CP-B $\gamma$ B <sup>c</sup>			~20 000	2.0	29				0.7/5.1 <sup>b</sup>
B $\gamma$ B-L $\beta$ B2		20 960	22 500	6.0	~1				2.1/5.1 <sup>b</sup>
<i>Bovine <math>\gamma</math>S-crystallin</i>									
B $\gamma$ S	(1–177)	20 796	21 400	7.0	~0				7.0
B $\gamma$ S-5	(6–177)	20 362	20 870	7.0	~0				7.4
B $\gamma$ S-N	(1–91)	10 513	10 710	7.0	~0				6.6
B $\gamma$ S-C	(93–177)	10 174	10 310	7.0	~0				6.0
B $\gamma$ S[N + C] <sup>d</sup>		20 687	15 500 <sup>f</sup>	7.0	~0				
<i>Human <math>\gamma</math>S-crystallin</i>									
H $\gamma$ S	(1–177)	20 876	21 500	7.0	~0	75 ± 1	84 ± 0	4.0 ± 0.5	8.0
H $\gamma$ S-N	(1–90)	10 480	10 990	7.0	~0	70 ± 1	42 ± 5	4.0 ± 0.5	7.0
H $\gamma$ S-C	(91–177)	10 413	10 710	7.0	~0	78 ± 1	48 ± 5	4.5 ± 0.5	7.6
H $\gamma$ S[N + C] <sup>d</sup>		20 893	10 180	7.0	~0				

<sup>a</sup> B $\gamma$ B, B $\gamma$ S, and H $\gamma$ S refer to bovine  $\gamma$ B-crystallin, bovine  $\gamma$ S-crystallin and human  $\gamma$ S-crystallin.  $\gamma$ B-N,  $\gamma$ B-C,  $\gamma$ S-N,  $\gamma$ S-C stand for the isolated N- and C-terminal domains, and numbers in round and square brackets for residue numbers and equimolar mixtures of domains, respectively.  $M_{\text{calc}}$ ,  $M_{\text{obs}}$ : molecular masses, from ultracentrifugal analysis;  $z$ : calculated net charge at given pH values;  $T_m$ : temperature of thermal denaturation;  $\Delta G$  and  $\Delta G^*$ : Gibbs free energy at 20°C (kJ/mol) and corrected for given molecular masses, respectively;  $c_{1/2,\text{urea}}$ : transition midpoints of urea denaturation. Data from Mayr et al. (1994, 1997), Palme et al. (1997, 1998a, b), Jaenicke (1999) and Wenk et al. (2000).

<sup>b</sup> Transition midpoints of urea denaturation for the N- and C-terminal domains of intact wild-type B $\gamma$ B and F56 mutants differing in critical interdomain interactions.

<sup>c</sup> Isolated N-terminal domains do not differ in  $c_{1/2,\text{urea}}$ . At  $z = 0$ , B $\gamma$ B-N (F56A) shows anomalous dimerisation.

<sup>d</sup> In analytical ultracentrifugation, equimolar mixtures of the N- and C-terminal domains do not indicate significant domain association at protein concentrations up to 5 mg/ml.

<sup>e</sup> In circular permutants of B $\gamma$ B with the sequence (87–174)-L-(1–84), varying the length of the glycine linker (L) from G<sub>3</sub> to G<sub>5</sub> has no effect on the stability and the monomeric state of the construct.

<sup>f</sup> The sedimentation coefficients of the separate domains and their mixture differ by ~25%.

interpreted with care as reversibility of the unfolding reaction was not demonstrated in an unambiguous way. Thus, the data may not meet the requirements for a sound thermodynamic analysis.

Qualitatively, unfolding/refolding experiments clearly indicate that  $\beta$ B2-crystallin is much less stable than  $\gamma$ -crystallins in spite of the structural similarity of the domains and domain interactions (Fig. 11). This is surprising, bearing in mind that increased states of association belong to the most effective strategies of protein stabilization (Jaenicke and Sterner, 2002).

The domain and subunit interactions of  $\beta$ B2-crystallin are effected in an unpredictable way when altering the linker peptides or the N- and C-terminal extensions that protrude from the surface of the dumb-bell shaped monomers at both termini. Truncation mutants ( $\beta$ B2 $\Delta_{NC}$ ), with the N- and C-terminal “arms” removed, were shown to form  $\beta$ B2-crystallin dimers and tetramers. Subjecting the tetramer fraction to urea denaturation and subsequent renaturation yielded exclusively the native dimer, proving that in free solution this represents the most stable form of the protein (Trinkl et al., 1994). Comparing the X-ray structures, the truncated form of the tetramer has a set of domain interactions very similar to the native lattice tetramer, however, the structures differ in the relative orientation of the two sets of four domains (Norledge et al., 1997b).

The N-terminal domain of  $\beta$ B2-crystallin provides another example of where higher-order interactions cause mutual stabilization of the protomer fold (Jaenicke, 1999). Pinpointing the structural basis for the lower stability is difficult, considering that pairwise comparisons of the various N- and C-terminal domains of  $\beta$ - and  $\gamma$ -crystallins show only around 30% sequence identity. However, in native  $\beta$ B2-crystallin, the N-terminal domain is stabilized at the expense of the C-terminal one. A contribution to this stability redistribution may reside in asymmetric structural features of the interface, namely the covering of a surface hydrophobic patch on the N-terminal domain by a constrained sequence extension from the C-terminal one. This mutual stabilization between non-identical domains probably contributes to the observed heterologous pairing of the N- and C-terminal domains in native  $\beta$ B2-crystallin: the C-terminal domain only forms monomers in solution, whereas the N-terminal domain provides a more favourable partner (Wielgmann et al., 1999).

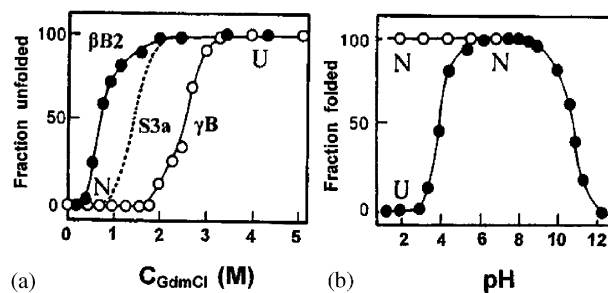


Fig. 11. Unfolding transitions of bovine  $\gamma$ B- and rat  $\beta$ B2-crystallin. (a) GdmCl-dependent equilibrium unfolding of  $\gamma$ B-crystallin (open symbols) and  $\beta$ B2-crystallin (closed symbols), monitored by maximum fluorescence emission in 0.1 M Na-phosphate pH 6.0. The dotted line illustrates the relatively low intrinsic stability of Ca<sup>2+</sup>-free Spherulin 3a from *Physarum polycephalum* (Kretschmar, 1999). (b) pH-induced unfolding of  $\gamma$ B- (open symbols) and  $\beta$ B2-crystallin (closed symbols), monitored by 315 nm fluorescence emission in Gly/HCl, citrate/H<sub>3</sub>PO<sub>4</sub>, Tris/HCl and Gly/NaOH at 0.1 M ionic strength (Jaenicke, 1999).

It is intriguing that at some stage during the evolution of the two-domain  $\beta$ B2-crystallin the N-terminal domain has effectively evolved a structural dependence on the C-terminal domain (Clout et al., 2000). The  $\beta$ B2-crystallin polypeptide chain is involved in domain swapping (Bax et al., 1990; Schlunegger et al., 1997) and it has been invoked to have a role in solubilizing crystallin hetero-oligomers in the eye lens by subunit exchange (Slingsby and Bateman, 1990; Bateman and Slingsby, 1992). Both processes require the N-terminal domain to become unpaired from that of the C-terminal. It may be that both the solubilizing and the exchanging role of  $\beta$ B2-crystallin is aided by the ease of unfolding of the N-terminal domain.

### 3.5. Stability of microbial $\beta\gamma$ -crystallin proteins

The common denominator of eye-lens  $\gamma$ -crystallins and their structural homologs in microorganisms is their high intrinsic stability. For Spherulin 3a or Protein S,  $\text{Ca}^{2+}$  serves as a highly efficient extrinsic stabilizing agent, enhancing both the thermodynamic and kinetic stability. Both Spherulin 3a and Protein S are involved in stress protection, the first as a water binding nutrient storage, the second as a cuticular spore envelope that can easily be solubilized again by chelating the stabilizing  $\text{Ca}^{2+}$ -ions. The value of these microbial protein data is that they clearly show that their calcium sites function as “highly efficient extrinsic stabilizing agents”. It is possible, given the low free water content in the core of lenses, that significant  $\text{Ca}^{2+}$  binding may occur to  $\beta\gamma$ -crystallin, although their binding sites are unlikely to be equivalent to those conserved in Protein S and Spherulin 3a (see Section 2.4.1).

#### 3.5.1. Spherulin 3a from *Physarum polycephalum*

In its native form, the 103 residue single-domain recombinant Spherulin 3a polypeptide chain forms a stable dimer of 22 kDa molecular mass. Due to its exposed cysteine residue (Cys 4), in the absence of reducing agents, intermolecular disulfide exchange causes covalent cross-linking to tetramers and higher polymers. In order to avoid these side reactions, the Cys4Ser mutant was produced. Being indistinguishable from the wild-type protein in all its physical properties, it was used to compare the stability of Spherulin 3a with that of bovine  $\gamma$ B-crystallin. In spite of the decrease in entropy of the denatured state, disulfide cross-linking has no significant effect on the denaturation reaction. In order to exclude irreversible perturbations of the two-state mechanism, in the following the cysteine-free mutant will be considered (Kretschmar et al., 1999a, b).

Calorimetric and spectroscopic analyses clearly showed that Spherulin 3a shares the high stability of its eye-lens homologs: in the absence of  $\text{Ca}^{2+}$ , its denaturation profiles range between those of  $\gamma$ B- and  $\beta$ B2-crystallin, the tertiary structure being destabilized at  $\text{pH} < 4$ , the secondary structure at  $\text{pH} < 3$  (Fig. 11a). Guanidine- and temperature-induced denaturation occur at  $c_{1/2, \text{GdmCl}} = 1.5 \text{ M}$  and  $T_m = 54^\circ\text{C}$ , respectively, both depending on concentration due to the dimeric state of the protein (Kretschmar et al., 1999a). In spite of this concentration dependence (and in contrast to the  $\beta$ B2-crystallin dimer), thermal and chemical equilibrium unfolding transitions obey the two-state model according to  $\text{N}_2 \rightleftharpoons 2\text{U}$ , allowing thermodynamic parameters to be determined. As has been mentioned, this is by no means trivial. The Gibbs free energy of stabilization is  $81 \pm 8 \text{ kJ/mol}$ , close to the above value for  $\gamma$ S-crystallin. No significant differences were found between the free energies calculated from calorimetric enthalpies ( $\Delta H_{\text{cal}}$ ) and  $T_m$ ; in addition, the free energy derived from thermal unfolding was confirmed by the spectroscopic

results obtained from GdmCl-induced unfolding transitions at different temperatures (Kretschmar and Jaenicke, 1999). Apart from the high *intrinsic* stability, there are two further contributions which further enhance the stability of Spherulin 3a; these are *extrinsic* as well as *kinetic stabilization* originating from high-affinity  $\text{Ca}^{2+}$ -binding. As shown by spectral analysis, Spherulin 3a contains one high-affinity and one low-affinity  $\text{Ca}^{2+}$ -binding site per subunit. Unfolding in the absence and in the presence of  $\text{Ca}^{2+}$  gives evidence for extreme thermodynamic and kinetic stabilization of the protein:  $\Delta G_{\text{stab}}$  is shifted from 81 to 137 kJ/mol (dimer),  $T_m$  from 53°C to 69°C, and the half-time of unfolding from 8 min (in 2.5 M GdmCl) to > 9 h (in 7.5 M GdmCl) (Fig. 12). The fact that the  $\text{Ca}^{2+}$  concentration in the spherules is sufficient for the complete complexation of the stress protein suggests that under condition of physiological stress the high expression of Spherulin 3a provides *Physarum polycephalum* with an extremely potent compatible solute (Kretschmar et al., 1999b; Kretschmar and Jaenicke, 1999).

### 3.5.2. Protein S from *Myxococcus xanthus*

In contrast to  $\gamma$ B-crystallin, which undergoes irreversible aggregation upon thermal unfolding, Protein S folds reversibly and it may therefore serve as a model in characterizing the thermodynamic properties of simple two-domain eye-lens crystallins such as  $\gamma$ B-crystallin. In addition, the kinetic characterization of this two-domain protein provided direct evidence that domain interactions can slow down the rate of unfolding, although as outlined in Section 2.4.1, the mode of domain pairing is different from the crystallins.

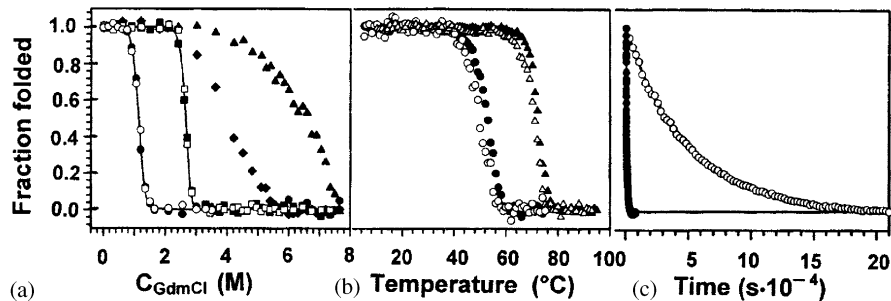


Fig. 12. Thermodynamic and kinetic stability of Spherulin 3a in 25 mM Mops buffer pH 7.0, in the absence and in the presence of  $\text{Ca}^{2+}$  (Kretschmar et al., 1999b). (a) GdmCl-induced equilibrium transitions of Spherulin 3a (40  $\mu\text{g}/\text{ml}$ ), monitored by fluorescence emission at 25°C. Renaturation was started from the fully denatured protein (after 16 h in 6 M GdmCl). In the absence of  $\text{Ca}^{2+}$ , unfolding/refolding after 1 day (●/○); in the presence of 3 mM  $\text{CaCl}_2$ : unfolding after 2 days (▲), unfolding after 4 weeks (◆), and unfolding/ refolding after 8 weeks (■/□). (b) Temperature-induced equilibrium transition of Spherulin 3a, monitored by dichroic absorption in the presence of 0.8 M GdmCl. Thermal denaturation was performed at 0.1 (open symbols) and 1.0 mg/ml protein concentration (closed symbols), either in the presence (△,▲) or in the absence of  $\text{Ca}^{2+}$  (○,●).  $\text{Ca}^{2+}$ -binding and enhanced Spherulin 3a concentration stabilize the protein, the latter due to the concentration-dependent shift of the monomer–dimer equilibrium to the native dimer. (c) Unfolding kinetics of Spherulin 3a, monitored by fluorescence emission at 40  $\mu\text{g}/\text{ml}$ . Kinetic traces at 2.5 M GdmCl for the  $\text{Ca}^{2+}$ -free protein (●), or at 7.5 M GdmCl for the  $\text{Ca}^{2+}$ -saturated protein (○). Using GdmSCN to accomplish full denaturation of  $\text{Ca}^{2+}$ -Spherulin 3a, and extrapolating both the GdmSCN- and the GdmCl-dependent unfolding kinetics to zero denaturant concentration, the rate-constants in the absence and in the presence of  $\text{Ca}^{2+}$  were found to be  $6.1 \times 10^{-6}$  and  $0.8 \times 10^{-6} \text{ s}^{-1}$ , respectively; thus, the  $\text{Ca}^{2+}$ -saturated protein is kinetically stabilized, showing an 8-fold decrease in its unfolding rate.

Protein S and its isolated domains, Protein S-N (Ala2→Val89) and Protein S-C (M-Gln90→Ser173-H<sub>6</sub>) were expressed in *E. coli* and isolated as recombinant proteins, Protein S in authentic form according to its spectral and hydrodynamic properties (Wenk and Mayr, 1998; Wenk and Jaenicke, 1999). X-ray analysis of the isolated N-terminal domain allowed two Ca<sup>2+</sup>-binding sites per domain to be localized (Fig. 9) (Wenk et al., 1999). Remarkably, these binding sites are very similar to those observed in Spherulin 3a (Clout et al., 2001). Removal of calcium by chelating agents such as EDTA leads to a destabilization of the protein (see below).

The Ca<sup>2+</sup>-binding monomeric two-domain crystallin homolog Protein S from *Myxococcus xanthus* shares not only its topology with  $\gamma$ B-crystallin, but also the difference in stability of its domains. The stability and Ca<sup>2+</sup>-binding were monitored by spectral and calorimetric techniques (Wenk and Mayr, 1998; Wenk and Jaenicke, 1999). The combination of the two approaches allowed both the mechanism and the thermodynamics of unfolding/refolding to be analyzed. Regarding Ca<sup>2+</sup>-binding and its extrinsic stabilizing effect, the monomeric two-domain Protein S follows the same pattern as the single-domain Spherulin 3a. Spectral changes show that the ligand alters the tertiary, but not the secondary structure of Protein S and its isolated domains; a 10% increase in sedimentation rate suggests that compaction of the molecule contributes to the extrinsic stabilization (Wenk et al., 1999). With its  $\gamma$ B-crystallin like topology, intact Protein S not only shows enhanced stability but also increased cooperativity of its equilibrium unfolding transitions, to the extent that, in the presence of Ca<sup>2+</sup>, the bimodal profiles are transformed to single sharp peaks (Fig. 13). Chemical and thermal unfolding in the absence and in the presence of Ca<sup>2+</sup> are fully reversible. Comparing the intact protein and its isolated domains, calorimetric experiments allow significant differences in the stability and cooperativity, as well as in the mechanism of their N→U transitions to be unravelled (Table 7).

In the case of the intact protein, independent folding/unfolding of the domains is observed only at low or high pH, when charge repulsion (plus Ca<sup>2+</sup> release) and the chaotropic effect of the denaturant are superimposed. The same holds for the thermal transitions at 10–90°C, in the absence of Ca<sup>2+</sup>. At neutral pH, both domains undergo a highly cooperative single transition; the bimodal profile is no longer observed. In the presence of Ca<sup>2+</sup>,  $\Delta G_{\text{PS-N}}$  exceeds  $\Delta G_{\text{PS-C}}$ ; obviously, in the intact two-domain protein, domain interactions result in an apparent destabilization of the N-domain with a concomitant increase in stability of the C-terminal half of the molecule. The thermal analysis of the monophasic profiles confirms two-state behaviour; in contrast, intact two-domain Protein S can only be fitted assuming two transitions, the first attributable to the C-terminal half (including the loss of domain interactions), the second to the N-terminal half. Comparing the calorimetric profiles of the isolated domains, similar values for the change in molar heat capacity ( $\Delta C_p$ ) and enthalpy ( $\Delta H$ ) are observed, as one would predict for proteins with similar size and fold (Myers et al., 1995). On the other hand, there is a striking difference between the melting points of the two domains, reflecting the significantly higher thermodynamic stability of the N-terminal domain compared to its C-terminal counterpart. In the case of the isolated domains, the effects are similar but less pronounced; the intrinsic stability of the C-domain in intact Protein S exceeds the stability of Protein S-C, whereas for the N-domain the opposite holds true. Ca<sup>2+</sup> binding, apart from enhancing both  $\Delta G_{\text{stab}}$  and the cooperativity of unfolding, also strengthens the interactions between the separate domains such that in the presence of Ca<sup>2+</sup> a 1:1 mixture of Protein S-N and Protein S-C is able to form liganded “nicked protein Protein S” (Wenk et al., 1999).

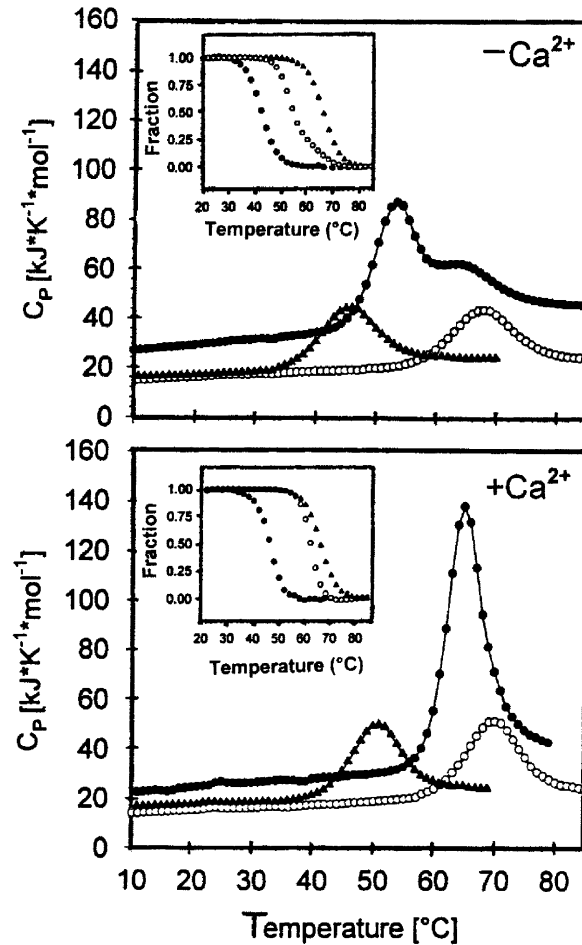


Fig. 13. Extrinsic stabilization of Protein S and its isolated domains by  $\text{Ca}^{2+}$  ions. Comparison of differential-scanning calorimetric profiles of Protein S and its domains in the absence and presence of  $\text{Ca}^{2+}$ . Protein S (PS) (●), PS-N (○), PS-C (▲) in 20 mM sodium cacodylate pH 7. *Upper frame*: in the presence of 1 mM EDTA; *lower frame*: in the presence of 3 mM  $\text{CaCl}_2$ . *Inserts*: Normalized temperature-induced unfolding transitions monitored by absorbance at 286 nm in the absence and in the presence of  $\text{Ca}^{2+}$  (Wenk, 1999; Wenk and Jaenicke, 1999).

Considering the unfolding/refolding *kinetics* for the isolated domains, only mono-exponential traces were obtained, as for other small all- $\beta$  proteins (Capaldi and Radford, 1998). In the case of intact Protein S, only the unfolding can be fitted with one exponential, whereas refolding shows biphasic kinetics, indicating folding intermediates. In spite of their different stabilities, both Protein S-N and Protein S-C unfold at the same rate ( $k_{\text{N} \rightarrow \text{U}} \approx 9 \times 10^{-5} \text{ s}^{-1}$ ); in intact Protein S, the unfolding rate of the cooperative unit of the interacting domains is slowed down 100-fold, indicating that the two-domain protein is kinetically stabilized (Table 7). In summary, Protein S exhibits a close similarity to other modular proteins that were shown to gain stability by domain interactions, in some cases to the extent that the truncated proteins were found to require their complementary parts for proper folding and assembly (Jaenicke, 1999).

Table 7

Structure, thermodynamics and kinetics of protein S and its separate domains in the absence and presence of stabilizing  $\text{Ca}^{2+}$ -ions<sup>a</sup>

	Protein S	Protein S-N	Protein S-C
Residues	172 (A2-S173) <sup>b</sup>	88 (A2-V89) <sup>b</sup>	91 (M-Q90-S173 + 6H) <sup>c</sup>
Molecular mass (kDa)			
MS	18.661	9.384	10.249
AUC <sup>d</sup>	19.6 ± 1.2	9.5 ± 0.2	10.2 ± 0.3
$s_{20,w}$ (S)	−/+ $\text{Ca}^{2+}$	1.90/2.12	1.43/1.45
$T_m$ (°C)	−/+ $\text{Ca}^{2+}$	N <sup>e</sup> : 52/64	68/70
	−/+ $\text{Ca}^{2+}$	C <sup>e</sup> : 64/65	45/50
$\Delta G_{\text{cal}}$ (kJ/mol)	−/+ $\text{Ca}^{2+}$	N <sup>e</sup> : 29/39	18/26
	−/+ $\text{Ca}^{2+}$	C <sup>e</sup> : 16/25	15/20
$\Delta G_{\text{urea}}$ (kJ/mol)	−/+ $\text{Ca}^{2+}$	21 ± 2/31 ± 3	15 ± 2/20 ± 2
$k_{\text{N} \rightarrow \text{U}}$ (s <sup>−1</sup> )	−/+ $\text{Ca}^{2+}$	−/−1	21/21
$k_{\text{U} \rightarrow \text{N}}$ (s <sup>−1</sup> )	−/+ $\text{Ca}^{2+}$	9.0 × 10 <sup>−7</sup>	8.5 × 10 <sup>−5</sup>

<sup>a</sup> 20 mM sodium cacodylate pH 7.0, plus 1 mM EDTA or 3 mM  $\text{CaCl}_2$ , 20°C.

MS, mass spectroscopy; AUC, sedimentation equilibria in anal. ultracentrifuge;  $s_{20,w}$ ; sedimentation coefficient;  $T_m$ ,  $\Delta G_{\text{cal}}$  and  $\Delta G_{\text{urea}}$  temperature and free energy of denaturation from calorimetry at 20–85°C and urea denaturation;  $k_{\text{N} \rightarrow \text{U}}$  and  $k_{\text{U} \rightarrow \text{N}}$ , microscopic rate constants of unfolding in chaotropic agents, and subsequent folding in the absence of denaturant. −/+  $\text{Ca}^{2+}$  refer to data in the absence and in the presence of 3 mM  $\text{CaCl}_2$ . Data from Wenk (1999), Wenk and Jaenicke (1999) and Wenk et al. (1999).

<sup>b</sup> The N-terminal Met residues are cleaved off by *E. coli* methionyl aminopeptidase.

<sup>c</sup> To avoid degradation, recombinant Protein S-C was prepared with a His<sub>6</sub>-tag.

<sup>d</sup> Results from sedimentation equilibria at 0.2–2.3 mg/ml initial protein concentration in the absence and in the presence of  $\text{Ca}^{2+}$  did not differ.

<sup>e</sup> For Protein S, N<sup>e</sup> and C<sup>e</sup> refer to the N- and C-terminal domains of the intact two-domain protein.

## 4. Multicomponent systems

### 4.1. Transparency in multicomponent macromolecular systems

From a physical point of view, as explained by Trokel as early as 1962 (Trokel, 1962), lens transparency is limited by the scattering of visible light. The transmitted light intensity  $I_t$  through a lens of thickness  $l$  may be simply written as a function of the incident intensity  $I_0$  and of an extinction coefficient  $\tau$ :

$$I_t = I_0 \exp(-\tau l) \quad (7)$$

where the extinction coefficient corresponds to the integral of the scattered intensity  $I_s$ :

$$\tau = \int I_s / I_0 \quad (8)$$

The scattered intensity is itself proportional to the concentration,  $c$  (in g/cm<sup>3</sup>), of the macromolecular scatterers, the crystallins, to their molecular mass,  $M$ , and refractive index increment,  $\partial n / \partial c$ , according to

$$I_s \sim cM \partial n / \partial c \quad (9)$$

and in concentrated solutions is in addition modulated because of protein distribution. When  $\tau = 0$ , all the incident light is transmitted and the lens is transparent. When  $\tau$  increases, the lens progressively turns opaque. As calculated by Trokel for the human lens, if crystallins were independent scatterers, about 70% of the incident light would be scattered, giving the lens a turbid aspect. Yet different protein distributions may reduce the scattering. Trokel proposed that the “high concentration of proteins in the lens must be accompanied by a degree of local order approaching a paracrystalline state”. Subsequently, it was shown by Benedek that at a sufficiently high concentration a liquid-like order was sufficient to maintain transparency (Benedek, 1971). That this holds true was finally demonstrated by X-ray scattering experiments. Making use of calf-lens cortical cytoplasmic extracts, it was shown that beyond a limiting protein concentration the scattered intensity is strongly affected by the short-range order of the scattering particles, to the effect that at the physiological protein level scattering was quenched (Delaye and Tardieu, 1983; Tardieu and Delaye, 1988). To quantify the concentration-dependent quenching, the scattered intensity is multiplied by a “structure factor”,  $S(c)$ , according to

$$I_s \sim cM \frac{\partial n}{\partial c} S(c) \quad (10)$$

Thus, both transparency and high refraction derive from the high protein concentration in the liquid-like, “glassy” interior of the fibre cells.

#### 4.2. Intra- and inter-molecular interactions and associations

The three-dimensional structure of the crystallins and their assembly to form complex cellular structures are determined, as they are for all proteins, by two classes of *non-covalent*, “weak” *interactions forces*, sometimes simply called interactions or interaction potentials, electrostatic and hydrophobic. The electrostatic interactions, either attractive or repulsive, include coulombic interactions, multipolar effects and more “sequence specific” interactions like ion pairing or hydrogen bonding (Kauzmann, 1969; Israelachvili, 1985). Hydrophobic interactions imply van der Waals forces and hydration effects. The concept of hydration forces (Parsegian et al., 1986; Ben Naim, 1987) refers to macromolecules and water hydrogen bonding interactions, and the possible effects of preferential orientation of the water molecules near polar or hydrophobic surfaces (Israelachvili, 1985; van Oss and Good, 1988; van Oss, 1993). Due to the superposition of significant enthalpic and entropic increments, the temperature dependence of the interaction forces is complex and their contribution to protein folding and stability still the subject of controversy (Baldwin and Eisenberg, 1987; Privalov and Gill, 1988; Dill, 1990; Creighton, 1991; Jaenicke, 1991a, b; Franks, 1995; Makhatadze and Privalov, 1995; Pace et al., 1996; Jaenicke and Böhm, 2001; Thornton, 2001). Attempts to analyze the molecular basis of the high stability of the crystallins are complicated by the fundamental question of how the marginal Gibbs free energy of stabilization of a given protein or a set of proteins is accumulated from the massive contributions of attractive and repulsive potentials between several thousand atoms.

Association implies the formation of intra- or inter-macromolecular contacts and therefore an additional step, dehydration (Jaenicke, 1987). Local water–protein interactions are replaced by a new network of ion pairing or hydrogen bonding or hydrophobic contacts. Self-assembly to yield homo- or hetero-oligomers requires specific recognition between partners whereas aggregation usually results from non specific contacts (Jaenicke and Seckler, 1997). To gain insight into

crystallin associations, NMR spectroscopy has been shown to be a promising approach because signals assigned to flexible terminal extensions, such as the  $\gamma$ S-crystallin N-terminal extension (Cooper et al., 1994b), the  $\alpha$ -crystallin C-terminal extension (Carver et al., 1994a, b) and the  $\beta$ B2-crystallin N- and C-terminal extensions (Carver et al., 1993b) allow the detection of protein-protein contacts. This technique also allows for contacts in crystallin mixtures and nuclear or cortical lens homogenates to be compared (Cooper et al., 1994a).

#### 4.3. Interactions at a distance and transparency

The “anomalous” scattering behaviour of the eye lens in terms of the relationship between interaction and protein distribution in solution, that governs transparency, osmotic pressure, and phase diagrams (i.e. phase separation and crystallization), is becoming well understood (Vérétout et al., 1989; Muschol and Rosenberger, 1995; Lomakin et al., 1996; Malfois et al., 1996; Haas et al., 1999). Macromolecular distribution in solution is governed by interactions at a distance that, given the protein shapes and sizes, can be measured with light, X-ray or neutron scattering. From such data, the underlying interaction potentials can be calculated (Belloni, 1986, 1988; Hansen and McDonald, 1986). Studies were conducted on monodisperse solutions of model proteins of different molecular weight, sizes, compactness, charge and isoelectric point as a function of the environment, pH, ionic strength, and temperature. They have shown that, once folded, the protein behaviour in physiological conditions (i.e. in low ionic strength solutions) can be essentially accounted for by a few forces: hard sphere repulsion, van der Waals attraction and coulombic electrostatic forces. This combination of forces is usually designated in the colloid field as the “DLVO potential”. Hard sphere interactions mean that two particles cannot interpenetrate, that they occupy an “excluded” volume. The interaction energy is infinite on contact and zero elsewhere. The van der Waals forces are short-range, about 3 Å, with a strength of the order of  $-2.8k_B T$  (where  $k_B$  is the Boltzmann constant and  $T$  the absolute temperature) increasing with decreasing temperature (Malfois et al., 1996). With monodisperse solutions of identical particles, the average charge is the same (whatever the particle) and the coulombic interactions are repulsive, except at the isoelectric point (pI), where they cancel. In the presence of higher salt concentrations or of additives like neutral polymers, an additional attraction is observed (Tardieu et al., 1999, 2002). More subtle interactions, for instance charge fluctuations at the surface, may also play a role, especially at the pI (Belloni and Spalla, 1997). They are weaker and more difficult to analyze.

Using these tools, the scattering behaviour of the eye lens can be explained in terms of the various types of weak interactions between the crystallin components. First, the mixture of crystallins in the cytoplasm of the lens was found to display an overall repulsive interaction determined essentially by the dominating effect of  $\alpha$ -crystallin (Delaye and Tardieu, 1983). Then, the study of lens  $\alpha$ -crystallin solutions at pH 6.8 and at different ionic strengths demonstrated that  $\alpha$ -crystallins behave as charged spheres (Vérétout et al., 1989) (Fig. 14). Therefore, the effects of non-ideality could be described over a large range of protein concentration, ionic strength and temperature with only two parameters, the charge and the radius of the equivalent sphere. The charge was found to be about 50 and the radius around 165 Å, which means that the  $\alpha$ -crystallin excluded volume is about twice the dry volume. In other words, the quaternary assembly is an open non-compact structure (Vérétout et al., 1989). The calculation of the structure factor

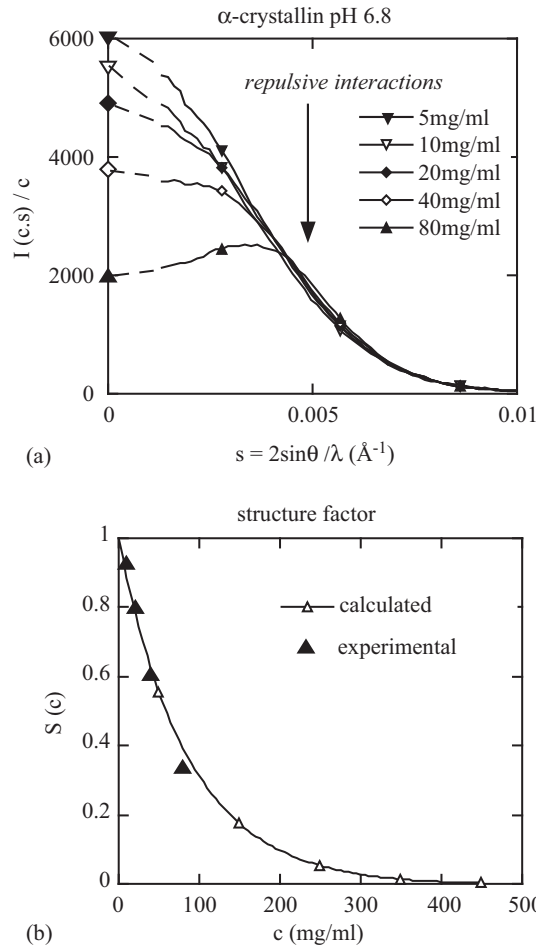


Fig. 14. SAXS curves showing repulsive interactions between  $\alpha$ -crystallins. *Top*: Normalized X-ray scattering curves (full lines),  $I(c,s)/c$ , recorded as a function of scattering angle,  $s = 2 \sin \theta / \lambda$ , for different values of  $\alpha$ -crystallin concentration (from Finet, 1999) close to physiological conditions, i.e. at pH 6.8 in phosphate buffer, ionic strength 150 mM. The normalized intensity at the origin decreases with protein concentration, which is typical of repulsive interactions. The extrapolation to the origin of the X-ray scattering curves (dotted lines),  $I(c,0)/c$ , is proportional to the normalized light scattering,  $I_s/c$  of an  $\alpha$ -crystallin solution at concentration  $c$ , i.e. to the structure factor  $S(c)$  (Eq. (10)). It can be seen that, because of the repulsive interactions, the normalized light scattering decreases rapidly when the protein concentration increases. *Bottom*: The experimental light scattering (structure factor) is compared to the theoretical one, calculated from Eq. (11).

relevant for lens transparency is simple since at physiological ionic strength the charge, screened by the salt, only plays a role in the vicinity of the macromolecular surface (to prevent aggregation) and the calculation reduces to (Carnahan and Starling, 1969):

$$S(c) = [1 - \phi(c)]^4 / [1 + 4\phi(c) + 4\phi(c)^2 - 4\phi(c)^3 + \phi(c)^4] \quad (11)$$

where  $\phi(c)$  is the volume fraction occupied by the  $\alpha$ -crystallins at concentration  $c$ . For a compact structure,  $\phi(c) \approx 0.75c$ , for  $\alpha$ -crystallins  $\phi(c) \approx 1.5c$ . In the case of  $\alpha$ -crystallin,  $S(c)$  decreases more rapidly with protein concentration which means stronger repulsive interactions with  $\alpha$ -crystallins

than with compact proteins. As a consequence, when concentrated,  $\alpha$ -crystallins tend to show an even distribution without periodical order which in turn reduces light scattering and favours high transparency (Tardieu and Delaye, 1988; V  r  tout et al., 1989). Moreover, under conditions where the quaternary structure remained native, i.e. up to 60  C, from pH 6 to about 8 and even in the presence of up to 2 M salt, the interaction between  $\alpha$ -crystallins remained repulsive (Finet, 1999). The only way to make an  $\alpha$ -crystallin interaction attractive is through the addition of polymers like polyethylene glycol (Finet and Tardieu, 2001). Under such conditions, a phase separation of  $\alpha$ -crystallin can eventually be induced.

From these studies it was concluded that, theoretically, transparency could have been achieved in many ways by using proteins with adequate combinations of molecular weight and compactness (see Eqs. (10)–(11)). If only transparency is considered, many different proteins might have done as well as  $\alpha\beta\gamma$ -crystallins (Tardieu & V  r  tout, 1991).

#### 4.4. $\beta$ - and $\gamma$ -crystallin interactions, phase separation

The physical state of the cytoplasmic protein solution within lens fibre cells depends critically on temperature, crystallin composition and a variety of other parameters (such as pH and ionic strength) and is prone to *fluid–fluid phase separation* (Benedek, 1971). For example, lowering the temperature of a calf lens below 15  C, leads to “cold cataract” as the result of a separation of the concentrated cytoplasmic protein solution into a coexisting protein-rich and a protein-poor phase. The existence of a phase separation and the shape of the “coexistence curve”, i.e. the concentrations of the protein-rich and protein-poor phase as a function of temperature (Fig. 15), is now well explained by the underlying interaction potentials, using the concepts that have been developed in liquid state physics to study colloids. Briefly, such phase separations occur when the macromolecules interact through short-range attractive potentials. With monodisperse solutions, when the potential range is less (or more) than one third of the macromolecular diameter, the phase separation is metastable (or stable) with respect to the crystal phase. In the lens, at physiological pH,  $\gamma$ -crystallins interact mainly through short-range attractive van der Waals forces since their isoelectric point is around 7. It has been shown (Lomakin et al., 1996; Malfois et al., 1996) that such a potential was sufficient to account for the shape of the phase separation diagram. In a  $\gamma$ -crystallin mixture, crystallization does not occur because of heterogeneity. With individual  $\gamma$ -crystallin components, the coexistence curve was indeed found below the solubility curve (Benedek, 1997). The interactions may be changed through modifications of the environment. When the pH is either increased or decreased from the physiological value, the  $\gamma$ -crystallin net charge increases, the interactions become less attractive (even showing coulombic repulsion) and the phase separation disappears (Finet, 1999).

The spatial fluctuation in the protein density from one phase to the other produces sufficient light scattering to cause opacification of the lens. The process is reversible and upon raising the temperature, the lens becomes clear again (Tanaka and Benedek, 1975). The onset of opacity is easily detectable with light scattering. Since the actual temperature of phase separation ( $T_c$ ) depends on the net attractive inter-protein interaction energy, it rises as the inter-protein interaction increases. Thus, the increase in light scattering accompanying the phase separation provides a means to quantify the net attraction within the multicomponent system of the eye lens. If the  $T_c$  increased above body temperature, the eye lens cytoplasm would

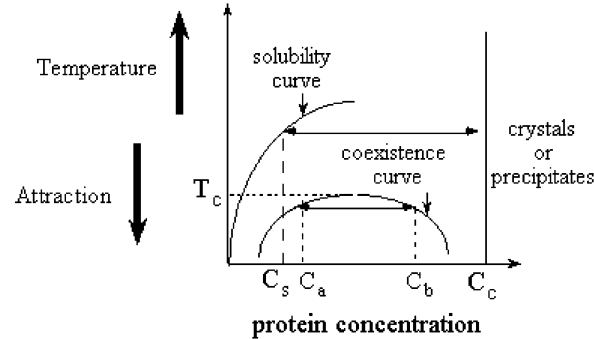


Fig. 15. A protein phase diagram. Schematic representation of the phase diagram observed as a function of temperature with DLVO-type potentials, i.e. with a potential that includes a short range attractive component increasing with decreasing temperature. Below the solubility curve, the phases at thermodynamic equilibrium are the crystal or precipitate at concentration  $C_c$  and the solution at concentration  $C_s$ . However, since crystal nucleation usually occurs after a lag time, when the temperature is rapidly decreased below the coexistence curve, a fluid–fluid phase separation may be observed first, metastable with respect to crystallization, between a protein poor phase at concentration  $C_a$  and a protein rich phase at concentration  $C_b$ .

turn opaque. There is no indication, however, that such liquid–liquid phase separations occur in ageing cataract.

Under physiological conditions (pH 6.8, 17–150 mM KCl),  $\beta$ - and  $\gamma$ -crystallins were found to differ (Tardieu et al., 1992). In mixtures, whereas interactions between  $\gamma$ -crystallins are attractive, increasing with decreasing temperature until phase separation occurs,  $\beta$ -crystallins present weakly repulsive interactions. Individual  $\beta$ -crystallins may turn attractive with decreasing temperature. However, solubility curves have been measured for only some of them. There are indications that the length of the N-terminal extensions of the  $\beta$ -crystallins affects the strength of their interaction:  $\beta$ A3-crystallin is more soluble than  $\beta$ A1-crystallin, the solubility of truncated  $\beta$ B1-crystallin is markedly temperature dependent being less soluble than full-length  $\beta$ B1-crystallin at lower temperatures (Bateman et al., 2001). It is thus possible that in vivo post-translational modifications of the  $\beta$ -crystallins promote attractive interaction and phase separation of these proteins.

$\gamma$ -Crystallins cluster into three groups characterized by increasing values of phase separation temperature  $T_c$  (the shape of the coexistence curve remains the same): the extreme case is mammalian  $\gamma$ S-crystallin which does not display phase separation, intermediary is typified by bovine  $\gamma$ B- and  $\gamma$ D-crystallin, and high  $T_c$  is typified by  $\gamma$ E- and  $\gamma$ F-crystallin (Siezen et al., 1988; Norledge et al., 1997a). The changes in phase separation temperatures reflect small differences in attractive potentials. The interaction between bovine  $\gamma$ -crystallins has also been studied by small angle X-ray scattering (SAXS). At physiological pH i.e. close to the  $\gamma$ -crystallin isoelectric point, the interactions between individual  $\gamma$ B-,  $\gamma$ D-, and  $\gamma$ E-crystallins are attractive (Fig. 16 top; Finet, 1999), where the attraction is stronger for  $\gamma$ E than for  $\gamma$ D- and  $\gamma$ B-crystallin. Under the same conditions, the interaction between  $\gamma$ S-crystallin, either bovine or human, which lacks phase separation, is neutral (Skouri-Panet et al., 2001; Fig. 16 bottom). In terms of physicochemical properties, the  $\gamma$ S-crystallin therefore appears intermediate between  $\beta$ -crystallins and the other  $\gamma$ A-F-crystallins.

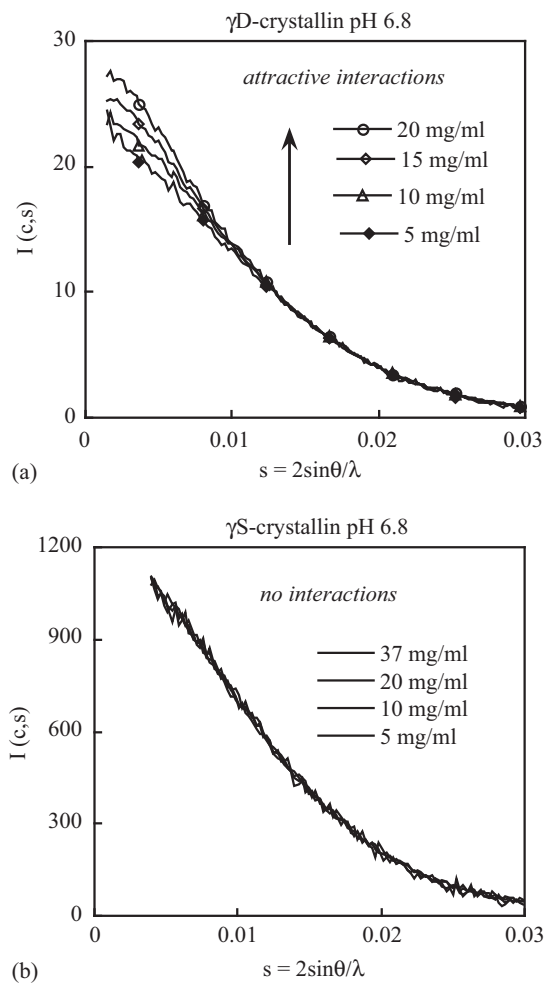


Fig. 16. SAXS curves showing attractive and neutral interactions in  $\gamma$ -crystallins. Normalized X-ray scattering curves recorded near physiological conditions, pH 6.8 ionic strength 150 mM as a function of protein concentration. *Top*:  $\gamma$ D-crystallins, and *Bottom*:  $\gamma$ S-crystallins. It can be seen that with  $\gamma$ D-crystallins the normalized intensity near the origin increases with protein concentration, which is indicative of attractive interactions. In contrast, the normalized intensity recorded with  $\gamma$ S-crystallins is invariant with protein concentration. No interactions, either attractive or repulsive, can be detected. When the pH is changed from 6.8 to 4.5, both  $\gamma$ D and  $\gamma$ S-crystallin interactions become repulsive.

The overall distribution of the  $\gamma$ -crystallin family within a particular lens shows a correlation with these attractive properties. By considering phase separation in terms of interaction potentials, new ideas have emerged to account for the protein distribution in the lens. As the propensity to phase separate leads to the formation of concentrated phases, proteins with a high  $T_c$  have good packing properties. The ability of attractive interactions to promote high protein concentrations can be illustrated in a different way. The osmotic pressure of a protein solution is a function of both protein concentration and interaction. If a protein solution in a dialysis bag is equilibrated against another macromolecular solution at constant osmotic pressure, the final protein concentration is higher if it exhibits attractive interactions rather than repulsive interactions. It is known that a protein concentration gradient exists from the centre to the

periphery of most lenses. This produces a refractive index gradient which contributes to the lens optical quality. It is also known that the osmotic pressure within the lens is constant. Each cell in the lens is equivalent to a dialysis bag in equilibrium with neighbouring cells. Since the interactions of the  $\alpha$ -,  $\beta$ -, and  $\gamma$ -crystallin mixture are more attractive in the nucleus than in the cortex, it is most likely that the protein concentration gradient within the eye lens originates from constant osmotic pressure coupled to differential interactive properties of  $\alpha$ -,  $\beta$ -, and  $\gamma$ -crystallins (Vérétout and Tardieu, 1989). This hypothesis could also be valid for the distribution of the individual  $\gamma$ -crystallins. In rodents, the high  $T_c$  proteins are synthesized early and therefore are enriched in the core region (see Section 1.1.4.2). Low  $T_c$   $\gamma$ -crystallins occupy an intermediary position along the refractive index gradient, while  $\gamma$ S-crystallin is located in the low refractive index outer regions of the lens as a result of synthesis after birth. Once a condensed phase has been stabilized, other processes may play a role to transform a liquid phase into a glass, as for example in the rat lens core.

Now that an increasing number of proteins have been tested for their interactions in solution, the uniqueness of the  $\gamma$ -crystallins is even more striking. Indeed, the monomeric  $\gamma$ -crystallins function close to their isoelectric point, which seems unusual for a protein that has to function at a high protein concentration. Under physiological conditions where the ionic strength is quite low, attraction largely originates from van der Waals forces. However, van der Waals forces decrease with increasing oligomeric size, as a result of a decrease in compactness as compared to monomers (Tardieu et al., 1987). These two features, pI around 7 and a monomeric compact structure, seem to be the only way in the protein world to have attractive interactions under physiological conditions. Moreover, these attractive interactions vary slightly from one  $\gamma$ -crystallin to the other, the extreme case being  $\gamma$ S-crystallin where the interactions are neutral. How to achieve such a fine tuning of the interactions is not understood yet and might be linked to the particular sets of arginine containing-ion pairs on the protein surface that are characteristic of  $\gamma$ -crystallin 3D structures (Chirgadze et al., 1996; Kumaraswamy et al., 1996; Norledge et al., 1997a; Basak et al., 2003). Whatever the molecular origin,  $\gamma$ -crystallins are a family of proteins capable of high solubility under extremely crowded conditions, presumably without competing with the hydration of other protein molecules, and yet close to a critical point for phase separation that provides a low-energy mechanism for the creation of a very high refractive index medium.

## 5. Lens $\alpha$ -crystallins and chaperone function

sHsps usually associate into high molecular weight monodisperse or polydisperse oligomers, able to protect against stress through the binding of a variety of partially unfolded substrates.  $\alpha$ -Crystallin was demonstrated by Horwitz in 1992 (Horwitz, 1992) to exhibit such chaperone properties *in vitro*. On the basis of these results, Horwitz proposed that  $\alpha$ -crystallin would bind  $\beta$ -crystallin or  $\gamma$ -crystallin at the onset of their denaturation, thus preventing further precipitation and lens opacity. There is some evidence that the conformational state of the substrate  $\beta\gamma$ -crystallins can be described as early unfolding intermediates on the irreversible pathway towards aggregation and precipitation (Das et al., 1999; Treweek et al., 2000). Accounting for up to 50% of the protein mass in the human lens,  $\alpha$ -crystallin would prevent opalescence of the eye lens over a long period of time. Only after “titrating out” the chaperone would the concentration

of irreversibly denatured protein rise to the critical concentration at which aggregation occurs (Goldberg et al., 1991; Jaenicke and Creighton, 1993; Jaenicke and Seckler, 1997; Welch et al., 1998; Beissinger et al., 1999; Thirumalai and Lorimer, 2001) and would ageing cataract ensue. In the past years a lot of evidence has been gathered showing that  $\alpha$ -crystallin does protect the  $\beta$ - and  $\gamma$ -crystallins as well as other proteins from aggregation in vitro (see Section 5.1 and Horwitz, 2003). In addition,  $\alpha$ -crystallin can protect from adduct formation (for review, see Harding, 2002), again in vitro. In the ageing lens, high molecular weight (HMW) forms of  $\alpha$ -crystallin are found that resemble the  $\alpha$ -crystallin chaperone complexes formed in vitro as well as the HMW complexes from a young lens when exposed to an external insult (for review, see Horwitz, 2003).

The chaperone-like activity of  $\alpha$ -crystallin has been the subject of numerous studies and functional models have been suggested (Carver et al., 1994a, b; Derham and Harding, 1999; MacRae, 2000; Abgar et al., 2001). The properties of  $\alpha$ -crystallin and related small heat shock proteins have been reviewed extensively (Goldberg et al., 1991; Jaenicke and Creighton, 1993; Jaenicke and Seckler, 1997; Ehrnsperger et al., 1998; Welsh and Gaestel, 1998; Beissinger et al., 1999; Horwitz et al., 1999; Thirumalai and Lorimer, 2001; Arrigo and Müller, 2002; van Montfort et al., 2002; Horwitz, 2003). One of the earlier criticisms of the original hypothesis rested on the need for heating  $\alpha$ -crystallin in order to demonstrate binding to destabilized  $\beta$ - and  $\gamma$ -crystallins, and thus the simple heating assay was replaced with less stable model substrates, or other denaturing protocols were suggested (Abgar et al., 2000; Rajaraman et al., 2001; Santhoshkumar and Sharma, 2001). Using a variety of such assays, it was found that both  $\alpha$ A- and  $\alpha$ B-crystallin exhibit high chaperone efficiency, binding misfolded proteins with high affinity and stoichiometry (Jaenicke and Creighton, 1993; Merck et al., 1993; Jaenicke, 1996a; Beissinger and Buchner, 1998; Ehrnsperger et al., 1998; Horwitz et al., 1999; Clark and Muchowski, 2000; Ganea and Harding, 2000) but without substrate release (Lee et al., 1997; Ehrnsperger et al., 1998; Berr et al., 2000). In living cells the bound protein substrates are held until either directed to the proteolysis machinery or passed onto ATP-dependent chaperones for refolding (Wickner et al., 1999). There is evidence that ATP enhances the function of  $\alpha$ -crystallin as a molecular chaperone (Muchowski et al., 1999; Wang and Spector, 2000).

The dynamic character of the  $\alpha$ -crystallin quaternary structure with the occurrence of temperature dependent subunit exchange was demonstrated and analyzed (Bova et al., 1997; Sun et al., 1998; Putilina et al., 2003). Fluorescence Resonance Energy Transfer (FRET) was found particularly useful to demonstrate that subunits, from recombinant  $\alpha$ A- or  $\alpha$ B-crystallin, can reversibly exchange between oligomers. Subunit exchange was also detected for other small heat shock proteins such as Hsp27, Hsp16.9, and Hsp16.5 (Bova et al., 2000, 2002; van Montfort et al., 2001; Sobott et al., 2002). The studies also demonstrated that subunit exchange might be partially inhibited in the presence of bound substrates. There are obvious differences between the chaperone action of the proposed hollow sphere  $\alpha$ B-crystallin model and chaperone models which assume substrate seclusion within an *Anfinsen cage*, especially with respect to the conformational variability and polydispersity of the assembly structure (Beissinger and Buchner, 1998; Saibil, 2000). It may be that these characteristics are essential for a molecular chaperone in the crowded environment of the lens.

### 5.1. The interaction between $\alpha$ -crystallin and $\beta$ - and $\gamma$ -crystallins

In the physiological context of the lens, it is important to consider whether  $\alpha$ -crystallin does protect against cataract by delaying the formation of light-scattering aggregates formed from

denatured crystallins. Yet only a few chaperone studies with  $\beta$ - and  $\gamma$ -crystallins as substrates have been performed (Boyle and Takemoto, 1994; Wang and Spector, 1994; Raman et al., 1995; Bours, 1996; Das et al., 1999; Weinreb et al., 2000) without any correlation with subunit exchange. As reviewed in Sections 3.3 and 3.4 (see also Table 5), although  $\alpha$ -crystallin seems less stable than many  $\beta$ - and  $\gamma$ -crystallins, the consequences of unfolding are not the same. Most of the  $\beta$ - and  $\gamma$ -crystallins start to aggregate at the onset of their denaturation, whereas  $\alpha$ -crystallins remain soluble for a long time, even if the average number of subunits changes with the extent of denaturation. As expected, preferential interactions or associations between  $\alpha$ -crystallin and other lens proteins in a complex mixture of crystallins could not be found at body temperature (Tardieu, A., unpubl. res.). Therefore,  $\alpha$ -crystallin does not need to chaperone native  $\beta$ - and  $\gamma$ -crystallins to maintain transparency, although it does appear to have a role in solubilization of the  $\gamma$ -crystallins (see Section 1.1.4.1).

Experiments were therefore performed at higher temperatures, but with attention also to changes in the  $\alpha$ -crystallin (Putilina et al., 2003). The chaperone activity of “lens”  $\alpha$ -crystallins towards  $\beta_{\text{LOW}}$ - and various  $\gamma$ -crystallins at the onset of their denaturation, at 60 and 66°C respectively, was studied at high and low crystallin concentrations using Small Angle X-ray Scattering (SAXS) and Fluorescence Energy Transfer (FRET). The crystallins were from calf lenses except for (recombinant) human  $\gamma$ S-crystallin. SAXS data demonstrated an irreversible doubling in molecular weight and a corresponding increase in size of  $\alpha$ -crystallins at temperatures above 60°C. Further increase is observed at 66°C. More subtle conformational changes accompanied the increase in size as shown by changes in the environment around tryptophan and cysteine residues. These temperature-induced changes in  $\alpha$ -crystallin were found necessary for the association with  $\beta_{\text{LOW}}$ - (but not  $\beta_{\text{HIGH}}$ -) and  $\gamma$ -crystallins to occur. FRET experiments using labelled subunits showed that the heat modified  $\alpha$ -crystallins retained their ability to exchange subunits and that, at 37°C, the rate of exchange was increased depending upon the temperature of incubation, 60°C or 66°C. Association with  $\beta_{\text{LOW}}$  (60°C) or various  $\gamma$ -crystallins (66°C) resulted at 37°C in decreased subunit exchange in proportion to bound ligands. Therefore,  $\beta_{\text{LOW}}$ - and  $\gamma$ -crystallins were compared for their capacity to associate with  $\alpha$ -crystallins and inhibit subunit exchange. Quite unexpectedly for a highly conserved protein family, differences were observed between the individual  $\gamma$ -crystallin family members. The strongest effect was observed for  $\gamma$ S-, followed by human  $\gamma$ S-,  $\gamma$ E-,  $\gamma$ A- and  $\gamma$ F-,  $\gamma$ D-,  $\gamma$ B-crystallin. The order of interaction of the  $\gamma$ -crystallins thus correlates with thermodynamic stability (see Section 3.4). Moreover, fluorescence properties of  $\alpha$ -crystallins in the presence of bound  $\beta_{\text{LOW}}$ - and  $\gamma$ -crystallins indicated that the formation of  $\beta_{\text{LOW}}/\alpha$ - or  $\gamma/\alpha$ -crystallin complexes involved various binding sites. The changes in subunit exchange associated with the chaperone properties of  $\alpha$ -crystallins towards the other lens crystallins demonstrate the dynamic character of the heat activated  $\alpha$ -crystallin structure.

At the protein concentrations used for the FRET experiments, the  $\alpha$ - $\beta$ - $\gamma$ -crystallin complexes were soluble. The chaperone-like activity of the  $\alpha$ -crystallin versus  $\beta_{\text{LOW}}$ - and  $\gamma$ -crystallin, i.e. the ability to prevent temperature induced precipitation of the  $\beta_{\text{LOW}}/\gamma$ -crystallin, was also studied with protein concentrations varying from about 2 mg/ml up to 20 mg/ml. Whatever the protein concentration, the  $\alpha$ - $\beta$ -crystallin complexes remained soluble for a long time. Instead, once formed, the  $\alpha$ - $\gamma$ -crystallin complexes precipitated as a function of time. Such a differential

behaviour in vitro could indicate that  $\gamma$ -crystallins represent a more important cataract risk than  $\beta$ -crystallins.

### 5.2. Specificity of the $\alpha$ -crystallin chaperone behaviour

The experiments outlined in Section 5.1 emphasize the importance of conformational changes in both  $\alpha$ - and  $\beta_{\text{LOW}}/\gamma$ -crystallin for association to take place. On the contrary, the chaperone activity of human recombinant  $\alpha$ A- or  $\alpha$ B-crystallin towards other partially unfolded substrates, like insulin or lactalbumin, or thermally denatured dehydrogenases or citrate synthase does not require the  $\alpha$ -crystallin structural transition (e.g. Andley et al., 1996; Horwitz et al., 1998b; Rajaraman et al., 1998; Abgar et al., 2000; Berr et al., 2000; Reddy et al., 2000). A thermodynamic analysis based on detection of direct binding by electron spin resonance showed that  $\alpha$ A-crystallin was able to sort a range of model T4 lysozyme mutants in order of their stability (Mchaourab et al., 2002). This study suggested a mechanism whereby the crystallin chaperone has two modes of interaction, involving binding of substrates with distinct conformational states, one more native-like and one nearer the global unfolded state. It is clear then that  $\alpha$ -crystallin can recognize and bind unfolded proteins over a range of temperatures, and hence its chaperone function is maintained over a range of conformations (including sizes). For it to work in the lens at body temperature, the  $\beta$ - and  $\gamma$ -crystallins would have to be “preferentially” denatured in order to have the opportunity of binding the low temperature form of the chaperone, or stress conditions would have to promote formation of the higher-molecular weight form of the  $\alpha$ -crystallin at body temperature. One possibility is that less stable regions of  $\alpha$ -crystallin are the first to respond to stress and on changing their conformation trigger an “activated” form of  $\alpha$ -crystallin. The consequence to the assembly might be that this “structural change” induces weaker subunit-subunit packing, consistent with the increase in subunit-exchange. Although heating studies show a dramatic increase in the size and binding activity of the  $\alpha$ -crystallin chaperone, it could be envisaged that there occurs a gradual increase in polydispersity of the ageing body-temperature form of  $\alpha$ -crystallin as it binds non-native  $\alpha$ -crystallin subunits. This binding, at the expense of its “native” interface contacts, may contribute to the increase in  $\alpha$ -crystallin binding activity towards other crystallins, in time for their eventual demise. Phosphorylated or deamidated subunits would freely exchange with the parent oligomer (Ito et al., 2001; Kamei et al., 2001). The R120G mutation appears like an extreme case where the associative properties undergo severe modifications and where the chaperone property of  $\alpha$ -crystallin is exhausted (Vicart et al., 1998; Bova et al., 1999).

Clues to a general structural mechanism of substrate binding of eukaryotic sHsps reside in the observation that the “active” structural component is likely to involve a temperature-regulated subassembly species with elements of conformational disorder. The hierarchy of the eukaryotic sHsp assembly shows that the fold of the plant N-terminal domain is absolutely dependent on the final assembly, and that the “ $\alpha$ -crystallin domain” is stabilized by assembly partners (Fig. 4). During a heat shock, the structural unit of exchange, having unfolded N-terminal regions and “a destabilized  $\alpha$ -crystallin domain”, could provide both substrate binding surfaces as well as assembly interfaces.

Different  $\alpha$ -crystallin peptides have been identified as functional elements in chaperone activity (Sharma et al., 1997, 1998). One of these peptides (residues 71–88 of  $\alpha$ A-crystallin) overlaps with a

putative substrate-binding site of small heat shock proteins (Sharma et al., 1998). According to the sHsp 3D structures that have been determined, this proposed binding site is covered with the C-terminal extension of another monomer and would become exposed during subunit exchange via dissociation from the parent oligomer and thus become available for interactions with substrates (van Montfort et al., 2001). A second putative binding site was allocated to the N-terminal part, involving aromatic residues (Sharma et al., 1998). Recent studies using mutated  $\alpha$ -crystallin also demonstrated the involvement of the C-terminal extension in its chaperone activity at 37°C towards insulin (Pasta et al., 2002). However, all binding interfaces that have been proposed were identified at low temperatures (25–37°C) and may have different properties at the temperatures at which lens in vitro heterocomplexes are formed.

## 6. Post-translational modification of crystallins

### 6.1. Crystallins are extensively modified, outcomes are varied

Over a long lifetime, crystallins may undergo a wide variety of irreversible, covalent modifications, caused by proteolysis, deamidation, oxidation, Maillard reactions, radiation-induced radicals and adduct formation, among others (for recent review, see Harding, 2002). The technical improvements in mass spectroscopy and 2D gel electrophoresis have made it possible to document a greater number of changes to a whole range of crystallin residues (Lund et al., 1996; Hanson et al., 1998; Lampi et al., 1998; Ma et al., 1998; Hanson et al., 2000; MacCoss et al., 2002; Lapko et al., 2002a, b, 2003b; Zhang et al., 2003). The nature of the modification, the residue location and the stability of the host crystallin domain or assembly will all have an impact on the level of structural change. The critical changes for lens transparency are those that destabilize or reduce the solubility of native crystallin structures. With recombinant mutant proteins it is possible to model some of the in vivo modifications and to test the effect of some of these modifications on the properties of the proteins. Unfortunately, only a few such studies have as yet been undertaken. The focus of these studies has been on stability.

Specific molecular features that perturb overall crystallin solubility (and short-range interactions) are poorly understood. The phenotypes of some human missense mutations suggest that the high solubility of native crystallins may in fact be easily decreased by seemingly innocuous changes, e.g. Arg58His in  $\gamma$ D-crystallin in aculeiform cataract (Pande et al., 2001). For the very stable crystallins, it is likely that modifications would need to be severe before unfolding was a greater problem than reduced solubility. Deamidation of asparagine, however, can be a marker of more radical damage (see below) as can disulphide crosslinks between cysteines that are known to be distal and buried in the native protein. In these cases the question revolves around whether the modification initiates unfolding or follows it. It is much less obvious that clipping of extensions, or deamidation of glutamine does adversely affect the stability of a crystallin, the effect of these modifications may be on solubility or oligomer assembly. Indeed, human  $\beta$ -crystallin remains soluble in spite of extensive modification (Zhang et al., 2003). Oligomers formed by intermolecular disulphide crosslinks of accessible cysteines can also markedly increase  $T_c$  as has been shown for the model bovine proteins  $\gamma$ B- and  $\gamma$ D-crystallin (Asherie et al., 1998). It has been suggested that the progressive juvenile-onset hereditary cataract linked to the Arg14Cys

human  $\gamma$ D crystallin mutation is due to disulfide-linked oligomers and aggregates caused by two exposed cysteines (Pande et al., 2000).

### 6.2. Crystallins are modified at an early age

Post-translational modification of the crystallins is often considered to cause their insolubilization in the ageing lens (although it is recognized that denatured proteins may be preferentially modified). When specific crystallins were targets of age-related studies, the surprising finding was the early age at which full modification appears to have occurred. All human crystallins, except for  $\beta$ B2-crystallin (Zhang et al., 2001), are extensively modified. These modifications are already apparent at age 3, and the pattern of a 17 yr old lens is very much like that of 54–55 year old lenses (Lampi et al., 1998). Takemoto and Boyle (1998) have estimated the rate of deamidation of a single residue (Asn 101) of human  $\alpha$ A-crystallin in the core of the lens to be about 15–20 yr, again showing that this process is essentially complete by age 40. Complete deamidation of  $\gamma$ -crystallins at various sites is also seen at an early age (Hanson et al., 1998). High levels of intramolecular disulfide bonding have been reported in soluble  $\gamma$ -crystallins from young human lenses (Hanson et al., 1998). Some of these intramolecular disulfide crosslinks are incompatible with protein solubility and are difficult to reconcile with the in vitro finding that  $\gamma$ S-crystallin more readily forms intermolecular disulfide bridges (Skouri-Panet et al., 2001).

### 6.3. The effect of clipping the arms of the crystallins

Both  $\alpha$ A- and  $\alpha$ B-crystallin have a flexible C-terminal tail. These C-terminal tails are hydrophilic and thought to be essential for a correct  $\alpha$ -crystallin assembly and solubility. In the ageing lens, some C-terminal truncation of the  $\alpha$ -crystallins is found. In the human lens the most common truncation is that of the C-terminal Ser from  $\alpha$ A-crystallin,  $\alpha$ B-lacking the C-terminal Lys can also be detected (Ma et al., 1998). Larger C-terminal truncations have also been reported. In the rodent lens, truncation of  $\alpha$ -crystallin is more common and more extensive than in the human lens, and the truncated forms are selectively insolubilized (Ueda et al., 2002). The properties of (recombinant) proteins mimicking the most common truncated forms of  $\alpha$ A- and  $\alpha$ B-crystallins in the human lens have not been reported. However, recombinant  $\alpha$ B-crystallin lacking the C-terminal tail performed almost as well as wild type  $\alpha$ B-crystallin in preventing insulin aggregation, but was much less efficient in preventing the thermal aggregation of citrate synthetase (Kokke et al., 2001). A 17 amino acid C-terminal truncation of human  $\alpha$ A-crystallin also impairs its ability to prevent thermal aggregation of human aldose reductase (Andley et al., 1996), probably due to a lesser solubility of the chaperoning complex. It is unknown whether the stability of truncated  $\alpha$ -crystallin is decreased.

$\beta$ B1-Crystallin is one of the crystallins that is extensively truncated with time. Complete loss of both the N- and C-terminal extension did not affect its stability as measured by urea denaturation (Lampi et al., 2002a). Similarly, the loss of the N-terminal arm of (bovine)  $\gamma$ S-crystallin had no effect on the stability of this protein (Wenk et al., 2000).  $\beta$ A1-crystallin can be considered a truncated version of  $\beta$ A3-crystallin. Again, loss of part of the N-terminal arm has no effect on the stability of the protein, indeed, the stability is marginally increased (Werten et al., 1996, Bateman et al., 2003). Finally, the stability of a rat  $\beta$ B2-crystallin mutant lacking both N- and C-terminal

arms has been reported to be less than that of the full length protein (Trinkl et al., 1994; Table 3). N-terminally, but not C-terminally, truncated  $\beta$ B2-crystallin has been detected in the lens of a 70 year old donor (Srivastava and Srivastava, 2003). In summary, from the presently available evidence, clipping of the arms of the crystallins is unlikely to have a major effect on protein stability. If clipping has a consequence for lens transparency, it is more likely due to changes in solubility or, in the case of the  $\beta$ -crystallins, in assembly. For example, the assembly of  $\beta$ H-crystallin is dependent on the full-length  $\beta$ B1-crystallin. Progressive truncation of the N-terminal extension causes disassembly of  $\beta$ H-crystallin (David et al., 1996; Ajaz et al., 1997).

#### 6.4. Deamidation

Deamidation is a common and early modification of human crystallins (Lampi et al., 1998; Ma et al., 1998) although not of mouse crystallins (Ueda et al., 2002). Deamidation of both Gln and Asn can be spontaneous but in the case of Gln it can also be catalyzed by transglutaminase. In vitro crystallins are a substrate of transglutaminase (Velasco and Lorand, 1987; Lorand et al., 1991; Groenen et al., 1994a; Shridas et al., 2001) and transglutaminase is present in the lens (Hidasi et al., 1995; Murthy et al., 1998; Raghunath et al., 1999). Given the prevalence of deamidated Gln in human crystallins, the possibility that crystallin deamidation is a regulated enzymatic process which is part of the normal maturation of the human lens should be further investigated.

Only a single study of a recombinant deamidated crystallin has been reported, namely of human  $\beta$ B1(Gln204Glu)-crystallin (Kim et al., 2002; Lampi et al., 2002a). The mutated site is located in the C-terminal domain and involved in interdomain interactions [see the topologically equivalent Q (Fig. 3) in  $\gamma$ S-C-terminal domain interface structure (Fig. 6c)]. A comparison of the urea denaturation of the modified protein with the wild type showed that the denaturation curve of the deamidated protein has two transitions, one with a midpoint at 4.2 M urea, the second at 7.1 M urea. In contrast, the curve of the wild type protein showed only a single transition at 5.9 M urea. Using a spin label attached to a Cys in the N-terminal domain, it was shown that the N-terminal domain is less stable in the deamidated protein than in the wild type protein, while the C-terminal domain is more stable. The increased stability of the C-terminal domain is presumably due to the additional charge, the decrease in stability of the N-terminal domain indicates that, as in  $\beta$ B2-crystallin, the N-terminal domain is stabilized by the interaction with the C-terminal domain. Presumably, in the deamidated protein the interface between the N- and C-terminal domains is disturbed. These data show that the major effect of deamidation of  $\beta$ B1-crystallin at Gln 204 is not one of stability: that of the N-terminal domain decreases, that of the C-terminal domain increases. The major effect is on assembly and aggregation: the mutant protein was less resistant to precipitation during heating, the flexibility of the N-terminal arm was decreased (Lampi et al., 2002a), and the mutant protein could not be fully refolded from urea, unlike the wild type protein (Kim et al., 2002).

Some age-related deamidations are difficult to model using recombinant proteins. When deamidation of an Asn residue has occurred via the succinimidyl intermediate resulting in the addition of extra carbon to the polypeptide backbone, it can be identified by the presence of  $\beta$ -aspartate, but not easily reproduced in vitro (Geiger and Clarke, 1987; Voorter et al., 1988; Fujii et al., 2001). In general this modification in proteins tends to be correlated with flexibility of the

native backbone chain (Aswad et al., 2000). The structure of the C-terminal domain of human  $\gamma$ S-crystallin (Purkiss et al., 2002) shows that a  $\beta$ -aspartate, identified at the site of Asn 143 (equivalent to residue 138 in the  $\gamma$ B numbering scheme (Figs. 3 and 17) that is deamidated in cataract (Takemoto, 2001), is located in a highly ordered structural region. This modification would be destabilizing if it occurred to the folded protein (Fig. 17). A more global study of the deamidation sites of  $\gamma$ S-crystallin from nuclear cataractous lenses showed more deamidation in the disulphide bonded-water-insoluble protein compared with water-soluble components and that surface exposure was a prerequisite for deamidation (Lapko et al., 2002a). It has been argued that these results are consistent with the hypothesis that the change in surface charge causes conformational changes which are followed by disulphide bonds and then by crystallin insolubility (Lapko et al., 2002a). Nevertheless, the overall level of  $\beta$ -aspartate in the human lens was found to be correlated only with age, not with cataract (van den Oetelaar and Hoenders, 1989b).

### 6.5. Disulfide bond formation in $\gamma$ S-crystallin

The data on the separate N and C domains of  $\gamma$ S-crystallin show that the domain interaction contributes little to the stability of the full length  $\gamma$ S-crystallin, suggesting that the domains easily dissociate (see Section 3.4.2). As domain dissociation may be one of the reasons why  $\gamma$ S-crystallin is particularly sensitive to oxidation, a combination of small angle X-ray scattering and chromatography was used to characterize the effect of oxidation on the solution structure of

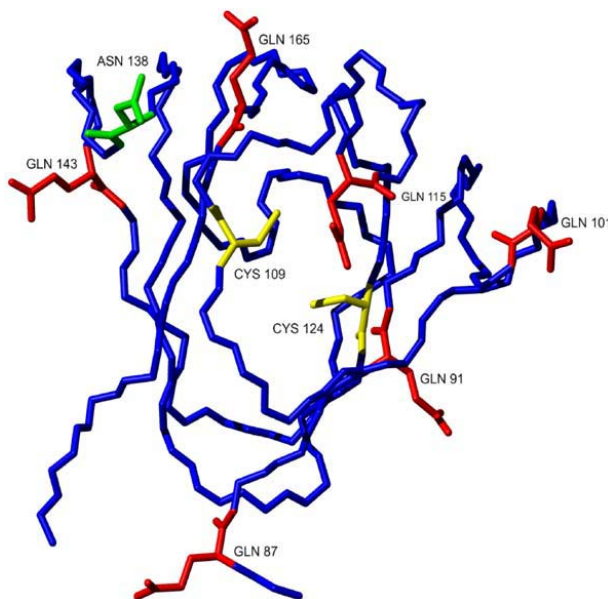


Fig. 17.  $\gamma$ S-crystallin C-terminal domain cysteine and amide accessibilities. The two cysteines in the C-terminal domain of human  $\gamma$ S-crystallin are completely buried having zero solvent accessibility. The Asn 143 (topologically equivalent to Asn 138 of bovine  $\gamma$ B-crystallin, green), that is deamidated involving  $\beta$ -aspartate formation, occurs on the conserved folded  $\beta$ -hairpin. Gln 106 (topologically equivalent to Gln 101 of  $\gamma$ B-crystallin, and Gln 120 (topologically equivalent to Gln 115 in  $\gamma$ B-crystallin) are both accessible and found to be deamidated in cataract (based on Fig. 5 from Purkiss et al. (2002) reproduced with permission from Journal of Biological Chemistry).

human  $\gamma$ S-crystallin (Skouri-Panet et al., 2001). No dissociation of  $\gamma$ S-crystallin into domains was observed upon oxidation, instead,  $\gamma$ S-crystallin formed dimers, linked by intermolecular disulfide bridges. This dimerization was readily reversible by DTT. At least one of the cysteines involved in the disulfide bridge is Cys 24 (topologically equivalent to Cys 20 in  $\gamma$ B-crystallin) as mutation of this cysteine to serine abolished the dimerization.

Oxidative dimerization of a protein can be destabilizing. However, the  $\gamma$ S-crystallin dimer behaved in this respect like the native monomer, showing that this dimer is as stable as the monomer, and that Cys 24 is likely to be quite exposed on the surface. Potentially, the exposed –SH of  $\gamma$ S-crystallin is of adaptive value and has a physiological role as an oxygen sink unless trapped by intramolecular disulfide bonds or blocked by methylation.

### 6.6. Protection by methylation

Recently it has been shown that specific cysteines in human  $\gamma$ B-,  $\gamma$ C-,  $\gamma$ D- and  $\gamma$ S-crystallins are methylated (Lapko et al., 2002b, 2003b). It is argued that this prominent modification can protect crystallins from more damaging oxidation and crosslinking reactions. The small size of the modification would be expected to keep destabilization of a native crystallin domain to a minimum.

## 7. Conclusions

In the last years a lot of progress has been made in characterizing the crystallins. Yet major gaps in our knowledge remain. The 3D structure of the  $\alpha$ -crystallin monomer and its oligomeric assembly, for example, is still unknown in spite of many efforts, although there is now fold information on the common domain from distant relatives. For the  $\beta$ -crystallins the domain fold is known, but we lack insight into its assembly (including even the rules for *intra versus intermolecular* domain pairing) and thus one of the essentials for understanding lens transparency. Only in the case of  $\gamma$ -crystallins, where the problem of assembly does not arise, can it be said that the structure is understood. At first sight, the  $\gamma$ -crystallins could be considered as inert space fillers. Yet, the variance in expression patterns during development or between species, for example rodents and man, the lack of all  $\gamma$ -crystallins except for  $\gamma$ S-crystallin in birds and reptiles, and the separate expansion of this gene family in fish and amphibians suggest that  $\gamma$ -crystallins have been subjected to strong selective pressure during evolution and that specific sets of  $\gamma$ -crystallins have been selected to fulfil specific functions. The unique attractive interaction between these proteins suggests a role in tuning the protein packing: it allows the lens to reach high protein concentrations without a large increase in osmotic pressure. This property, coupled with the high intrinsic stability of these proteins, comes in very useful when a hard, round lens is required. It would be easier to mould this protein family to the particular optical needs of particular species than to recruit novel proteins which share these unique properties.

The conservation of the  $\beta$ -crystallin sequences during evolution suggests, as we have argued above (Section 1.1.5), that the  $\beta$ -crystallins are essential components of the vertebrate transparent lens although, unlike the  $\gamma$ -crystallins, high stability is a variable feature for the family of  $\beta$ -crystallins. Their main role in the mature lens fibre cell may also be space filling, with controlled

assembly of the  $\beta$ -crystallins yielding the required mixture of polydisperse oligomers. The 3D studies have shown that the  $\beta$ -crystallins use structural mechanisms such as domain swapping coupled with interface selection and subunit-exchange to generate a wide range of oligomer diversity. It has not been possible to reproduce the *in vivo* assembly of  $\beta$ -crystallins *in vitro* (see Section 2.3.3). Of the recombinant human  $\beta$ -crystallins studied thus far, it would appear that assembly is based on heterodimers and  $\beta$ B2-crystallin homodimers. It is not clear how *in vivo* those heterodimeric partners are provided. For instance, are the newly synthesized monomers assembled into homodimers as they come off the ribosome assembly line and left to find their favoured partners in the crowded cytoplasm by subunit exchange, or do the monomers need a chaperone? It would be of interest to determine whether chaperoning by  $\alpha$ -crystallin plays a role in  $\beta$ -crystallin assembly. Alternatively (or in addition), they may need a chaperone later in assembly in order to form  $\beta$ H-crystallins from the smaller heteromers.  $\beta$ B2-crystallin has been suggested to be the stabilizing (or solubilizing) agent for the other  $\beta$ -crystallins (see also Zhang et al., 2003). However, in the newborn mouse lens,  $\beta$ B2-crystallin is only a minor component (Ueda et al., 2002). In this lens,  $\beta$ H-crystallin must be assembled without the aid of  $\beta$ B2-crystallin. This difference in  $\beta$ -crystallin spectrum between the human and rodent lens may be correlated with the need to concentrate proteins in the rodent lens core into a glass, after which time solubility is no longer an issue. However, in the human lens, solution conditions have to prevail over many decades. The long-term expression over the whole lifespan in human lens of a molecule such as  $\beta$ B2-crystallin with the ability to domain swap and subunit exchange with other members of the  $\beta$ -crystallin family may be needed to solubilize and stabilize other  $\beta$ -crystallins.

A further unknown is the effect of post-translational modification on  $\beta$ -crystallin assembly. The early timing of the truncations (in mouse and man) and deamidations (in man) of these proteins suggests a developmental process rather than age-related decay (Lampi et al., 1998, 2002b; Werten et al., 1999; Ueda et al., 2002). Given the high selective pressure of visual acuity, these post-translational modifications are likely to be of adaptive value. The most obvious possibility is that these are required for protein packing in the water-poor centre of the lens. The few available studies show that truncation changes not only the  $\beta$ -crystallin assembly properties but also affects its solubility in terms of the transition from a liquid to precipitate phase. A decrease in solubility (and possibly an increase in  $T_c$ ) would threaten transparency and contribute to age-related cataract. It is thus of obvious importance to understand the functional consequence of these modifications.

$\alpha$ -Crystallin has a multifunctional role in transparency. Biophysical arguments show that a protein oligomer with the properties of  $\alpha$ -crystallin is required for establishment of the transparent state. The requirement for  $\alpha$ -crystallin in lens morphogenesis may stem from the cytoprotective properties it shares with other heat shock proteins. In 1992 Horwitz proposed a function for  $\alpha$ -crystallin in age-related cataract:  $\alpha$ -crystallin could maintain lens transparency by chaperoning misfolded or damaged proteins in the crowded fibre cells and thus preventing aggregation (Horwitz, 1992). The most likely substrates for  $\alpha$ -crystallin would be the crystallins that are the least stable, and at the same time the most prone to irreversible aggregation following unfolding at ambient temperature. With respect to stability, the most susceptible crystallins are those that unfold (irreversibly) in the presence of relatively low denaturant concentrations. Some acidic  $\beta$ -crystallins fulfil all three risk criteria of low energetic stability, indications of irreversible

unfolding, and low solubility, whereas  $\beta$ B2-crystallin and  $\alpha$ -crystallin itself belong to the group of crystallins where the major risk is unfolding (see Table 5).

Obviously, age-related cataract involves the superposition of post-translational covalent modifications onto the age-related conformational effects.  $\alpha$ -Crystallin is also subject to covalent modifications such as phosphorylation, deamidation and loss of the C-terminal tail. Since the  $\alpha$ -crystallin tertiary and quaternary structures are still unknown, it is difficult to anticipate what conformational changes and quaternary structure reorganizations accompany the covalent modifications. These structural changes may of course modify in turn the chaperone activity of  $\alpha$ -crystallin. Denatured  $\alpha$ -crystallin is likely to be a substrate for the native  $\alpha$ -crystallin chaperone as well. Binding of its own denatured subunits will contribute to the polydispersity of  $\alpha$ -crystallin, and might therefore be of adaptive value. From the stability data derived using chemical denaturants, it would be predicted that the  $\alpha$ -crystallin chaperone will be fully titrated with non-native  $\alpha$ - and  $\beta$ -crystallins before the highly stable unmodified  $\gamma$ -crystallins have unfolded, unless there are specific *in vivo* conditions that destabilize  $\gamma$ -crystallins before  $\alpha$ -crystallins. These are unlikely to be temperature-related and more likely to involve covalent modification of reactive side chains such as oxidation of cysteines. It is clear from the few known human hereditary cataracts caused by point (missense) mutations in  $\gamma$ -crystallin that their effect is a reduction in protein solubility (rather than stability). This would suggest that surface modifications are more likely to result in associations, crystals, or fibres of folded protein which are unlikely to be recognized by the  $\alpha$ -crystallin chaperone. In general it is to be expected that by the time unmodified stable crystallins unfold, there will be no  $\alpha$ -crystallin chaperone capacity left, it will be saturated with acidic  $\beta$ -crystallins, oxidized  $\gamma$ -crystallins and possibly  $\alpha$ -crystallin subunits. It is unclear how the broad spectrum of modifications contributes to the likelihood of the modified protein requiring a chaperone and thus to cataractogenesis, as it depends on the effect on the solubility, stability and conformation of a particular protein, and when in that protein's life history it occurs.

One question that also needs to be considered is how the chaperoning by  $\alpha$ -crystallin affects its biophysical function in establishing transparency. Blocking the repulsive properties of  $\alpha$ -crystallin by substrate binding would lead to changes in the short-range order of the crystallins. At the end point of titrating the  $\alpha$ -crystallin chaperone activity, most of the  $\alpha$ -crystallin would become insoluble. Indeed, this is found in the older human lens (Ma et al., 1998) when the lens, although not classified as having cataract, is less transparent than young. A possible model for a lens depleted of  $\alpha$ -crystallin is the  $\alpha$ A-crystallin knock-out mouse. In the lens of this mutant, part of the  $\gamma$ -crystallin fraction is selectively insolubilized (Horwitz, 2003). Such insolubilization is unlikely to be due to protein unfolding, as  $\gamma$ -crystallins are very stable proteins, but may well be the result of phase separation or precipitation. If so, this would illustrate that depleting the fibre cell of  $\alpha$ -crystallin during ageing, either by complexing with  $\beta$ - or  $\gamma$ -crystallins, or because  $\alpha$ -crystallin itself becomes insoluble, disturbs transparency by changing the properties of the concentrated protein mixture. Paradoxically then, a chaperoning function of  $\alpha$ -crystallin would cause depletion of  $\alpha$ -crystallin and thereby cataract, an expression of the adaptive conflict of a multifunctional protein.

For lens function, not only protein solubility in the fibre cells located at the centre of the lens need to be maintained, but also the integrity of the epithelial cells and the still biosynthetically active cortical cells is required. Cells in other organs do age, and (rat) lens epithelial cells show the

same signs of ageing as cells in other tissues (Li et al., 1997; Pendergrass et al., 2001). In rodents, age-related cataract can be delayed by caloric restriction, which is well known to extend their lifespan (Wolf et al., 2000). In ageing cells all cellular defence systems including DNA repair, RNA surveillance and protein surveillance are attenuated (for review, see Franceschi et al., 2000; Söti and Csermely, 2002). Hence, ageing epithelial and cortical fibre cells would become more sensitive to oxidative and radiation damage. In addition, molecular misreading by RNA polymerase increases (van Leeuwen et al., 2000) causing faulty mRNAs to be made. Translation of such mRNAs obviously yields aberrant proteins. In particular, misfolded integral membrane proteins, including the highly expressed fibre cell proteins connexin and aquaporin, would threaten the osmotic balance of the lens cortical cells, an effect that could spread inwards to the lens core. Ageing of the outer lens cells could thus also be a cause of ageing cataract, although perhaps more likely of cortical cataract than of nuclear cataract.

In studies of *C. elegans* it was shown that lack of sHsps contributes to ageing (Hsu et al., 2003) and therefore the abundance of  $\alpha$ -crystallin in lens epithelial cell would be expected to delay ageing of these cells. Now that the technology for gene expression profiling of normal, cataractous and stressed lens cells is becoming available, additional candidate genes and proteins in the lens epithelium, that either contribute or are responsive to the damage of age-related cataract, will be defined. This will enable the elucidation of pathways involved in the breakdown of lens homeostasis (Spector et al., 2002; Hawse et al., 2003; Ruotolo et al., 2003).

Ageing involves the balance of three processes: presentation of insults, molecular damage and cytoprotection where the cellular system will break down at its weakest point. In age-related nuclear cataract, the exhaustion of a non-renewable resource, the  $\alpha$ -crystallin chaperone, is likely to be the limiting factor. In age-related cortical cataract, it may be the absence of cytoprotection, which is in earlier life supplied by  $\alpha$ -crystallin (see also Andley et al., 2001), that tips the balance. Thus, even though mechanistically different,  $\alpha$ -crystallin would still be a common theme in the two prevalent forms of age-related cataract.  $\alpha$ -Crystallin might be considered a therapeutic target for cortical cataract, although for nuclear cataract one should look at ways to keep the  $\beta$ - and  $\gamma$ -crystallin soluble, perhaps by targeting harmful post-translational modifications.

## Acknowledgements

We are very grateful to Drs. Rob van Montfort, Andrew Purkiss and Naomi Clout for pictures of crystallins. The work has been supported by an EU BioMed Grant (BMH4-CT98-3895). CS is grateful for the financial support of the Medical Research Council (London).

## References

- Aarts, H.J., Lubsen, N.H., Schoenmakers, J.G.G., 1989a. Crystallin gene expression during rat lens development. *Eur. J. Biochem.* 183, 31–36.
- Aarts, H.J., Jacobs, E.H., van Willigen, G., Lubsen, N.H., Schoenmakers, J.G., 1989b. Different evolution rates within the lens-specific beta-crystallin gene family. *J. Mol. Evol.* 28, 313–321.
- Abgar, S., Backmann, J., Aerts, T., Vanhoudt, J., Clauwaert, J., 2000. The structural differences between bovine lens alphaA- and alphaB-crystallin. *Eur. J. Biochem.* 267, 5916–5925.

- Abgar, S., Vanhoudt, J., Aerts, T., Clauwaert, J., 2001. Study of the chaperoning mechanism of bovine lens alpha-crystallin, a member of the alpha-small heat shock superfamily. *Biophys. J.* 80, 1986–1995.
- Ajaz, M.S., Ma, Z., Smith, D.L., Smith, J.B., 1997. Size of human lens beta-crystallin aggregates are distinguished by N-terminal truncation of betaB1. *J. Biol. Chem.* 272, 11250–11255.
- Alizadeh, A., Clark, J.I., Seeberger, T., Hess, J., Blankenship, T., Spicer, A., FitzGerald, P.G., 2002. Targeted genomic deletion of the lens-specific intermediate filament protein CP49. *Invest. Ophthalmol. Vis. Sci.* 43, 3722–3727.
- Andley, U.P., Mathur, S., Griest, T.A., Petrash, J.M., 1996. Cloning, expression, and chaperone-like activity of human alphaA-crystallin. *J. Biol. Chem.* 271, 31973–31980.
- Andley, U.P., Song, Z., Wawrousek, E.F., Brady, J.P., Bassnett, S., Fleming, T.P., 2001. Lens epithelial cells derived from alphaB-crystallin knockout mice demonstrate hyperproliferation and genomic instability. *FASEB J.* 15, 221–229.
- Antuch, W., Guntert, P., Wuthrich, K., 1996. Ancestral beta gamma-crystallin precursor structure in a yeast killer toxin. *Nat. Struct. Biol.* 3, 662–665.
- Aquilina, J.A., Benesch, J.L., Bateman, O.A., Slingsby, C., Robinson, C.V., 2003. Polydispersity of a mammalian chaperone: mass spectrometry reveals the population of oligomers in alphaB-crystallin. *Proc. Natl. Acad. Sci. USA* 100, 10611–10616.
- Arrigo, A.P., Müller, W.E.G. (Eds.), 2002. Small stress proteins. *Prog. Mol. Subcell. Biol.*, Vol. 28, Springer-Verlag, Berlin, 270pp.
- Asherie, N., Pande, J., Lomakin, A., Ogun, O., Hanson, S.R., Smith, J.B., Benedek, G.B., 1998. Oligomerization and phase separation in globular protein solutions. *Biophys. Chem.* 75, 213–227.
- Aswad, D.W., Paranandi, M.V., Schurter, B.T., 2000. Isoaspartate in peptides and proteins: formation, significance, and analysis. *J. Pharm. Biomed. Anal.* 21, 1129–1136.
- Bagby, S., Harvey, T.S., Eagle, S.G., Inouye, S., Ikura, M., 1994a. Structural similarity of a developmentally regulated bacterial spore coat protein to beta gamma-crystallins of the vertebrate eye lens. *Proc. Natl. Acad. Sci. USA* 91, 4308–4312.
- Bagby, S., Harvey, T.S., Eagle, S.G., Inouye, S., Ikura, M., 1994b. NMR-derived three-dimensional solution structure of protein S complexed with calcium. *Structure* 2, 107–122.
- Bagby, S., Harvey, T.S., Kay, L.E., Eagle, S.G., Inouye, S., Ikura, M., 1994c. Unusual helix-containing greek keys in development-specific Ca(2+)-binding protein S. <sup>1</sup>H, <sup>15</sup>N, and <sup>13</sup>C assignments and secondary structure determined with the use of multidimensional double and triple resonance heteronuclear NMR spectroscopy. *Biochemistry* 33, 2409–2421.
- Baldwin, R.L., Eisenberg, D., 1987. Protein Stability. In: Oxender, D.L., Fox, C.F. (Eds.), *Protein Engineering*. A.R. Liss, Inc., New York, pp. 127–148.
- Basak, A., Bateman, O., Slingsby, C., Pande, A., Asherie, N., Ogun, O., Benedek, G.B., Pande, J., 2003. High-resolution X-ray crystal structures of human  $\gamma$ D-crystallin (1.25A) and the R58H mutant (1.15A) associated with aculeiform cataract. *J. Mol. Biol.* 328, 1137–1147.
- Basak, A.K., Kroone, R.C., Lubsen, N.H., Naylor, C.E., Jaenicke, R., Slingsby, C., 1998. The C-terminal domains of gammaS-crystallin pair about a distorted twofold axis. *Protein Eng.* 11, 337–344.
- Bassnett, S., 2002. Lens organelle degradation. *Exp. Eye Res.* 74, 1–6.
- Bateman, O.A., Slingsby, C., 1992. Structural studies on beta H-crystallin from bovine eye lens. *Exp. Eye Res.* 55, 127–133.
- Bateman, O.A., Lubsen, N.H., Slingsby, C., 2001. Association behaviour of human betaB1-crystallin and its truncated forms. *Exp. Eye Res.* 73, 321–331.
- Bateman, O.A., Sarra, R., van Genesen, S.T., Kappe, G., Lubsen, N.H., Slingsby, C., 2003. The stability of human acidic beta-crystallin oligomers and hetero-oligomers. *Exp. Eye Res.* 77, 409–422.
- Bax, B., Lapatto, R., Nalini, V., Driessen, H., Lindley, P.F., Mahadevan, D., Blundell, T.L., Slingsby, C., 1990. X-ray analysis of beta B2-crystallin and evolution of oligomeric lens proteins. *Nature* 347, 776–780.
- Beissinger, M., Buchner, J., 1998. How chaperones fold proteins. *Biol. Chem.* 379, 245–259.
- Beissinger, M., Rutkat, K., Buchner, J., 1999. Catalysis, commitment and encapsulation during GroE-mediated folding. *J. Mol. Biol.* 289, 1075–1092.

- Belloni, L., 1986. Electrostatic interactions in colloidal solutions: comparison between primitive and one component models. *J. Chem. Phys.* 85, 519–526.
- Belloni, L., 1988. Self-consistent integral equation applied to the highly charged primitive model. *J. Chem. Phys.* 88, 5143–5148.
- Belloni, L., Spalla, O., 1997. Attraction of electrostatic origin between colloids. *J. Chem. Phys.* 107, 465–480.
- Benedek, G.B., 1971. Theory of transparency of the eye. *Appl. Opt.* 10, 459–473.
- Benedek, G.B., 1997. Cataract as a protein condensation disease: the proctor lecture. *Invest. Ophthalmol. Vis. Sci.* 38, 1911–1921.
- Benedek, G.B., Clark, I.J., Serrallach, E.N., Young, C.Y., Mengel, L., Sauke, T., Bagg, A., Benedek, K., 1979. Light scattering and reversible cataracts in the calf and human lens. *Philos. Trans. R. Soc. London A* 293, 329–340.
- Ben Naim, A., 1987. *Solvation Thermodynamics*. Plenum Press, New York, 246pp.
- Bennett, M.J., Choe, S., Eisenberg, D., 1994. Domain swapping: entangling alliances between proteins. *Proc. Natl. Acad. Sci. USA* 91, 3127–3131.
- Bennett, M.J., Schlunegger, M.P., Eisenberg, D., 1995. 3D domain swapping: a mechanism for oligomer assembly. *Protein Sci.* 4, 2455–2468.
- Berbers, G.A.M., Boermann, O.C., Bloemendal, H., de Jong, W.W., 1982. Primary gene products of bovine beta-crystallin and reassociation behaviour of its aggregates. *Eur. J. Biochem.* 128, 495–502.
- Berbers, G.A., Hoekman, W.A., Bloemendal, H., de Jong, W.W., Kleinschmidt, T., Braunitzer, G., 1984. Homology between the primary structures of the major bovine beta-crystallin chains. *Eur. J. Biochem.* 139, 467–479.
- Bernier, F., Seligy, V.L., Pallotta, D., Lemieux, G., 1986. Changes in gene-expression during spherulation in *Physarum polycephalum*. *Biochem. Cell. Biol.* 64, 337–343.
- Bernier, F., Lemieux, G., Pallotta, D., 1987. Gene families encode the major encystment-specific proteins of *Physarum polycephalum* plasmodia. *Gene* 59, 265–277.
- Berr, K., Wassenberg, D., Lilie, H., Behlke, J., Jaenicke, R., 2000. Epsilon-crystallin from duck eye lens comparison of its quaternary structure and stability with other lactate dehydrogenases and complex formation with alpha-crystallin. *Eur. J. Biochem.* 267, 5413–5420.
- Bieri, O., Kiefhaber, T., 2000. Kinetic models in protein folding. In: Pain, R.H. (Ed.), *Mechanisms of Protein Folding* (Frontiers in Molecular Biology), Vol. 32. Oxford University Press, Oxford, pp. 34–64.
- Bindels, J.G., Koppers, A., Hoenders, H.J., 1981. Structural aspects of bovine beta-crystallins: physical characterization including dissociation–association behavior. *Exp. Eye Res.* 33, 333–343.
- Bloemendal, H., de Jong, W.W., 1991. Lens proteins and their genes. *Prog. Nucleic Acid Res. Mol. Biol.* 41, 259–281.
- Blundell, T.L., Lindley, P., Miller, L., Moss, D., Slingsby, C., Tickley, I., Turnell, B., Wistow, G., 1981. The molecular structure and stability of the eye lens: X-ray analysis of gamma-crystallin II. *Nature* 289, 771–777.
- Böhm, G., Jaenicke, R., 1994. Relevance of sequence statistics for the properties of extremophilic proteins. *Int. J. Pept. Protein Res.* 43, 97–106.
- Bours, J., 1996. Calf lens alpha-crystallin, a molecular chaperone, builds stable complexes with beta s- and gamma-crystallins. *Ophthalmic Res.* 28, 23–31.
- Bova, M.P., Ding, L.L., Horwitz, J., Fung, B.K., 1997. Subunit exchange of alphaA-crystallin. *J. Biol. Chem.* 272, 29511–29517.
- Bova, M.P., Yaron, O., Huang, Q., Ding, L., Haley, D.A., Stewart, P.L., Horwitz, J., 1999. Mutation R120G in alphaB-crystallin, which is linked to a desmin-related myopathy, results in an irregular structure and defective chaperone-like function. *Proc. Natl. Acad. Sci. USA* 96, 6137–6142.
- Bova, M.P., McHaourab, H.S., Han, Y., Fung, B.K., 2000. Subunit exchange of small heat shock proteins. Analysis of oligomer formation of alphaA-crystallin and Hsp27 by fluorescence resonance energy transfer and site-directed truncations. *J. Biol. Chem.* 275, 1035–1042.
- Bova, M.P., Huang, Q., Ding, L., Horwitz, J., 2002. Subunit exchange, conformational stability, and chaperone-like function of the small heat shock protein 16.5 from *Methanococcus jannaschii*. *J. Biol. Chem.* 277, 38468–38475.
- Boyle, D., Takemoto, L., 1994. Characterization of the alpha-gamma and alpha-beta complex: evidence for an in vivo functional role of alpha-crystallin as a molecular chaperone. *Exp. Eye Res.* 58, 9–15.
- Boyle, D.L., Takemoto, L., Brady, J.P., Wawrousek, E.F., 2003. Morphological characterization of the alphaA- and alphaB-crystallin double knockout mouse lens. *BMC Ophthalmol.* 3, 3.

- Brady, J.P., Garland, D., Duglas-Tabor, Y., Robison Jr, W.G., Groome, A., Wawrousek, E.F., 1997. Targeted disruption of the mouse alpha A-crystallin gene induces cataract and cytoplasmic inclusion bodies containing the small heat shock protein alphaB-crystallin. *Proc. Natl. Acad. Sci. USA* 94, 884–889.
- Brady, J.P., Garland, D.L., Green, D.E., Tamm, E.R., Giblin, F.J., Wawrousek, E.F., 2001. AlphaB-crystallin in lens development and muscle integrity: a gene knockout approach. *Invest. Ophthalmol. Vis. Sci.* 42, 2924–2934.
- Brakenhoff, R.H., Aarts, H.J., Reek, F.H., Lubsen, N.H., Schoenmakers, J.G.G., 1990. Human gamma-crystallin genes. A gene family on its way to extinction. *J. Mol. Biol.* 216, 519–532.
- Branden, C., Tooze, J., 1998. *Introduction to Protein Structure*, 2nd Edition. Garland Publ., New York, p. 27.
- Bron, A.J., Vrensen, G.F., Koretz, J., Maraini, G., Harding, J.J., 2000. The ageing lens. *Ophthalmologica* 214, 86–104.
- Burgio, M.R., Kim, C.J., Dow, C.C., Koretz, J.F., 2000. Correlation between the chaperone-like activity and aggregate size of alpha-crystallin with increasing temperature. *Biochem. Biophys. Res. Commun.* 268, 426–432.
- Capaldi, A.P., Radford, S.E., 1998. Kinetic studies of beta-sheet protein folding. *Curr. Opin. Struct. Biol.* 8, 86–92.
- Carnahan, N.F., Starling, K.E., 1969. Equation of state for non attracting rigid spheres. *J. Chem. Phys.* 51, 635–636.
- Carpenter, J.F., Clegg, J.S., Crowe, J.H., Somero, G.N., 1993. Compatible solutes and macromolecular stability. *Cryobiology* 30, 201–241.
- Carver, J.A., Aquilina, J.A., Truscott, R.J., 1993a. An investigation into the stability of alpha-crystallin by NMR spectroscopy; evidence for a two-domain structure. *Biochim. Biophys. Acta* 1164, 22–28.
- Carver, J.A., Cooper, P.G., Truscott, R.J.W., 1993b. 1H-NMR spectroscopy of beta B2-crystallin from bovine eye lens. Conformation of the N- and C-terminal extensions. *Eur. J. Biochem.* 213, 313–320.
- Carver, J.A., Aquilina, J.A., Cooper, P.G., Williams, G.A., Truscott, R.J.W., 1994a. Alpha-crystallin: molecular chaperone and protein surfactant. *Biochim. Biophys. Acta* 1204, 195–206.
- Carver, J.A., Aquilina, J.A., Truscott, R.J., 1994b. A possible chaperone-like quaternary structure for alpha-crystallin. *Exp. Eye Res.* 59, 231–234.
- Chambers, C., Russell, P., 1991. Deletion mutation in an eye lens beta-crystallin. An animal model for inherited cataracts. *J. Biol. Chem.* 266, 6742–6746.
- Chirgadze, Y.N., Driessen, H.P.C., Wright, G., Sunngby, C., Hay, R.E., Lindley, P.F., 1996. Structure of the bovine eye lens  $\gamma$ D( $\gamma$  IIIb)-crystallin at 1.95Å. *Acta Cryst. D52*, 712–721.
- Chow, R.L., Lang, R.A., 2001. Early eye development in vertebrates. *Annu. Rev. Cell Dev. Biol.* 17, 255–296.
- Civil, A., van Genesen, S.T., Klok, E.J., Lubsen, N.H., 2000. Insulin and IGF-I affect the protein composition of the lens fibre cell with possible consequences for cataract. *Exp. Eye Res.* 70, 785–794.
- Civil, A., van Genesen, S.T., Lubsen, N.H., 2002. C-Maf, the gammaD-crystallin Maf-responsive element and growth factor regulation. *Nucleic Acids Res.* 30, 975–982.
- Clark, J.I., Muchowski, P.J., 2000. Small heat-shock proteins and their potential role in human disease. *Curr. Opin. Struct. Biol.* 10, 52–59.
- Clout, N.J., Slingsby, C., Wistow, G.J., 1997. Picture story. An eye on crystallins. *Nat. Struct. Biol.* 4, 685.
- Clout, N.J., Basak, A., Wieligmann, K., Bateman, O.A., Jaenicke, R., Slingsby, C., 2000. The N-terminal domain of betaB2-crystallin resembles the putative ancestral homodimer. *J. Mol. Biol.* 304, 253–257.
- Clout, N.J., Kretschmar, M., Jaenicke, R., Slingsby, C., 2001. Crystal structure of the calcium-loaded spherulin 3a dimer sheds light on the evolution of the eye lens betagamma-crystallin domain fold. *Struct. Fold. Design* 9, 115–124.
- Cooper, P.G., Carver, J.A., Truscott, R.J.W., 1993. 1H-NMR spectroscopy of bovine lens beta-crystallin. The role of the betaB2-crystallin C-terminal extension in aggregation. *Eur. J. Biochem.* 213, 321–328.
- Cooper, P.G., Aquilina, J.A., Truscott, R.J.W., Carver, J.A., 1994a. Supramolecular order within the lens: 1H NMR spectroscopic evidence for specific crystallin–crystallin interactions. *Exp. Eye Res.* 59, 607–616.
- Cooper, P.G., Carver, J.A., Aquilina, J.A., Ralston, G.B., Truscott, R.J., 1994b. 1H NMR spectroscopic comparison of gamma S- and gamma B-crystallins. *Exp. Eye Res.* 59, 211–220.
- Coulombre, J.L., Coulombre, A.J., 1963. Lens development: fibre elongation and lens orientation. *Science* 142, 1489–1490.
- Creighton, T.E., 1991. Stability of folded conformations. *Curr. Opin. Struct. Biol.* 1, 5–16.
- Csermely, P., 2001. Chaperone overload is a possible contributor to ‘civilization diseases’. *Trends Genet.* 17, 701–704.

- Dams, T., Jaenicke, R., 1999. Stability and folding of dihydrofolate reductase from the hyperthermophilic bacterium *Thermotoga maritima*. *Biochemistry* 38, 9169–9178.
- Darwin, C., 1859. *The Origin of Species by Means of Natural Selection*. J. Murray, London.
- Das, B.K., Liang, J.J., 1997. Detection and characterization of alpha-crystallin intermediate with maximal chaperone-like activity. *Biochem. Biophys. Res. Commun.* 236, 370–374.
- Das, B.K., Liang, J.J., 1998. Thermodynamic and kinetic characterization of calf lens gammaF-crystallin. *Int. J. Biol. Macromol.* 23, 191–197.
- Das, K.P., Choo-Smith, L.P., Petrash, J.M., Surewicz, W.K., 1999. Insight into the secondary structure of non-native proteins bound to a molecular chaperone alpha-crystallin. An isotope-edited infrared spectroscopic study. *J. Biol. Chem.* 274, 33209–33212.
- Datta, S.A., Rao, C.M., 2000. Packing-induced conformational and functional changes in the subunits of alpha-crystallin. *J. Biol. Chem.* 275, 41004–41010.
- David, L.L., Lampi, K.J., Lund, A.L., Smith, J.B., 1996. The sequence of human betaB1-crystallin cDNA allows mass spectrometric detection of betaB1 protein missing portions of its N-terminal extension. *J. Biol. Chem.* 271, 4273–4279.
- de Jong, W.W., 1981. Evolution of lens and crystallins. In: Bloemendal, H. (Ed.), *Molecular and Cellular Biology of the Eye Lens*. Wiley, New York, pp. 221–278.
- de Jong, W.W., Caspers, G.-J., Leunissen, J.A.M., 1998. Genealogy of the alpha-crystallin–small heat-shock protein superfamily. *Int. J. Biol. Macromol.* 22, 151–162.
- Delaye, M., Tardieu, A., 1983. Short-range order of crystallin proteins accounts for eye lens transparency. *Nature* 302, 415–417.
- den Dunnen, J.T., Moormann, R.J., Lubsen, N.H., Schoenmakers, J.G.G., 1986. Concerted and divergent evolution within the rat gamma-crystallin gene family. *J. Mol. Biol.* 189, 37–46.
- Derham, B.K., Harding, J.J., 1999. Alpha-crystallin as a molecular chaperone. *Prog. Retin. Eye Res.* 18, 463–509.
- Dill, K.A., 1990. Dominant forces in protein folding. *Biochemistry* 29, 7133–7155.
- Di Maro, A., Pizzo, E., Cubellis, M.V., D'Alessio, G., 2002. An intron-less betagamma-crystallin-type gene from the sponge *Geodia cydonium*. *Gene* 299, 79–82.
- Dirks, R.P., van Genesen, S.T., Krüse, J.J., Jorissen, L., Lubsen, N.H., 1998. Extralenticular expression of the rodent betaB2-crystallin gene. *Exp. Eye Res.* 66, 267–269.
- Dobson, C.M., 1999. Protein misfolding, evolution and disease. *Trends Biochem. Sci.* 24, 329–332.
- Doerwald, L., Nijveen, H., Civil, A., van Genesen, S.T., Lubsen, N.H., 2001. Regulatory elements in the rat betaB2-crystallin promoter. *Exp. Eye Res.* 73, 703–710.
- Doss-Pepe, E.W., Carew, E.L., Koretz, J.F., 1998. Studies of the denaturation patterns of bovine alpha-crystallin using an ionic denaturant, guanidine hydrochloride and a non-ionic denaturant, urea. *Exp. Eye Res.* 67, 657–679.
- Ehrnsperger, M., Buchner, J., Gaestel, M., 1998. Small heat-shock proteins. In: Fink, A.L., Goto, Y. (Eds.), *Molecular Chaperones in the Life Cycle of Proteins: Structure, Function and Mode of Action*. M. Dekker, New York, Basel, Hong Kong, pp. 533–575.
- Ehrnsperger, M., Lilie, H., Gaestel, M., Buchner, J., 1999. The dynamics of Hsp25 quaternary structure. Structure and function of different oligomeric species. *J. Biol. Chem.* 274, 14867–14874.
- Faber, S.C., Robinson, M.L., Makarenkova, H.P., Lang, R.A., 2002. Bmp signaling is required for development of primary lens fiber cells. *Development* 129, 3727–3737.
- Feil, I.K., Malfois, M., Hendle, J., van der Zandt, H., Svergun, D.I., 2001. A novel quaternary structure of the dimeric alpha-crystallin domain with chaperone-like activity. *J. Biol. Chem.* 276, 12024–12029.
- Fernald, R.D., 1997. The evolution of eyes. *Brain Behav. Evol.* 50, 253–259.
- Fernald, R.D., Wright, S.E., 1983. Maintenance of optical quality during crystalline lens growth. *Nature* 301, 618–620.
- Finet, S., 1999. Interactions entre protéines en solution : étude par diffusion des rayons X aux petits angles du lysozyme et des protéines du cristallin : Application à la cristallisation. Ph.D. Thesis, University Paris 6.
- Finet, S., Tardieu, A., 2001. Alpha-crystallin interaction forces studied by SAXS and numerical simulations. *J. Cryst. Growth* 232, 40–49.
- Franceschi, C., Valensin, S., Bonafè, M., Paolisso, G., Yashin, A.I., Monti, D., DeBenedictis, G., 2000. The network and the remodeling theories of aging: historical background and new perspectives. *Exp. Gerontol.* 35, 879–896.

- Franks, F., 1995. Protein destabilization at low temperatures. *Adv. Protein Chem.* 46, 105–139.
- Fu, L., Liang, J.J., 2002. Unfolding of human lens recombinant betaB2- and gammaC-crystallins. *J. Struct. Biol.* 139, 191–198.
- Fujii, N., Matsumoto, S., Hiroki, K., Takemoto, L., 2001. Inversion and isomerization of Asp-58 residue in human alphaA-crystallin from normal aged lenses and cataractous lenses. *Biochim. Biophys. Acta* 1549, 179–187.
- Ganea, E., Harding, J.J., 2000. Alpha-crystallin assists the renaturation of glyceraldehyde-3-phosphate dehydrogenase. *Biochem. J.* 345, 467–472.
- Garland, D.L., Douglas-Tabor, Y., Jimenez-Asensio, J., Datiles, M.B., Magno, B., 1996. The nucleus of the human lens: demonstration of a highly characteristic protein pattern by two-dimensional electrophoresis and introduction of a new method of lens dissection. *Exp. Eye Res.* 62, 285–291.
- Geiger, T., Clarke, S., 1987. Deamidation, isomerization, and racemization at asparaginyl and aspartyl residues in peptides. Succinimide-linked reactions that contribute to protein degradation. *J. Biol. Chem.* 262, 785–794.
- Goldberg, M.E., Rudolph, R., Jaenicke, R., 1991. A kinetic study of the competition between renaturation and aggregation during the refolding of denatured-reduced egg white lysozyme. *Biochemistry* 30, 2790–2797.
- Grainger, R.M., 1992. Embryonic lens induction: shedding light on vertebrate tissue determination. *Trends Genet.* 8, 349–355.
- Groenen, P.J., Grootjans, J.J., Lubsen, N.H., Bloemendal, H., de Jong, W.W., 1994a. Lys-17 is the amine-donor substrate site for transglutaminase in betaA3-crystallin. *J. Biol. Chem.* 269, 831–833.
- Groenen, P.J.T.A., Merck, K.B., de Jong, W.W., Bloemendal, H., 1994b. Structure and modifications of the junior chaperone alpha-crystallin. From lens transparency to molecular pathology. *Eur. J. Biochem.* 225, 1–19.
- Haas, C., Drenth, J., Wilson, W.W., 1999. Relation between the solubility of proteins in aqueous solutions and the second virial coefficient of the solution. *J. Phys. Chem. B.* 103, 2808–2811.
- Haley, D.A., Horwitz, J., Stewart, P.L., 1998. The small heat-shock protein, alphaB-crystallin, has a variable quaternary structure. *J. Mol. Biol.* 277, 27–35.
- Haley, D.A., Bova, M.P., Huang, Q.L., Mchaourab, H.S., Stewart, P.L., 2000. Small heat-shock protein structures reveal a continuum from symmetric to variable assemblies. *J. Mol. Biol.* 298, 261–272.
- Hansen, J.P., McDonald, I.R., 1986. *Theory of Simple Liquids*. Academic Press, New York.
- Hanson, S.R., Smith, D.L., Smith, J.B., 1998. Deamidation and disulfide bonding in human lens gamma-crystallins. *Exp. Eye Res.* 67, 301–312.
- Hanson, S.R.A., Hasan, A., Smith, D.L., Smith, J.B., 2000. The major in vivo modifications of the human water-insoluble lens crystallins are disulfide bonds, deamidation, methionine oxidation and backbone cleavage. *Exp. Eye Res.* 71, 195–207.
- Harding, J.J., 2002. Viewing molecular mechanisms of ageing through a lens. *Ageing Res. Rev.* 1, 465–479.
- Hawse, J.R., Hejtmancik, J.F., Huang, Q., Sheets, N.L., Hosack, D.A., Lempicki, R.A., Horwitz, J., Kantorow, M., 2003. Identification and functional clustering of global gene expression differences between human age-related cataract and clear lenses. *Mol. Vis.* 9, 515–537.
- Hemmingsen, J.M., Gernert, K.M., Richardson, J.S., Richardson, D.C., 1994. The tyrosine corner: a feature of most Greek key beta-barrel proteins. *Protein Sci.* 3, 1927–1937.
- Hendriks, W., Leunissen, J., Nevo, E., Bloemendal, H., de Jong, W.W., 1987. The lens protein alpha A-crystallin of the blind mole rat, *Spalax ehrenbergi*: evolutionary change and functional constraints. *Proc. Natl. Acad. Sci. USA* 84, 5320–5324.
- Héon, E., Priston, M., Schorderet, D.F., Billingsley, G.D., Girard, P.O., Lubsen, N., Munier, F.L., 1999. The gamma-crystallins and human cataracts: a puzzle made clearer. *Am. J. Hum. Genet.* 65, 1261–1267.
- Herbrink, P., van Westreenen, H., Bloemendal, H., 1975. Further studies on the polypeptide chains of beta-crystallin. *Exp. Eye Res.* 20, 541–548.
- Hidasi, V., Adany, R., Muszbek, L., 1995. Localization of transglutaminase in human lenses. *J. Histochem. Cytochem.* 43, 1173–1177.
- Horwitz, J., 1992. Alpha-crystallin can function as a molecular chaperone. *Proc. Natl. Acad. Sci. USA* 89, 10449–10453.
- Horwitz, J., 2003. Alpha-crystallin. *Exp. Eye Res.* 76, 145–153.
- Horwitz, J., Huang, Q.-L., Ding, L., Bova, M.P., 1998a. Lens alpha-crystallin: chaperone-like properties. *Methods Enzymol.* 290, 365–383.

- Horwitz, J., Bova, M., Huang, Q.L., Ding, L., Yaron, O., Lowman, S., 1998b. Mutation of alpha B-crystallin: effects on chaperone-like activity. *Int. J. Biol. Macromol.* 22, 263–269.
- Horwitz, J., Bova, M.P., Ding, L.L., Haley, D.A., Stewart, P.L., 1999. Lens alpha-crystallin: function and structure. *Eye* 13, 403–408.
- Hsu, A.L., Murphy, C.T., Kenyon, C., 2003. Regulation of aging and age-related disease by DAF-16 and heat-shock factor. *Science* 300, 1142–1145.
- Hughes, A., 1996. Seeing cones in living eyes. *Nature* 380, 393–394.
- Huxley, F., 1990. *The Eye: the Seer and the Seen*. Thames, and Hudson, London.
- Inouye, S., Inouye, M., McKeever, B., Sarma, R., 1980. Preliminary crystallographic data for protein S, a development-specific protein of *Myxococcus xanthus*. *J. Biol. Chem.* 255, 3713–3714.
- Israelachvili, J.N., 1985. *Intermolecular and Surface Forces*. Academic Press, London.
- Ito, H., Kamei, K., Iwamoto, I., Inaguma, Y., Nohara, D., Kato, K., 2001. Phosphorylation-induced change of the oligomerization state of alpha B-crystallin. *J. Biol. Chem.* 276, 5346–5352.
- Iwaki, T., Kume-Iwaki, A., Goldman, J.E., 1990. Cellular distribution of alpha B-crystallin in non-lenticular tissues. *J. Histochem. Cytochem.* 38, 31–39.
- Jacob, M.H., 2000. *Theorien der elementaren Faltung im Test am Kälteschockprotein CspB*. Ph.D. Dissertation, University of Bayreuth.
- Jaenicke, R., 1987. Folding and association of proteins. *Prog. Biophys. Mol. Biol.* 49, 117–237.
- Jaenicke, R., 1991a. Protein folding: local structures, domains and association. *Biochemistry* 30, 3147–3161.
- Jaenicke, R., 1991b. Protein stability and molecular adaptation to extreme conditions. *Eur. J. Biochem.* 202, 715–728.
- Jaenicke, R., 1996. Protein folding and association: in vitro studies for self-organization and targeting in the cell. *Curr. Top. Cell Regul.* 34, 209–314.
- Jaenicke, R., 1998. Protein self-organization in vitro and in vivo: partitioning between physical biochemistry and cell biology. *Biol. Chem.* 379, 237–243.
- Jaenicke, R., 1999. Stability and folding of domain proteins. *Prog. Biophys. Mol. Biol.* 71, 155–241.
- Jaenicke, R., Böhm, G., 1998. The stability of proteins in extreme environments. *Curr. Opin. Struct. Biol.* 8, 738–748.
- Jaenicke, R., Böhm, G., 2001. Thermostability of proteins from *Thermotoga maritima*. *Methods Enzymol.* 334, 438–469.
- Jaenicke, R., Creighton, T.E., 1993. Junior chaperones:  $\alpha$ -crystallins of the vertebrate eye lens are members of the family of small heat-shock proteins, sharing with other family members the ability to “chaperone” protein folding. *Curr. Biol.* 3, 234–235.
- Jaenicke, R., Seckler, R., 1997. Protein misassembly in vitro. *Adv. Protein Chem.* 50, 1–59.
- Jaenicke, R., Slingsby, C., 2001. Lens crystallins and their microbial homologs: structure, stability, and function. *Crit. Rev. Biochem. Mol. Biol.* 36, 435–499.
- Jaenicke, J., Sterner, R., 2002. Life at high temperature. In: *The Prokaryotes*, 3rd Edition (electronic), Latest Update Release: 3. 9. 2002. Springer, New York, pp. 1–56.
- Jencks, W.P., 1969. *Catalysis in Chemistry and Enzymology*. McGraw-Hill, New York.
- Jimenez-Asensio, J., Gonzalez, P., Zigler, J.S.Jr, Garland, D.L., 1995. Glyceraldehyde 3-phosphate dehydrogenase is an enzyme-crystallin in diurnal geckos of the genus *Phelsuma*. *Biochem. Biophys. Res. Commun.* 209, 796–802.
- Kaiser, D., Maniol, C.C., Dworkin, M., 1979. Myxobacteria: cell interactions, genetics, and development. *Annu. Rev. Microbiol.* 33, 595–639.
- Kamei, A., Hamaguchi, T., Matsuura, N., Masuda, K., 2001. Does post-translational modification influence chaperone-like activity of alpha-crystallin? I. Study on phosphorylation. *Biol. Pharm. Bull.* 24, 96–99.
- Kauzmann, W., 1969. Some factors in the interpretation of protein denaturation. *Adv. Protein Chem.* 14, 1–69.
- Kim, K.K., Kim, R., Kim, S.-H., 1998. Crystal structure of a small heat-shock protein. *Nature* 394, 595–599.
- Kim, Y.H., Kapfer, D.M., Boekhorst, J., Lubsen, N.H., Bachinger, H.P., Shearer, T.R., David, L.L., Feix, J.B., Lampi, K.J., 2002. Deamidation, but not truncation, decreases the urea stability of a lens structural protein, betaB1-crystallin. *Biochemistry* 41, 14076–14084.
- Kirby, A.J., 1980. *Adv. Phys. Org. Chem.* 17, 183–278.
- Klein, B.E., Klein, R., Lee, K.E., 2002. Incidence of age-related cataract over a 10-year interval: the Beaver Dam Eye Study. *Ophthalmology* 109, 2052–2057.

- Kmoch, S., Brynda, J., Asfaw, B., Bezouska, K., Novak, P., Rezacova, P., Ondrova, L., Filipec, M., Sedlacek, J., Elleder, M., 2000. Link between a novel human gammaD-crystallin allele and a unique cataract phenotype explained by protein crystallography. *Hum. Mol. Genet.* 9, 1779–1786.
- Knapp, S., Ladenstein, R., Galinski, E.A., 1999. Extrinsic protein stabilization by the naturally occurring osmolytes beta-hydroxyectoine and betaine. *Extremophiles* 3, 191–198.
- Kokke, B.P., Boelens, W.C., de Jong, W.W., 2001. The lack of chaperone like activity of *Caenorhabditis elegans* Hsp12.2 cannot be restored by domain swapping with human alphaB-crystallin. *Cell Stress Chaperones* 6, 360–367.
- Koretz, J.F., Handelman, G.H., 1988. How the human eye focuses. *Sci. Am.* 259, 92–99.
- Kosinski-Collins, M.S., King, J., 2003. In vitro unfolding, refolding, and polymerization of human gammaD crystallin, a protein involved in cataract formation. *Protein Sci.* 12, 480–490.
- Koteiche, H.A., Mchaourab, H.S., 1999. Folding pattern of the alpha-crystallin domain in alphaA-crystallin determined by site-directed spin labeling. *J. Mol. Biol.* 294, 561–577.
- Kretschmar, M., 1999. Struktur, Stabilität, Faltung und Funktion von S3a aus *Physarum polycephalum*. Ph.D. Dissertation, University of Regensburg.
- Kretschmar, M., Jaenicke, R., 1999. Stability of a homo-dimeric Ca(2+)-binding member of the beta gamma-crystallin superfamily: DSC measurements on spherulin 3a from *Physarum polycephalum*. *J. Mol. Biol.* 291, 1147–1153.
- Kretschmar, M., Mayr, E.M., Jaenicke, R., 1999a. Homo-dimeric spherulin 3a: a single-domain member of the beta gamma-crystallin superfamily. *Biol. Chem.* 380, 89–94.
- Kretschmar, M., Mayr, E.M., Jaenicke, R., 1999b. Kinetic and thermodynamic stabilization of the betagamma-crystallin homolog spherulin 3a from *Physarum polycephalum* by calcium binding. *J. Mol. Biol.* 289, 701–705.
- Kröger, R.H., Campbell, M.C., Munger, R., Fernald, R.D., 1994. Refractive index distribution and spherical aberration in the crystalline lens of the African cichlid fish *Haplochromis burtoni*. *Vis. Res.* 34, 1815–1822.
- Kumaraswamy, V.S., Lindley, P.F., Slingsby, C., Glover, I.D., 1996. An eye-lens protein-water structure: 1.2Å resolution structure of  $\gamma$ D-crystallin at 150k. *Acta Cryst. D* 52, 611–622.
- Lampi, K.J., Ma, Z., Shih, M., Shearer, T.R., Smith, J.B., Smith, D.L., David, L.L., 1997. Sequence analysis of betaA3, betaB3, and betaA4 crystallins completes the identification of the major proteins in young human lens. *J. Biol. Chem.* 272, 2268–2275.
- Lampi, K.J., Ma, Z., Hanson, S.R., Azuma, M., Shih, M., Shearer, T.R., Smith, D.L., Smith, J.B., David, L.L., 1998. Age-related changes in human lens crystallins identified by two-dimensional electrophoresis and mass spectrometry. *Exp. Eye Res.* 67, 31–43.
- Lampi, K.J., Oxford, J.T., Bachinger, H.P., Shearer, T.R., David, L.L., Kapfer, D.M., 2001. Deamidation of human beta B1 alters the elongated structure of the dimer. *Exp. Eye Res.* 72, 279–288.
- Lampi, K.J., Kim, Y.H., Bachinger, H.P., Boswell, B.A., Lindner, R.A., Carver, J.A., Shearer, T.R., David, L.L., Kapfer, D.M., 2002a. Decreased heat stability and increased chaperone requirement of modified human betaB1-crystallins. *Mol. Vis.* 8, 359–366.
- Lampi, K.J., Shih, M., Ueda, Y., Shearer, T.R., David, L.L., 2002b. Lens proteomics: analysis of rat crystallin sequences and two-dimensional electrophoresis map. *Invest. Ophthalmol. Vis. Sci.* 43, 216–224.
- Lansbury, P.T., 1999. Evolution of amyloid: what normal protein folding may tell us about fibrillogenesis and disease. *Proc. Natl. Acad. Sci. USA* 96, 3342–3344.
- Lapko, V.N., Smith, D.L., Smith, J.B., 2002a. S-methylated cysteines in human lens gamma S-crystallins. *Biochemistry* 41, 14645–14651.
- Lapko, V.N., Purkiss, A.G., Smith, D.L., Smith, J.B., 2002b. Deamidation in human gamma S-crystallin from cataractous lenses is influenced by surface exposure. *Biochemistry* 41, 8638–8648.
- Lapko, V.N., Smith, D.L., Smith, J.B., 2003a. Expression of betaA2-crystallin in human lenses. *Exp. Eye Res.* 77, 383–385.
- Lapko, V.N., Smith, D.L., Smith, J.B., 2003b. Methylation and carbamylation of human gamma-crystallins. *Protein Sci.* 12, 1762–1774.
- Lee, G.J., Roseman, A.M., Saibil, H.R., Vierling, E., 1997. A small heat shock protein stably binds heat-denatured model substrates and can maintain a substrate in a folding-competent state. *EMBO J.* 16, 659–671.
- Leenders, W.P., van Genesen, S.T., Schoenmakers, J.G.G., van Zoelen, E.J.J., Lubsen, N.H., 1997. Synergism between temporally distinct growth factors: bFGF, insulin and lens cell differentiation. *Mech. Dev.* 67, 193–201.

- Li, Y., Yan, Q., Wolf, N.S., 1997. Long-term caloric restriction delays age-related decline in proliferation capacity of murine lens epithelial cells in vitro and in vivo. *Invest. Ophthalmol. Vis. Sci.* 38, 100–107.
- Liang, J.J., Sun, T.X., Akhtar, N.J., 2000. Heat-induced conformational change of human lens recombinant alphaA- and alphaB-crystallins. *Mol. Vis.* 6, 10–14.
- Lindner, R.A., Ralston, G.B., 1995. Effects of dextran on the self-association of human spectrin. *Biophys. Chem.* 57, 15–25.
- Lindner, R.A., Ralston, G.B., 1997. Macromolecular crowding: effects on actin polymerisation. *Biophys. Chem.* 66, 57–66.
- Liu, C.W., Asherie, N., Lomakin, A., Pande, J., Ogun, O., Benedek, G.B., 1996. Phase separation in aqueous solutions of lens gamma-crystallins: special role of gamma s. *Proc. Natl. Acad. Sci. USA* 93, 377–382.
- Lomakin, A., Asherie, N., Benedek, G.B., 1996. Monte-Carlo study of phase separation in aqueous protein solutions. *J. Chem. Phys.* 104, 1646–1656.
- Lorand, L., Parameswaran, K.N., Velasco, P.T., 1991. Sorting-out of acceptor–donor relationships in the transglutaminase-catalyzed cross-linking of crystallins by the enzyme-directed labeling of potential sites. *Proc. Natl. Acad. Sci. USA* 88, 82–83.
- Lubsen, N.H., Aarts, H.J.M., Schoenmakers, J.G.G., 1988. The evolution of lenticular proteins: the beta- and gamma-crystallin super gene family. *Prog. Biophys. Mol. Biol.* 51, 47–76.
- Lund, A.L., Smith, J.B., Smith, D.L., 1996. Modifications of the water-insoluble human lens alpha-crystallins. *Exp. Eye Res.* 63, 661–672.
- Ma, Z.X., Hanson, S.R.A., Lampi, K.J., David, L.L., Smith, D.L., Smith, J.B., 1998. Age-related changes in human lens crystallins identified by HPLC and mass spectrometry. *Exp. Eye Res.* 67, 21–30.
- MacCoss, M.J., McDonald, W.H., Saraf, A., Sadygov, R., Clark, J.M., Tasto, J.J., Gould, K.L., Wolters, D., Washburn, M., Weiss, A., Clark, J.I., Yates 3rd, J.R., 2002. Shotgun identification of protein modifications from protein complexes and lens tissue. *Proc. Natl. Acad. Sci. USA* 99, 7900–7905.
- MacRae, T.H., 2000. Structure and function of small heat shock/alpha-crystallin proteins: established concepts and emerging ideas. *Cell. Mol. Life Sci.* 57, 899–913.
- Magabo, K.S., Horwitz, J., Piatigorsky, J., Kantorow, M., 2000. Expression of betaB(2)-crystallin mRNA and protein in retina, brain, and testis. *Invest. Ophthalmol. Vis. Sci.* 41, 3056–3060.
- Makhatadze, G.I., Privalov, P.L., 1995. Energetics of protein structure. *Adv. Protein Chem.* 47, 307–425.
- Malfois, M., Bonneté, F., Belloni, L., Tardieu, A., 1996. A model of attractive interactions to account for fluid–fluid phase separation of protein solutions. *J. Chem. Phys.* 105, 3290–3300.
- Mayr, E.M., Jaenicke, R., Glockshuber, R., 1994. Domain interactions and connecting peptides in lens crystallins. *J. Mol. Biol.* 235, 84–88.
- Mayr, E.M., Jaenicke, R., Glockshuber, R., 1997. The domains in gammaB-crystallin: identical fold-different stabilities. *J. Mol. Biol.* 269, 260–269.
- McAvoy, J.W., 1978. Cell division, cell elongation and distribution of alpha-, beta- and gamma-crystallins in the rat lens. *J. Embryol. Exp. Morphol.* 44, 149–165.
- McAvoy, J.W., Chamberlain, C.G., 1989. Fibroblast growth factor (FGF) induces different responses in lens epithelial cells depending on its concentration. *Development* 107, 221–228.
- Mchaourab, H.S., Dodson, E.K., Koteiche, H.A., 2002. Mechanism of chaperone function in small heat shock proteins—two-mode binding of the excited states of T4 lysozyme mutants by alpha A-crystallin. *J. Biol. Chem.* 277, 40557–40566.
- Merck, K.B., Groenen, P.J., Voorter, C.E., de Haard-Hoekman, W.A., Horwitz, J., Bloemendal, H., de Jong, W.W., 1993. Structural and functional similarities of bovine alpha-crystallin and mouse small heat-shock protein. A family of chaperones. *J. Biol. Chem.* 268, 1046–1052.
- Michael, R., van Marle, J., Vrensen, G.F., van den Berg, T.J., 2003. Changes in the refractive index of lens fibre membranes during maturation—impact on lens transparency. *Exp. Eye Res.* 77, 93–99.
- Minton, A., 2000a. Effect of a concentrated “inert” macromolecular cosolute on the stability of a globular protein with respect to denaturation by heat and by chaotropes: a statistical-thermodynamic model. *Biophys. J.* 78, 101–109.
- Minton, A., 2000b. Implications of macromolecular crowding for protein assembly. *Curr. Opin. Struct. Biol.* 10, 34–39.

- Morimoto, R.I., Santoro, M.G., 1998. Stress-inducible responses and heat shock proteins: new pharmacologic targets for cytoprotection. *Nat. Biotechnol.* 16, 833–838.
- Mornon, J.P., Halaby, D., Malfois, M., Durand, P., Callebaut, I., Tardieu, A., 1998. Alpha-Crystallin C-terminal domain: on the track of an ig fold. *Int. J. Biol. Macromol.* 22, 219–227.
- Motohashi, H., Shavit, J.A., Igarashi, K., Yamamoto, M., Engel, J.D., 1997. The world according to Maf. *Nucleic Acids Res.* 25, 2953–2959.
- Muchowski, P.J., Hays, L.G., Yates, J.R., Clark, J.I., 1999. ATP and the core “alpha-Crystallin” domain of the small heat-shock protein alphaB-crystallin. *J. Biol. Chem.* 274, 30190–30195.
- Murthy, S.N., Velasco, P.T., Lorand, L., 1998. Properties of purified lens transglutaminase and regulation of its transamidase/crosslinking activity by GTP. *Exp. Eye Res.* 67, 273–281.
- Muschol, M., Rosenberger, F., 1995. Interactions in under- and supersaturated lysozyme solutions. Static and dynamic light scattering results. *J. Chem. Phys.* 103, 10424–10432.
- Myers, J.K., Pace, C.N., Scholz, J.M., 1995. Denaturant m values and heat capacity changes: relation to changes in accessible surface areas of protein unfolding. *Protein Sci.* 4, 2138–2148.
- Nguyen, T., Huang, H.C., Pickett, C.B., 2000. Transcriptional regulation of the antioxidant response element. Activation by Nrf2 and repression by MafK. *J. Biol. Chem.* 275, 15466–15473.
- Nicholl, I.D., Quinlan, R.A., 1994. Chaperone activity of alpha-crystallins modulates intermediate filament assembly. *EMBO J.* 13, 945–953.
- Norledge, B.V., Mayr, E.M., Glockshuber, R., Bateman, O.A., Slingsby, C., Jaenicke, R., Driessen, H.P., 1996. The X-ray structures of two mutant crystallin domains shed light on the evolution of multi-domain proteins. *Nat. Struct. Biol.* 3, 267–274.
- Norledge, B.V., Hay, R.E., Bateman, O.A., Slingsby, C., Driessen, H.P.C., 1997a. Towards a molecular understanding of phase separation in the lens: a comparison of the X-ray structures of two high Tc gamma-crystallins, gammaE and GammaF, with two low Tc gamma-crystallins, gammaB and gammaD. *Exp. Eye Res.* 65, 609–630.
- Norledge, B.V., Trinkl, S., Jaenicke, R., Slingsby, C., 1997b. The X-ray structure of a mutant eye lens beta B2-crystallin with truncated sequence extensions. *Protein Sci.* 6, 1612–1620.
- Ohno, A., Tate, S.-I., Seeram, S.S., Hiraga, K., Swindells, M.B., Oda, K., Kainosho, M., 1998. NMR structure of the *Streptomyces* metalloproteinase inhibitor, SMPI, isolated from *Streptomyces nigrescens* TK-23: another example of an ancestral beta gamma-crystallin precursor structure. *J. Mol. Biol.* 282, 421–433.
- Pace, C.N., Shirley, B.A., McNutt, M., Gajiwala, K., 1996. Forces contributing to the conformational stability of proteins. *FASEB J.* 10, 75–83.
- Palme, S., Slingsby, C., Jaenicke, R., 1997. Mutational analysis of hydrophobic domain interactions in gamma B-crystallin from bovine eye lens. *Protein Sci.* 6, 1529–1536.
- Palme, S., Jaenicke, R., Slingsby, C., 1998a. X-ray structures of three interface mutants of gammaB-crystallin from bovine eye lens. *Protein Sci.* 7, 611–618.
- Palme, S., Jaenicke, R., Slingsby, C., 1998b. Unusual domain pairing in a mutant of bovine lens gammaB-crystallin. *J. Mol. Biol.* 279, 1053–1059.
- Pan, F.M., Chang, W.C., Chao, Y.K., Chiou, S.H., 1994. Characterization of gamma-crystallins from a hybrid teleostean fish: multiplicity of isoforms as revealed by cDNA sequence analysis. *Biochem. Biophys. Res. Commun.* 202, 527–534.
- Pande, A., Pande, J., Asherie, N., Lomakin, A., Ogun, O., King, J.A., Lubsen, N.H., Walton, D., Benedek, G.B., 2000. Molecular basis of a progressive juvenile-onset hereditary cataract. *Proc. Natl. Acad. Sci. USA* 97, 1993–1998.
- Pande, A., Pande, J., Asherie, N., Lomakin, A., Ogun, O., King, J., Benedek, G.B., 2001. Crystal cataracts: human genetic cataract caused by protein crystallization. *Proc. Natl. Acad. Sci. USA* 98, 6116–6120.
- Parsegian, V.A., Rand, R.P., Fuller, N.L., Rau, D.C., 1986. Osmotic stress for the direct measurement of intermolecular forces. *Methods Enzymol.* 127, 400–416.
- Pasta, S.Y., Raman, B., Ramakrishna, T., Rao, Ch.M., 2002. Role of the C-terminal extensions of alpha-crystallins: swapping the C-terminal extension of alpha A-crystallin to alpha B-crystallin results in enhanced chaperone activity. *J. Biol. Chem.* 277, 45821–45828.
- Patil, C., Walter, P., 2001. Intracellular signaling from the endoplasmic reticulum to the nucleus: the unfolded protein response in yeast and mammals. *Curr. Opin. Cell Biol.* 13, 349–355.

- Peek, R., McAvoy, J.W., Lubsen, N.H., Schoenmakers, J.G.G., 1992. Rise and fall of crystallin gene messenger levels during fibroblast growth factor induced terminal differentiation of lens cells. *Dev. Biol.* 152, 152–160.
- Pendergrass, W.R., Penn, P.E., Li, J., Wolf, N.S., 2001. Age-related telomere shortening occurs in lens epithelium from old rats and is slowed by caloric restriction. *Exp. Eye. Res.* 73, 221–228.
- Perl, D., Welker, C., Schindler, T., Schroder, K., Marahiel, M.A., Jaenicke, R., Schmid, F.X., 1998. Conservation of rapid two-state folding in mesophilic, thermophilic and hyperthermophilic cold shock proteins. *Nat. Struct. Biol.* 5, 229–235.
- Petsko, G.A., 2001. Structural basis of thermostability in hyperthermophilic proteins, or “there’s more than one way to skin a cat”. *Methods Enzymol.* 334, 469–478.
- Pfeil, W., 1998. *Protein Stability and Folding*. Springer, Berlin, Heidelberg, New York.
- Piatigorsky, J., Wistow, G.J., 1989. Enzyme/crystallins: gene sharing as an evolutionary strategy. *Cell* 57, 197–199.
- Piatigorsky, J., Wistow, G., 1991. The recruitment of crystallins: new functions precede gene duplication. *Science* 252, 1078–1079.
- Pierscionek, B.K., Augusteyn, R.C., 1992. Growth related changes to functional parameters in the bovine lens. *Biochim. Biophys. Acta.* 1116, 283–290.
- Privalov, P.L., 1979. Stability of proteins: small globular proteins. *Adv. Protein Chem.* 33, 167–241.
- Privalov, P.L., 1982. Stability of proteins. Proteins which do not present a single cooperative system. *Adv. Protein Chem.* 35, 193–231.
- Privalov, P.L., 1992. Physical basis of the stability of the folded conformations of proteins. In: Creighton, T.E. (Ed.), *Protein Folding*. Freeman, New York, pp. 83–126.
- Privalov, P.L., Gill, S.J., 1988. Stability of protein structure and hydrophobic interaction. *Adv. Protein Chem.* 39, 193–231.
- Purkiss, A.G., Bateman, O.A., Goodfellow, J.M., Lubsen, N.H., Slingsby, C., 2002. The X-ray crystal structure of human gammaS-crystallin C-terminal domain. *J. Biol. Chem.* 277, 4199–4205.
- Putilina, T., Skouri-Panet, F., Prat, K., Lubsen, N.H., Tardieu, A., 2003. Subunit exchange demonstrates a differential chaperone activity of calf alpha-crystallin towards beta<sub>LOW</sub>- and individual gamma-crystallins. *J. Biol. Chem.* 278, 13747–13756.
- Raghunath, M., Cankay, R., Kubitscheck, U., Fauteck, J.D., Mayne, R., Aeschlimann, D., Schlotzer-Schrehardt, U., 1999. Transglutaminase activity in the eye: cross-linking in epithelia and connective tissue structures. *Invest. Ophthalmol. Vis. Sci.* 40, 2780–2787.
- Rajaraman, K., Raman, B., Ramakrishna, T., Rao, C.M., 1998. The chaperone-like alpha-crystallin forms a complex only with the aggregation-prone molten globule state of alpha-lactalbumin. *Biochem. Biophys. Res. Commun.* 249, 917–921.
- Rajaraman, K., Raman, B., Ramakrishna, T., Rao, C.M., 2001. Interaction of human recombinant alphaA- and alphaB-crystallins with early and late unfolding intermediates of citrate synthase on its thermal denaturation. *FEBS Lett.* 497, 118–123.
- Rajini, B., Shridas, P., Sundari, C.S., Muralidhar, D., Chandani, S., Thomas, F., Sharma, Y., 2001. Calcium binding properties of gamma-crystallin: calcium ion binds at the Greek key beta gamma-crystallin fold. *J. Biol. Chem.* 276, 38464–38471.
- Raman, B., Ramakrishna, T., Rao, C.M., 1995. Rapid refolding studies on the chaperone-like alpha-crystallin. Effect of alpha-crystallin on refolding of beta- and gamma-crystallins. *J. Biol. Chem.* 270, 19888–19892.
- Ray, M.E., Wistow, G.J., Su, Y.A., Meltzer, P.S., Trent, J.M., 1997. AIM1, a novel non-lens member of the betagamma-crystallin superfamily, is associated with the control of tumorigenicity in human malignant melanoma. *Proc. Natl. Acad. Sci. USA* 94, 3220–3234.
- Reddy, G.B., Das, K.P., Petrash, J.M., Surewicz, W.K., 2000. Temperature-dependent chaperone activity and structural properties of human alphaA- and alphaB-crystallins. *J. Biol. Chem.* 275, 4565–4570.
- Ring, B.Z., Cordes, S.P., Overbeek, P.A., Barsh, G.S., 2000. Regulation of mouse lens fiber cell development and differentiation by the Maf gene. *Development* 127, 307–317.
- Rivas, G., Fernandez, J.A., Minton, A.P., 1999. Direct observation of the self-association of dilute proteins in the presence of inert macromolecules at high concentration via tracer sedimentation equilibrium: theory, experiment, and biological significance. *Biochemistry* 38, 9379–9388.

- Robinson, K.M., Taube, J.R., Reed, N.A., Duncan, M.K., 2003. Role of betaB2-crystallin in fertility. Invest. Ophthalmol. Vis. Sci. 44, E-Abstract 2136.
- Röll, B., van Boekel, M.A.M., Amons, R., de Jong, W.W., 1995. RhoB-crystallin, an aldose reductase-like lens protein in the gecko *Lepidodactylus lugubris*. Biochem. Biophys. Res. Commun. 217, 452–458.
- Röll, B., Amons, R., de Jong, W.W., 1996. Vitamin A<sub>2</sub> bound to cellular retinol-binding protein as ultraviolet filter in the eye lens of the gecko *Lygodactylus picturatus*. J. Biol. Chem. 271, 10437–10440.
- Rosinke, B., Renner, C., Mayr, E.-M., Jaenicke, R., Holak, T.A., 1997. Ca<sup>2+</sup>-loaded spherulin 3a from *Physarum polycephalum* adopts the prototype gamma-crystallin fold in aqueous solution. J. Mol. Biol. 271, 645–655.
- Rudolph, R., Siebendritt, R., Nessler, G., Sharma, A.K., Jaenicke, R., 1990. Folding of an all-beta protein: independent domain folding in gamma II-crystallin from calf eye lens. Proc. Natl. Acad. Sci. USA 87, 4625–4629.
- Ruotolo, R., Grassi, F., Percudani, R., Rivetti, C., Martorana, D., Maraini, G., Otonello, S., 2003. Gene expression profiling in human age-related nuclear cataract. Mol. Vis. 9, 538–548.
- Saibil, H., 2000. Molecular chaperones: containers and surfaces for folding, stabilising or unfolding proteins. Curr. Opin. Struct. Biol. 10, 251–258.
- Sandilands, A., Hutcheson, A.M., Long, H.A., Prescott, A.R., Vrensen, G., Loster, J., Klopp, N., Lutz, R.B., Graw, J., Masaki, S., Dobson, C.M., MacPhee, C.E., Quinlan, R.A., 2002. Altered aggregation properties of mutant gamma-crystallins cause inherited cataract. EMBO J. 21, 6005–6014.
- Santhoshkumar, P., Sharma, K.K., 2001. Analysis of alpha-crystallin chaperone function using restriction enzymes and citrate synthase. Mol. Vis. 7, 172–177.
- Santini, S.A., Mordente, A., Meucci, E., Miggiano, G.A., Martorana, G.E., 1992. Conformational stability of bovine alpha-crystallin. Evidence for a destabilizing effect of ascorbate. Biochem. J. 287, 107–112.
- Schlunegger, M.P., Bennett, M.J., Eisenberg, D., 1997. Oligomer formation by 3D domain swapping: a model for protein assembly and misassembly. Adv. Protein Chem. 50, 61–122.
- Sharma, K.K., Kaur, H., Kester, K., 1997. Functional elements in molecular chaperone alpha-crystallin: identification of binding sites in alpha B-crystallin. Biochem. Biophys. Res. Commun. 239, 217–222.
- Sharma, K.K., Kaur, H., Kumar, G.S., Kester, K., 1998. Interaction of 1, 1'-bi(4-anilino)naphthalene-5, 5'-disulfonic acid with alpha-crystallin. J. Biol. Chem. 273, 8965–8970.
- Shridas, P., Sharma, Y., Balasubramanian, D., 2001. Transglutaminase-mediated cross-linking of alpha-crystallin: structural and functional consequences. FEBS Lett. 499, 245–250.
- Siezen, R.J., Anello, R.D., Thomson, J.A., 1986. Interactions of lens proteins. Concentration dependence of beta-crystallin aggregation. Exp. Eye Res. 43, 293–303.
- Siezen, R.J., Thomson, J.A., Kaplan, E.D., Benedek, G.B., 1987. Human lens gamma-crystallins: isolation, identification, and characterization of the expressed gene products. Proc. Natl. Acad. Sci. USA 84, 6088–6092.
- Siezen, R.J., Wu, E., Kaplan, E.D., Thomson, J.A., Benedek, G.B., 1988. Rat lens gamma-crystallins. Characterization of the six gene products and their spatial and temporal distribution resulting from differential synthesis. J. Mol. Biol. 199, 475–490.
- Sinha, D., Esumi, N., Jaworski, C., Kozak, C.A., Pierce, E., Wistow, G., 1998. Cloning and mapping the mouse Crygs gene and non-lens expression of gammaS-crystallin. Mol. Vis. 4, 8.
- Skouri-Panet, F., Bonneté, F., Prat, K., Bateman, O.A., Lubsen, N.H., Tardieu, A., 2001. Lens crystallins and oxidation: the special case of gammaS. Biophys. Chem. 89, 65–76.
- Slingsby, C., Bateman, O.A., 1990. Quaternary interactions in eye lens beta-crystallins: basic and acidic subunits of beta-crystallins favor heterologous association. Biochemistry 29, 6592–6599.
- Smith, G., Atchison, D.A., Pierscionek, B.K., 1992. Modeling the power of the aging human eye. J. Opt. Soc. Am. A 9, 2111–2117.
- Smolich, B.D., Tarkington, S.K., Saha, M.S., Stathakis, D.G., Grainger, R.M., 1993. Characterization of *Xenopus laevis* gamma-crystallin-encoding genes. Gene 128, 189–195.
- Sobott, F., Benesch, J.L.P., Vierling, E., Robinson, C.V., 2002. Subunit exchange of multimeric complexes-real-time monitoring of subunit exchange between small heat shock proteins by using electrospray mass spectrometry. J. Biol. Chem. 277, 38921–38929.
- Sonna, L.A., Fujita, J., Gaffin, S.L., Lilly, C.M., 2002. Invited review: effects of heat and cold stress on mammalian gene expression. J. Appl. Physiol. 92, 1725–1742.

- Söti, C., Csermely, P., 2002. Chaperones and aging: role in neurodegeneration and in other civilizational diseases. *Neurochem. Int.* 41, 383–389.
- Spector, A., Li, D., Ma, W., Sun, F., Pavlidis, P., 2002. Differential amplification of gene expression in lens cell lines conditioned to survive peroxide stress. *Invest. Ophthalmol. Vis. Sci.* 43, 3251–3264.
- Srinivasan, A.N., Nagineni, C.N., Bhat, S.P., 1992. Alpha A-crystallin is expressed in non-ocular tissues. *J. Biol. Chem.* 267, 23337–23341.
- Srivastava, O.P., Srivastava, K., 2003. BetaB2-crystallin undergoes extensive truncation during aging in human lenses. *Biochem. Biophys. Res. Commun.* 301, 44–49.
- Sun, T.X., Liang, J.J., 1998. Intermolecular exchange and stabilization of recombinant human alphaA- and alphaB-crystallin. *J. Biol. Chem.* 273, 286–290.
- Sun, T.X., Akhtar, N.J., Liang, J.J., 1998. Subunit exchange of lens alpha-crystallin: a fluorescence energy transfer study with the fluorescent labeled alphaA-crystallin mutant W9F as a probe. *FEBS Lett.* 430, 401–404.
- Sun, T.X., Akhtar, N.J., Liang, J.J., 1999. Thermodynamic stability of human lens recombinant alphaA- and alphaB-crystallins. *J. Biol. Chem.* 274, 34067–34071.
- Surewicz, W.K., Olesen, P.R., 1995. On the thermal stability of alpha-crystallin: a new insight from infrared spectroscopy. *Biochemistry* 34, 9655–9660.
- Takemoto, L., 2001. Deamidation of Asn-143 of gamma S crystallin from protein aggregates of the human lens. *Curr. Eye Res.* 22, 148–153.
- Takemoto, L., Boyle, D., 1998. Determination of the in vivo deamidation rate of asparagine-101 from alpha-A crystallin using microdissected sections of the aging human lens. *Exp. Eye Res.* 67, 119–120.
- Tanaka, T., Benedek, G., 1975. Observation of protein diffusivity in intact human and bovine lenses with application to cataract. *Invest. Ophthalmol.* 14, 449–456.
- Tardieu, A., Delaye, M., 1988. Eye lens proteins and transparency: from light transmission theory to solution X-ray structural analysis. *Annu. Rev. Biophys. Chem.* 17, 47–70.
- Tardieu, A., Véréout, F., 1991. Biophysical analysis of eye lens transparency. In: Obrecht, G., Stark, L.W. (Eds.), *Presbyopia Research: From Molecular Biology to Visual Adaptation*. Plenum Press, New York, pp. 49–55.
- Tardieu, A., Laporte, D., Licinio, P., Krop, B., Delaye, M., 1986. Calf lens alpha-crystallin quaternary structure. A three-layer tetrahedral model. *J. Mol. Biol.* 192, 711–724.
- Tardieu, A., Laporte, D., Delaye, M., 1987. Colloidal dispersions of alpha-crystallin proteins. 1. Small angle X-ray analysis of the dispersion structure. *J. Phys.* 48, 1207–1215.
- Tardieu, A., Véréout, F., Krop, B., Slingsby, C., 1992. Protein interactions in the calf eye lens: interactions between beta-crystallins are repulsive whereas in gamma-crystallins they are attractive. *Eur. Biophys. J.* 21, 1–12.
- Tardieu, A., Le Verge, A., Malfois, M., Bonneté, F., Finet, S., Riès-Kautt, M., Belloni, L., 1999. Proteins in solution: from X-ray scattered intensities to interaction potentials. *J. Cryst. Growth* 196, 193–203.
- Tardieu, A., Bonneté, F., Finet, S., Vivarès, D., 2002. Understanding salt or PEG induced attractive interactions to crystallize biological macromolecules. *Acta Crystallogr. D* 58, 1549–1553.
- Tellam, R.L., Sculley, M.J., Nicol, L.W., Wills, P.R., 1983. The influence of poly(ethylene glycol) 6000 on the properties of skeletal-muscle actin. *Biochem. J.* 213, 651–659.
- Thirumalai, D., Lorimer, G., 2001. Chaperonin-mediated protein folding. *Annu. Rev. Biophys. Struct. Biol.* 30, 245–269.
- Thornton, J.M., 2001. The Hans Neurath Award lecture of The Protein Society: proteins—a testament to physics, chemistry, and evolution. *Protein Sci.* 10, 3–11.
- Timasheff, S.N., Arakawa, T., 1997. Stabilization of protein structure by solvents. In: Creighton, T.E. (Ed.), *Protein Structure: A Practical Approach*. IRL, Oxford, pp. 349–364.
- Treweek, T.M., Lindner, R.A., Mariani, M., Carver, J.A., 2000. The small heat-shock chaperone protein, alpha-crystallin, does not recognize stable molten globule states of cytosolic proteins. *Biochim. Biophys. Acta* 1481, 175–188.
- Trinkl, S., Glockshuber, R., Jaenicke, R., 1994. Dimerization of beta B2-crystallin: the role of the linker peptide and the N- and C-terminal extensions. *Protein Sci.* 3, 1392–1400.
- Trokel, S., 1962. The physical basis for transparency of the crystalline lens. *Invest. Ophthalmol.* 1, 493–501.
- Ueda, Y., Duncan, M.K., David, L.L., 2002. Lens proteomics: the accumulation of crystallin modifications in the mouse lens with age. *Invest. Ophthalmol. Vis. Sci.* 43, 205–215.

- van Boekel, M.A., de Lange, F., de Grip, W.J., de Jong, W.W., 1999. Eye lens alphaA- and alphaB-crystallin: complex stability versus chaperone-like activity. *Biochim. Biophys. Acta* 1434, 114–123.
- van Boekel, M.A.M., van Aalten, D.M.F., Caspers, G.-J., Röhl, B., de Jong, W.W., 2001. Evolution of the aldose reductase-related gecko eye lens protein rhoB-crystallin: a sheep in wolf's clothing. *J. Mol. Evol.* 52, 239–248.
- van den Berg, B., Ellis, R.J., Dobson, C.M., 1999. Effects of macromolecular crowding on protein folding and aggregation. *EMBO J.* 18, 6927–6933.
- van den Berg, B., Wain, R., Dobson, C.M., Ellis, R.J., 2000. Macromolecular crowding perturbs protein refolding kinetics: implications for folding inside the cell. *EMBO J.* 19, 3870–3875.
- van den Heuvel, R., Hendriks, W., Quax, W., Bloemendal, H., 1985. Complete structure of the hamster  $\alpha$ A crystallin gene. Reflection of an evolutionary history by means of exon shuffling. *J. Mol. Biol.* 185, 273–284.
- van den Ijssel, P., Norman, D.G., Quinlan, R.A., 1999. Molecular chaperones: small heat shock proteins in the limelight. *Curr. Biol.* 9, R103–105.
- van den Oetelaar, P.J., Hoenders, H.J., 1989a. Folding-unfolding and aggregation–dissociation of bovine alpha-crystallin subunits; evidence for unfolding intermediates of the alpha A subunits. *Biochim. Biophys. Acta* 995, 91–96.
- van den Oetelaar, P.J., Hoenders, H.J., 1989b. Racemization of aspartyl residues in proteins from normal and cataractous human lenses: an aging process without involvement in cataract formation. *Exp. Eye Res.* 48, 209–214.
- Vanhoudt, J., Abgar, S., Aerts, T., Clauwaert, J., 2000. Native quaternary structure of bovine alpha-crystallin. *Biochemistry* 39, 4483–4492.
- van Leen, R.W., Breuer, M.L., Lubsen, N.H., Schoenmakers, J.G.G., 1987a. Developmental expression of crystallin genes: in situ hybridization reveals a differential localization of specific mRNAs. *Dev. Biol.* 123, 338–345.
- van Leen, R.W., van Roozendaal, K.E., Lubsen, N.H., Schoenmakers, J.G.G., 1987b. Differential expression of crystallin genes during development of the rat eye lens. *Dev. Biol.* 120, 457–464.
- van Leeuwen, F.W., Fischer, D.F., Kamel, D., Sluijs, J.A., Sonnemans, M.A.F., Benne, R., Swaab, D.F., Salehi, A., Hol, E.M., 2000. Molecular misreading: a new type of transcript mutation expressed during aging. *Neurobiol. Aging* 21, 879–891.
- van Montfort, R.L., Basha, E., Friedrich, K.L., Slingsby, C., Vierling, E., 2001. Crystal structure and assembly of a eukaryotic small heat shock protein. *Nat. Struct. Biol.* 8, 1025–1030.
- van Montfort, R., Slingsby, C., Vierling, E., 2002. Structure and function of the small heat shock protein/alpha-crystallin family of molecular chaperones. In: Horwich, A. (Ed.), *Protein Folding in the Cell*. *Adv. Protein Struct.* 59, 105–156.
- van Montfort, R.L.M., Bateman, O.A., Lubsen, N.H., Slingsby, C., 2003. Crystal structure of truncated human betaB1-crystallin. *Protein Sci.* 12, 2606–2612.
- van Oss, C.J., 1993. In: Westhof, E. (Ed.), *Water and Biological Macromolecules*. Macmillan Press, Houndmills and London, pp. 393–429.
- van Oss, C.J., Good, R.J., 1988. Orientation of the water molecules of hydration of human serum albumin. *J. Protein Chem.* 7, 179–183.
- van Rens, G.L., De Jong, W.W., Bloemendal, H., 1991. One member of the gamma-crystallin gene family, gamma s, is expressed in birds. *Exp. Eye Res.* 53, 135–138.
- van Rheede, T., Amons, R., Stewart, N., de Jong, W.W., 2003. Lactate dehydrogenase A as a highly abundant eye lens protein in platypus (*Ornithorhynchus anatinus*): epsilon-(v)-crystallin. *Mol. Biol. Evol.* 20, 994–998.
- Velasco, P.T., Lorand, L., 1987. Acceptor-donor relationships in the transglutaminase-mediated cross-linking of lens beta-crystallin subunits. *Biochemistry* 26, 4629–4634.
- Vérétout, F., Tardieu, A., 1989. The protein concentration gradient within eye lens might originate from constant osmotic pressure coupled to differential interactive properties of crystallins. *Eur. Biophys. J.* 17, 61–68.
- Vérétout, F., Delaye, M., Tardieu, A., 1989. Molecular basis of eye lens transparency. Osmotic pressure and X-ray analysis of alpha-crystallin solutions. *J. Mol. Biol.* 205, 713–728.
- Vicart, P., Caron, A., Guicheney, P., Li, Z., Prevost, M.C., Faure, A., Chateau, D., Chapon, F., Tome, F., Dupret, J.M., Paulin, D., Fardeau, M., 1998. A missense mutation in the alphaB-crystallin chaperone gene causes a desmin-related myopathy. *Nat. Genet.* 20, 92–95.
- Vita, C., Jaenicke, R., Fontana, A., 1989. Folding of thermolysin fragments: hydrodynamic properties of isolated domains and subdomains. *Eur. J. Biochem.* 183, 513–518.

- Voorter, C.E., de Haard-Hoekman, W.A., van den Oetelaar P, J., Bloemendal, H., de Jong, W.W., 1988. Spontaneous peptide bond cleavage in aging alpha-crystallin through a succinimide intermediate. *J. Biol. Chem.* 263, 19020–19023.
- Voorter, C.E., De Haard-Hoekman, W.A., Hermans, M.M., Bloemendal, H., De Jong, W.W., 1990. Differential synthesis of crystallins in the developing rat eye lens. *Exp. Eye Res.* 50, 429–437.
- Wang, K., Spector, A., 1994. The chaperone activity of bovine alpha crystallin. Interaction with other lens crystallins in native and denatured states. *J. Biol. Chem.* 269, 13601–13608.
- Wang, K., Spector, A., 2000. Alpha-crystallin prevents irreversible protein denaturation and acts cooperatively with other heat-shock proteins to renature the stabilized partially denatured protein in an ATP-dependent manner. *Eur. J. Biochem.* 267, 4705–4712.
- Wang, X., Garcia, C.M., Kwon, G., Guo, J., Wistow, G., Beebe, D.C., 2003. Expression and regulation of GAMMAS-crystallin in the lens epithelium: an epithelial “Stress Crystallin” Invest. Ophthalmol. Vis. Sci. 44, E-Abstract 2354.
- Weaver, A.J., Sullivan, W.P., Felts, S.J., Owen, B.A., Toft, D.O., 2000. Crystal structure and activity of human p23, a heat shock protein 90 co-chaperone. *J. Biol. Chem.* 275, 23045–23052.
- Weinreb, O., van Rijk, A.F., Dovrat, A., Bloemendal, H., 2000. In vitro filament-like formation upon interaction between lens alpha-crystallin and betaL-crystallin promoted by stress. Invest. Ophthalmol. Vis. Sci. 41, 3893–3897.
- Welch, W.J., Eggers, D.K., Hansen, W.J., Nagata, H., 1998. In: Fink, A.L., Goto, Y. (Eds.), *Molecular Chaperones in the Life Cycle of Proteins*. Marcel Dekker, New York, pp. 71–93.
- Welsh, M.J., Gaestel, M., 1998. Small heat-shock protein family: function in health and disease. *Ann. N.Y. Acad. Sci.* 851, 28–35.
- Wenk, M., 1999. Protein S aus *Myxococcus xanthus* und seine isolierten Domänen: Stabilität, Wechselwirkungen, Faltung und Struktur. Ph.D. Dissertation, University of Regensburg.
- Wenk, M., Jaenicke, R., 1999. Calorimetric analysis of the Ca(2+)-binding betagamma-crystallin homolog protein S from *Myxococcus xanthus*: intrinsic stability and mutual stabilization of domains. *J. Mol. Biol.* 293, 117–124.
- Wenk, M., Mayr, E.-M., 1998. *Myxococcus xanthus* spore coat protein S, a stress-induced member of the betagamma-crystallin superfamily, gains stability from binding of calcium ions. *Eur. J. Biochem.* 255, 604–610.
- Wenk, M., Baumgartner, R., Holak, T.A., Huber, R., Jaenicke, R., Mayr, E.M., 1999. The domains of protein S from *Myxococcus xanthus*: structure, stability and interactions. *J. Mol. Biol.* 286, 1533–1545.
- Wenk, M., Herbst, R., Hoeger, D., Kretschmar, M., Lubsen, N.H., Jaenicke, R., 2000. Gamma S-crystallin of bovine and human eye lens: solution structure, stability and folding of the intact two-domain protein and its separate domains. *Biophys. Chem.* 86, 95–108.
- Werten, P.J., Carver, J.A., Jaenicke, R., de Jong, W.W., 1996. The elusive role of the N-terminal extension of betaA3- and betaA1-crystallin. *Protein Eng.* 9, 1021–1028.
- Werten, P.J., Vos, E., De Jong, W.W., 1999. Truncation of betaA3/A1-crystallin during aging of the bovine lens: possible implications for lens optical quality. *Exp. Eye Res.* 68, 99–103.
- Werten, P.J., Röhl, B., van Aalten, D.M., de Jong, W.W., 2000. Gecko iota-crystallin: how cellular retinol-binding protein became an eye lens ultraviolet filter. *Proc. Natl. Acad. Sci. USA* 97, 3282–3287.
- Wickner, S., Maurizi, M.R., Gottesman, S., 1999. Posttranslational quality control: folding, refolding, and degrading proteins. *Science* 286, 1888–1893.
- Wieligmann, K., 2000. betaB2-Kristallin und Mutanten von betaB2-Kristallin: Stabilität, Wechselwirkungen, Faltung und Struktur. Ph.D. Dissertation, University of Regensburg.
- Wieligmann, K., Norledge, B., Jaenicke, R., Mayr, E.M., 1998. Eye lens betaB2-crystallin: circular permutation does not influence the oligomerization state but enhances the conformational stability. *J. Mol. Biol.* 280, 721–729.
- Wieligmann, K., Mayr, E.M., Jaenicke, R., 1999. Folding and self-assembly of the domains of betaB2-crystallin from rat eye lens. *J. Mol. Biol.* 286, 989–994.
- Wilf, J., Gladner, J.A., Minton, A.P., 1985. Acceleration of fibrin gel formation by unrelated proteins. *Thromb. Res.* 37, 681–688.
- Wistow, G., 1990. Evolution of a protein superfamily: relationships between vertebrate lens crystallins and microorganism dormancy proteins. *J. Mol. Evol.* 30, 140–145.
- Wistow, G., 1993. Lens crystallins: gene recruitment and evolutionary dynamism. *Trends Biochem. Sci.* 18, 301–306.
- Wistow, G., 1995. In: *Molecular Biology and Evolution of Crystallins*. Molecular Biology. Springer, Landes, Austin, TX, pp. 37–82.

- Wistow, G., Piatigorsky, J., 1987. Recruitment of enzymes as lens structural proteins. *Science* 236, 1554–1556.
- Wistow, G., Summers, L., Blundell, T., 1985. *Myxococcus xanthus* spore coat protein S may have a similar structure to vertebrate lens beta gamma-crystallins. *Nature* 315, 771–773.
- Wistow, G.J., Mulders, J.W., de Jong, W.W., 1987. The enzyme lactate dehydrogenase as a structural protein in avian and crocodilian lenses. *Nature* 326, 622–624.
- Wistow, G., Jaworski, C., Rao, P.V., 1995. A non-lens member of the beta gamma-crystallin superfamily in a vertebrate, the amphibian *Cynops*. *Exp. Eye Res.* 61, 637–639.
- Wistow, G., Bernstein, S.L., Wyatt, M.K., Behal, A., Touchman, J.W., Bouffard, G., Smith, D., Peterson, K., 2002. Expressed sequence tag analysis of adult human lens for the NEIBank Project: over 2000 non-redundant transcripts, novel genes and splice variants. *Mol. Vis.* 8, 171–184.
- Wolf, N.S., Li, Y., Pendergrass, W., Schneider, C., Turturro, A., 2000. Normal mouse and rat strains as models for age-related cataract and the effect of caloric restriction on its development. *Exp. Eye Res.* 70, 683–692.
- Wright, G., Basak, A.K., Wieligmann, K., Mayr, E.-M., Slingsby, C., 1998. Circular permutation of betaB2-crystallin changes the hierarchy of domain assembly. *Protein Sci.* 7, 1280–1285.
- Yu, N.-T., De Nagel, D.C., Pruett, P.L., Kuck Jr, J.F.R., 1985. Disulphide bond formation in the eye lens. *Proc. Natl. Acad. Sci. USA* 82, 207–214.
- Zarina, S., Slingsby, C., Jaenicke, R., Zaidi, Z.H., Driessen, H., Srinivasan, N., 1994. Three-dimensional model and quaternary structure of the human eye lens protein gamma S-crystallin based on beta- and gamma-crystallin X-ray coordinates and ultracentrifugation. *Protein Sci.* 3, 1840–1846.
- Zhang, Z., David, L.L., Smith, D.L., Smith, J.B., 2001. Resistance of human betaB2-crystallin to in vivo modification. *Exp. Eye Res.* 73, 203–211.
- Zhang, Z., Smith, D.L., Smith, J.B., 2003. Human beta-crystallins modified by backbone cleavage, deamidation and oxidation are prone to associate. *Exp. Eye Res.* 77, 259–272.
- Zigler Jr, J.S., Horwitz, J., Kinoshita, J.H., 1980. Human beta-crystallin I. Comparative studies on the beta<sub>1</sub>, beta<sub>2</sub> and beta<sub>3</sub>-crystallins. *Exp. Eye Res.* 31, 41–55.